

# REVERSE ENGINEERING OF EXISTING REINFORCED CONCRETE SLAB BRIDGES



T.L. (THOMAS) HARREWIJN

# Reverse Engineering of existing reinforced concrete slab bridges

by

T.L. Harrewijn

to obtain the degree of Master of Science  
at the Delft University of Technology,  
to be defended publicly on December the 13th, 2019.

Student number:	4292359	
Project duration:	March 1, 2019 – December 13, 2019	
Chair committee:	Dr. ir. Y. Yang,	Delft University of Technology
Former Chair committee:	Dr. ir. C. van der Veen	Delft University of Technology
Thesis committee	Dr. ir. E. O. L. Lantsoght,	Delft University of Technology and Universidad San Francisco de Quito (Republic Ecuador)
	Dr. ir. P. C. J. Hoogenboom,	Delft University of Technology
	ir. R. P. H. Vergoossen,	Royal HaskoningDHV (PhD-candidate Delft University of Technology)

*This thesis is confidential and cannot be made public until December 13th, 2021.*

Cover photos from <https://beeldbank.rws.nl>, © Rijkswaterstaat

An electronic version of this thesis is available at  
<http://repository.tudelft.nl/>.



# Preface

This thesis has been written as part of the Master of Science in Structural Engineering with a specialisation in Concrete Structures at Delft University of Technology. Over the last nine months I have been working on the thesis, in close collaboration with my supervisors at both the TU Delft and at Royal HaskoningDHV.

The challenge of learning a new specialisation in the field of structural engineering was my motivation for conducting this research. Ageing of the infrastructure is a worldwide problem and preserving the existing infrastructure is a large challenge the civil industry is facing today. In this work I present the findings of my research: Reverse Engineering of existing reinforced concrete slab bridges.

The contributions of all members of my committee are gratefully acknowledged. I thank Rob Vergoossen for his daily supervision and sharing his knowledge and experience in the field of conservation of existing structures. Furthermore, I would like to thank the cooperating company (Royal HaskoningDHV) where Rob is employed, for all helpful documents, features and colleagues assistance. I thank Eva Lantsoght for introducing me to the topic, welcoming my ideas for shaping the topic and continually offering supportive and constructive feedback. My academic writhing is significantly improved by Eva, who intensively helped me with writing and structuring the report. My thanks go to Pierre Hoogenboom for his active interest in my research and provoke thinking and inquiry. His friendly inquiries as to my progress during committee meetings and readiness to provide feedback were both useful and motivating. Furthermore, he introduced me to the field of probabilistic design and got me enthusiastic. Both Cor van der Veen and Yuguang Yang have fulfilled the role as chairman of the graduation committee. I received positive recognition for the usefulness of the research topic from both chairmen. From the role of my professor to that of chairman of my graduation committee, their readiness to always kindly provide assistance has been greatly appreciated.

Enjoy reading the report.

*Thomas Harrewijn  
Rotterdam, November 2019*

# Abstract

Most bridges in the Western European road networks are ageing. The vast majority of about 90% of these bridges have reinforced concrete as a building material. The traffic intensity, as well as the axle, and the average vehicle weight have increased since these structures were opened to traffic. Furthermore, the structural (design) codes have changed over the years. Therefore, there is a need to investigate if existing structures meet the safety/reliability level described by the current codes (Vergoossen, 2015). However, a frequently faced problem in practice is that the original design calculations and technical drawings of a large percentage of the existing bridges are unknown or lost. Especially for bridges in the lower road network, often designed for the lower load classes B/45 and maintained by a local government, the documentation is missing. The national road network, designed for load classes A/60 is maintained by the national government and faces the same problem but to a lesser extent. Bridges within this scope have different detailing rules and execution practices than used nowadays. Plain reinforcement was in general used which is bend-up at a support. Therefore, the study is twofold: first, Reverse Engineering is applied to determine the reinforcement of existing reinforced concrete slab bridges, second the capacity margin of RE bridges are examined with the current assessment codes.

A group of bridges with available documentation is Reverse Engineered by hand-calculations. The group includes rectangular slab bridges with and without edge beams. From the hand calculations it can be concluded that the main reinforcement can be Reverse Engineered without overestimating the capacity. However, the reinforcement in the edge beams is designed based on experience. The presumption is that the edge beams are designed for 100% of the permanent- and traffic loads from the mid-strip, but this should be further examined. The layout of the bend bars in the available technical drawings is only limited by the prescription from the former design code (GBV). The distribution in transverse reinforcement amounts is large and will not be further examined in this study. The restriction of a minimum transverse reinforcement of 20% of the main reinforcement is only recognised in former design.

A Reverse Engineering-tool is developed to automate the dimensioning of the required reinforcement according to the former design codes. This tool uses the year of design, load class and the geometric dimensions of the bridge as input parameters. A parametric study is performed to examine bridges from different design periods. Consequently, the Reverse Engineering-tool is used to assess the Reverse Engineered bridge according to the current assessment codes. The validation of the model shows for the majority of the Reverse Engineered bridges that the Reverse Engineered reinforcement is slightly less than the reinforcement amounts from the technical drawings. This proves a conservative approach where the actual structural capacity is underestimated. Consequently, an assessment of the Reverse Engineered bridge can be performed with sufficient robustness.

The uncertainty in the input parameters from the engineering factor, execution factor, design year and load class effects the structural capacity. The computer code ran with the input parameters having a normal distribution, showed the largest effect for the uncertainty in the design year and load class especially around 1940 and 1962. Therefore, the design year and load class are crucial in Reverse Engineering and assessment of an existing bridge.

The capacity margin of the Reverse Engineered bridges is assessed according to the current Eurocode based design codes. The traffic- and permanent load including load factors according to the general assessment codes from the NEN8700/NEN8701 and the RBK-1-1, and the decentralised load model from TNO are applied. The assessment with the Eurocode including the load factors from the NEN8700 showed Unity Checks for bending moment at the mid-supports and mid-spans of larger than 1.0, where the Unity Checks for shear forces resulted below 1.0, see Table 4.2. The assessment with the Decentralised load model showed Unity Checks for bending moment at the mid-supports and mid-spans and shear force below 1.0, see Table 4.2. In case the amount of support reinforcement is based on the amount of span reinforcement, the bending capacity margin at the mid-supports is insufficient for large spans.

Significant bending capacity margins are obtained in structural design of RC slab bridges in the period 1930-1970, see Figures 5.1 and 4.3. The main contribution of this research is that bridges designed between 1940



---

and 1962 show the most critical Unity Checks (load/capacity) for bending in the assessed period. In this period account the following design methods: The dynamic amplification factor (Section 2.4) introduced in the GBV1940 for concrete bridges, the traffic load class from the VOSB1933 (Section 2.3), the N-method (Section 2.2.3) to determine the cross-section capacity and the effective width method from the GBV1940 (Section 2.5) and from the Guyon Massonnet method (Section 2.5).

The capacity margin for shear is found to be almost independent of the design period, see figures 4.11. Here can be concluded that the slenderness of the bridge deck is the main contribution in the shear capacity.

Bridges designed in the period 1940-1962 with the support reinforcement based on the span reinforcement and with a span length >10m designed for load class B/45 (Figure 4.5), or with a span length of >11m designed for load class A/60 (Figure C.20), form the group with the most critical bending capacity. However, the size of the group of former bridges designed according to these conditions is unknown.

From the results can be concluded that bridges designed between 1940-1962 with RE reinforcement are found to be legally unsafe for bending according to the parametric assessment with the Eurocode.

# Contents

<b>Abstract</b>	<b>ii</b>
<b>Abbreviations</b>	<b>vi</b>
<b>List of Symbols</b>	<b>vii</b>
<b>1 Introduction</b>	<b>1</b>
1.1 Context . . . . .	1
1.2 Problem description . . . . .	1
1.3 Main goal . . . . .	2
1.4 Scope . . . . .	2
1.5 Thesis outline . . . . .	3
<b>2 Preliminary study</b>	<b>4</b>
2.1 State of the art . . . . .	4
2.2 Reinforced concrete slab bridges . . . . .	4
2.2.1 Classification of jargon. . . . .	5
2.2.2 Materials. . . . .	5
2.2.3 N-Method . . . . .	6
2.2.4 Crack method ('Breukmethode'). . . . .	8
2.2.5 Reinforcement . . . . .	12
2.3 Traffic load . . . . .	15
2.4 Dynamic amplification factor . . . . .	18
2.5 Concentrated load distribution . . . . .	18
2.5.1 Shear force distribution . . . . .	22
2.5.2 Loading in the longitudinal direction . . . . .	22
2.6 Force determination . . . . .	23
2.7 Former design changes . . . . .	23
2.8 Discussion . . . . .	24
<b>3 Reverse Engineering by hand calculations</b>	<b>25</b>
3.1 Introduction . . . . .	25
3.2 Uniformly distributed load . . . . .	25
3.3 Concentrated loads . . . . .	27
3.3.1 Edge beam . . . . .	28
3.3.2 Influence lines . . . . .	29
3.3.3 Shear force distribution of concentrated loading. . . . .	29
3.4 Reversed engineered bridges . . . . .	30
3.4.1 Bending capacity. . . . .	30
3.4.2 Actual reinforcement amounts. . . . .	31
3.5 Estimated required reinforcement . . . . .	32
3.6 Shear capacity . . . . .	34
3.7 Discussion . . . . .	36
3.8 Conclusion . . . . .	37
<b>4 Reverse Engineering and assessment by coding</b>	<b>38</b>
4.1 Introduction . . . . .	38
4.2 Assumptions . . . . .	39
4.3 Dimensioning of the main reinforcement. . . . .	40
4.4 Assessment for current traffic- and permanent loads . . . . .	41
4.4.1 Load reduction factors . . . . .	41
4.4.2 Reliability of existing bridges. . . . .	41

4.4.3	Crack width and Fatigue . . . . .	42
4.4.4	Current material properties . . . . .	42
4.5	Current capacity based on assessment codes . . . . .	42
4.5.1	Bending moment capacity . . . . .	42
4.5.2	Shear Capacity . . . . .	43
4.6	Reinforcement amounts based on former- and current structural design . . . . .	43
4.6.1	Span reinforcement . . . . .	44
4.6.2	Support reinforcement. . . . .	45
4.6.3	reinforcement difference ratio support/span . . . . .	46
4.7	Decentralised traffic load model . . . . .	46
4.8	Shear control . . . . .	48
4.9	Summary of the results . . . . .	50
4.10	Validation . . . . .	50
4.11	Limitations of the computer code. . . . .	51
4.12	Discussion . . . . .	51
<b>5</b>	<b>Sensitivity Analysis</b>	<b>53</b>
5.1	Introduction . . . . .	53
5.2	Sensitivity analysis . . . . .	55
5.3	Prioritisation of existing RC slab bridges for current traffic loading . . . . .	58
5.3.1	Risk quantified. . . . .	58
5.3.2	Possible extra capacity . . . . .	59
5.3.3	Possible reduced loading. . . . .	59
<b>6</b>	<b>Conclusion</b>	<b>60</b>
<b>7</b>	<b>Recommendations</b>	<b>62</b>
7.1	Recommendations for Reverse Engineering. . . . .	62
7.2	Recommendations for future research . . . . .	62
	<b>Bibliography</b>	<b>64</b>
	<b>List of Figures</b>	<b>66</b>
	<b>List of Tables</b>	<b>71</b>
<b>A</b>	<b>Appendix - Chapter 2: Literature</b>	<b>72</b>
A.1	Cross-sectional forces and stresses . . . . .	72
A.2	Crack width control. . . . .	74
<b>B</b>	<b>Appendix - Chapter 3: Reverse Engineering</b>	<b>79</b>
B.1	Force lines . . . . .	81
B.2	Shear force . . . . .	83
<b>C</b>	<b>Appendix - Chapter 4: Reverse Engineering</b>	<b>86</b>
C.1	Parametric geometry . . . . .	86
C.2	Assumption . . . . .	86
C.3	Reinforcement table . . . . .	91
C.4	Effective width . . . . .	91
C.5	Required reinforcement amounts and reinforcement ratio . . . . .	93
C.6	Assessment . . . . .	95
C.7	How accurate is the computer code? . . . . .	99
<b>D</b>	<b>Appendix - Chapter 5: Risk Analysis</b>	<b>101</b>
D.1	Geometrical uncertainties . . . . .	101
D.2	Reliability Methods . . . . .	105
D.3	Protocol. . . . .	105

# Abbreviations

API	Application programming interface
ASD	Allowable stress design
CC	Consequence class
DAF	Dynamic amplification factor
DC load model	Decentralised load model
EC	Eurocode
FEA	Finite element analysis
GBV	Gewapend Beton Voorschriften
GUI	Grafical user interface
L1	Length of an end-span
L2	Length of a mid-span
LRFD	Load and Resistance Factor Design
ODE	Ordinary differential equation
OSI	Open systems interconnection
RC	Reinforced concrete
RE	Reverse Engineering (or conjugated)
RHDHV	Royal HaskoningDHV
SAM	Steel area method
TS	Design Tandem
UDL	Uniformly distributed load
UC	Unity Check
ULS	Ultimate limit state
VB	Voorschriften Beton
VOSB	Voorschriften voor het Ontwerpen van Stalen Bruggen

# List of Symbols

The list of symbols shows both the current classification of symbols from the Eurocode and the former classification of symbols from the GBV code. However, for some cases either the current or former symbol is applicable. The symbols used in this thesis are divided below in Latin symbols and Greek symbols:

## Latin Symbols

Current	Former	Explanation
	$a$	longitudinal reinforcement spacing
	$a_1$	distance between bend main reinforcement
$A_c$	$F_b$	product of the height and the width of the slab or beam
$A_s$	$A$	area of the reinforcing steel in tension
	$A'$	area of the reinforcing steel in compression
$b$	$b$	element width
$b_1^*$		fictitious slab width
$B_{eff}$	$B$	effective slab width
$c_{nom}$	$c$	nominal concrete cover
$C$	$K$	concrete quality
$d$	$h$	effective height of the cross-section
	$d_s$	distance between the centre of an outer rebar to the nearest concrete edge
$e$	$e$	edge distance
$EI$	$EI$	bending stiffness
$\frac{EI}{b}$	$\rho_{xx}$	flexural rigidity per unit width
$E_c$	$E_b$	young's modulus of concrete
$E_s$	$E_a$	young's modulus of the reinforcing steel
$f_{yd}$		design strength of reinforcement steel
$GJ$	$\alpha$	torsional rigidity per unit width
$\frac{GJ}{b}$	$\gamma_{xy} = \gamma_{yx}$	average torsional stiffness
$h$	$h_t$	total element depth
$I_t$	$I$	moment of inertia of the total deck cross-section
$K_\alpha$	$K_\alpha$	principal coefficient of lateral distribution
$k_{cap}$		massive slab coefficient
$l_t$	$\Delta l$	crack distance
$l_{bd}$	$l_d$	anchorage length
$M$	$M$	bending moment
$M_{rep}$	$M_u$	bending moment at cracking
$M_{xx}$	$M_{l1}$	bending moment in the longitudinal direction
$M_{yy}$	$M_{l2}$	bending moment in the transverse direction
$M_{rd}$	$M$	resisting bending moment
	$\bar{N}'_b$	allowable concrete compression force
$N_{cu}$	$N'_{bu}$	ultimate concrete compression force
	$\bar{N}_a$	allowable steel tensile force
$F_{su}$	$N_{au}$	ultimate steel tensile force
$S$	$QR$	steel quality (hot rolled)
$C$	$QR_{(n)}$	steel quality (cold formed)
$r$	$r$	sattler coefficient
$V$	$T$ or $D$	shear force
$V_{Rd,c}$	$\rho$ or $\bar{\sigma}_b$	shear force resistance without reinforcement
$V_{Rd}$	$\rho$ or $\bar{\sigma}_{bmax}$	shear force resistance with stirrup reinforcement
$w_{max}$	$w_{max}$	maximum expected crack width
$x_u$	$X$	distance until the neutral axis in ULS
$\frac{5}{8}x$	$k_z$	distance resulting compressive force and the neutral axis
$z$	$z$	lever arm of the cross-sectional forces

## Greek Symbols

Current	Former	Explanation
$\alpha_e = \frac{E_s}{E_{cm}}$	$n = \frac{E_a}{E_b}$	ratio between the Young's moduli of steel and concrete
$\alpha_{trend}$		trend reduction factor
$\beta$		reliability index
$\epsilon_c$	$\epsilon'_b$	strain of concrete in compression
$\epsilon_s$	$\epsilon_a$	specific elongation of the rebar
$\epsilon_{cu}$	$\epsilon'_u$	maximum strain at cracking of the concrete
	$\gamma$	safety factor
$\gamma_c$		partial factor for concrete
$\gamma_s$		partial factor for steel
$\gamma_{Gj,sup}$		load factor for permanent loading
$\gamma_{Q,1}$		load factor for traffic loading
$\phi$	$\phi$	rebar diameter
	$\phi_k$	nominal diameter of ribbed reinforcement bars
$\Phi$	S	dynamic amplification factor
$\psi$		transient load factor
$\rho_l$		reinforcement ratio for the main reinforcement
$\tau$	$\sigma_b$	shear stress of the concrete
	$\sigma_{bmax}$	allowable shear stress of the concrete including stirrup reinforcement
	$\sigma'_b$	allowable compressive stress of the concrete
	$\sigma'_a$	allowable tensile stress of the reinforcing steel
	$\sigma_e$	the yield strength or 0.2 strain limit of steel divided by the safety factor ( $\gamma$ )
	$\sigma'_u$	maximum compressive stress in concrete in the cracked situation, which is equal to 0,6 times the cube strength
	$\Sigma \phi$	sum of the rebar diameters
$\tau_{bm}$	$\tau_d$	bond stress along the anchorage length
$\tau_{bd}$	$\bar{\tau}_d$	allowable bond stress along the anchorage length
$\theta$		angular rotation
	$\theta$	flexural stiffness
	$\omega_0$	tensile reinforcement in percentage of the effective cross-section
	$\omega'_0$	compression reinforcement in percentage of the effective cross-section



# Introduction

## 1.1. Context

In the Netherlands, the first reinforced concrete (RC) slab bridges were constructed at the beginning of the twentieth century. A combination of concrete and steel was used to construct the bridges, by commonly resisting the loads on the bridge. The first RC bridges were not designed according to a prescribed code, because no prescribed regulation existed at that time.

The first developed design code for RC structures in the Netherlands is the GBV1912 ('Gewapend Beton Voorschriften') published by Koninklijk Instituut van Ingenieurs (1912). The code prescribed standards for material qualities, execution methods, calculations and the design of RC. After every period of approximately ten years, a new version of the code was published including increased knowledge in mechanics, material properties and practical experiences. The Ministry responsible for the infrastructure (Directie van Waterstaat (1933)) published in 1933 the VOSB ('Voorschriften Ontwerpen Stalen Bruggen') design codes for steel bridges in addition to the GBV. In the VOSB1933 the imposed load determination for bridges is prescribed.

Bridges are categorised based on their type of loading in the VOSB. Three options were described: railway and tram loading and loading by normal traffic. In the VOSB, bridges designed for normal traffic are categorised for a specific load class depending on the destination in the road network. The first load classification was from A to D, where load class A is the load class for bridges in the national road network, where redirection of traffic is impossible. Load class B is the load class for bridges in the national road network, where accidentally very heavy traffic will pass. Load class C is not intended for heavy traffic and load class D only intended for light traffic such as pedestrians.

The government is the administrator of the national road network including the larger and the heavily loaded bridges. The municipalities are the administrator of the underlying road network including the bridges with a smaller span length of often <20m. At the beginning of the 1960s, the load classification has been adjusted to the change in traffic intensity and magnitude, leading to a different notation of load classes. In the VOSB1963, the classes are notated with a number and can be coincided with the previous notation. Load class 60 corresponds to load class A, load class 45 corresponds to load class B and load class 30 corresponds to load class C. A lighter load class than 30 is omitted since the VOSB1963.

Research from Mulder (2015) on behalf of the association 'Bouwend Nederland' shows as a result of their survey on bridges of municipalities, that most of the administration is not according to the standards. For example for a significant amount of RC bridges, the construction year, the former load class and the capacity are unknown. In more than half of the instances, maintenance assessment of the bridges scores 'moderate' to 'poor'. By estimation, only one-third of the former calculations and present reinforcement layout is known.

## 1.2. Problem description

Most bridges in the Dutch infrastructure networks are built before 1985 and are ageing. The traffic intensity, as well as the axle, and the average vehicle weight have increased since these structures were opened to traffic. On the other hand, the structural (design) codes have changed over the years. Therefore, there is a need to investigate if existing structures meet the safety/reliability level described by the current codes (Vergoossen, 2015).

The increase in traffic is also reflected in the higher (representative) traffic load model regarding the former codes. One of the changes is that in the current code there is hardly a difference between the traffic load for bridges in main roads like motorways and bridges in smaller roads like residential areas. In the design codes

up to the start of this century, there was a huge difference between the load level of bridges in main roads and the bridges in minor roads. This difference has been partly changed with a new traffic load model for bridges with span length up to 20 m, for roads with a maximum number of 125.000 trucks per lane per year. On the other hand, old(er) structures are designed with other materials and with different theory and formulae for their (ultimate) capacity. Also detailing rules and execution practice are different. For instance, in structures with plain reinforcement bars are bend-up and anchored by a hook. When those structures are recalculated with current design formulae this will result in a divergent capacity depending on the material properties. A frequently faced problem in practice is that the original design calculations and technical drawings of a large percentage of the existing bridge stock are unknown or lost. This is especially the case for bridges in the lower road network which are often designed for the lower load classes B/45 and maintained by a local government. Both phenomena result in the question if the current structural safety of those structures meets the requirement of the current assessment codes.

### 1.3. Main goal

This thesis aims to RE existing planless RC slab bridges and assess the structural safety of RE RC slab bridges, by addressing the following research question and subquestions:

*How can the main reinforcement of existing reinforced concrete slab bridges constructed with plain reinforcement be estimated, and what is the margin in structural capacity of the reverse engineered bridges according to the current assessment codes?*

- *In which topics does concrete structural bridge design differ according to the former design codes?*
- *How does the residual capacity of existing RC slab bridges constructed with plain reinforcement relate to the current traffic loading?*
- *What are the influences of the engineering factor and the execution factor on the Unity Checks of the reverse engineering method?*

The first subquestion studies former bridge design and is elaborated in Chapter 2. The second subquestion asks for capacity and load calculations and is executed in Chapters 3 and 4. The third subquestion examines the uncertainty in the method and is examined in Chapter 5.

### 1.4. Scope

This thesis will seek to Reverse Engineer (RE) RC slab bridges in minor roads constructed with plain reinforcement bars, mostly in possession of- or managed by a local government (province or municipality). An example of such a bridge can be seen on the front page of this report. This bridge was located between Amsterdam and Utrecht and crossed the former Rijksweg 2 but got demolished in order to realise the new A2 motorway. Furthermore, RC slab bridges designed by the GBV 1912/1918/1930/1940/1950/1962 and VOSB 1933/1938/1963 are assessed. The RE of the reinforcement and the validation of this process are executed with former load traffic classes A/B/C respectively 60/45/30, after which the current capacity of the existing bridge deck with former load traffic class B/C resp. 45/30 is assessed for current load models, in the ultimate limit state (ULS). The scope of this research limits itself to bridges with an intersection angle of minimal 80 gon ( $\approx 72^\circ$ ). Bridges with a larger skewness deviate in force transfer compared to bridges with a small or negligible skewness. Only rectangular deck cross-section and rectangular deck cross-sections with edge beams are included.

The scope of this thesis is a subsection of a larger goal in the assessment of existing structures. This larger goal aims to automatically assess any type of concrete bridge. This goal is prescribed by the following method: By scanning the geometry of existing concrete bridges, 3D-plots of the geometry can be obtained. Here minimal hindrance of traffic flow is caused. The geometry functions as input for a finite element computer model, where also the design year and traffic load class need to be inserted. In this computer model, the current capacity and current loading shall be estimated with assessment codes. This method needs to provide for an

automated assessment of existing concrete bridges.

## **1.5. Thesis outline**

In Chapter 2 a preliminary study towards the design and design codes of existing RC slab bridges is performed. Chapter 3 consists of RE by hand-calculations to get acquainted with former structural design. A sub-conclusion towards the scope for modelling of a RE-tool is made at the end of the chapter. Chapter 4 details the method and results of the RE tool, where the RE tool is validated by comparing the RE reinforcement with known reinforcement amounts from practical examples. In Chapter 5, the uncertainty in the RE process is examined and evaluated. In Chapter 6, conclusions are drawn regarding RE of existing RC slab bridges, their structural safety and their governing failure mode. Finally, recommendations are proposed for further research and the development in RE of existing structures. Several discussions are included throughout the report, at the end of a chapter. References to figures and tables in the Appendix are written in the text by the abbreviation of the appendix following with a number.

# 2

## Preliminary study

### 2.1. State of the art

Bouwend Nederland, an association of companies in the building- and infra industry collected information about maintenance and structural safety of bridges owned by municipalities in the Netherlands. The surveyed by Mulder (2015), 34% of the 403 contacted municipalities replied on the request, of which 69% are in possession of an actual overview of their bridges. Around 28% of the concrete bridges are built before 1970. Notable is that from 15% of the concrete bridges the design- or construction year is unknown. Actual numbers of bridges without plans are unknown but it is estimated that municipalities have around one-third of the plans of existing bridges in their possession.

A questionnaire regarding load rating procedures for bridges without plans in the United States by Cuaron et al. (2016) led to a response of thirty-three states. The survey showed that sixteen states own each more than a hundred concrete bridges without plans.

The state of the art of technical knowledge of existing RC slab bridges should be searched for internationally. For any bridge owner around the world responsible for the management and maintenance of existing bridges, problems occur in the administration of plans. Especially bridges designed before the appearance of the computer and before the possibility of digitally saving of documents have missing calculation reports and/or technical drawings. This makes the preservation of existing structures an internationally shared problem.

Several methods are known to rate bridges without plans. A widely used method is load testing of bridges in combination with theoretical analysis, to obtain the performance and capacity of the bridge.

A method proposed by Harris et al. (2015), uses results of load ratings derived from the entire batch of bridges in the Virginia Department Of Transportation. The relationship between various characteristics of a bridge with available plans can be extracted. These relationships are then used for predicting the load ratings for bridges without plans.

In this research, a method is proposed by RE RC slab bridges based on the former design codes and the available information. Limited research has been done to evaluate planless concrete bridges without the use of load testing, according to Cuaron et al. (2016). Likewise, the increase in traffic intensity leads to the question from Dieteren (2012): 'How to practically assess bridges designed for load class 45/30 resp. B/C'.

The research starts with a literature study to the former design codes and clarifies the development of knowledge along these codes. The first subquestion can be answered at the end of this chapter: In which topics does concrete structural bridge design differ according to the former design codes?

### 2.2. Reinforced concrete slab bridges

The RC slab bridge is a common design for a single or multiple span bridge since the beginning of the twentieth century, see the example in Figure 2.1. In former design, these type of structures are schematised with beam elements as is illustrated in Figure 2.2. The first design code for RC structures is the GBV, where after the VOSB codes were published for steel bridges including imposed traffic loading. Bridges are designed for load class A/60 in case the bridge is part of a national road, and load class B/45 in case the bridge is part of a lower network. Multiple span bridges often have a continuous deck structure leading to a statically indeterminate structure. The maximum mid-span length (L2) for this type of bridge is around 20m, where the end-spans (L1) often have a maximum length of  $0.8 \cdot$  mid-span length. These bridges often carry a maximum of two

traffic lanes in each driving direction. RC slab bridges are always constructed on-site. The construction on the building site is labour intensive using raw materials as reinforcement and concrete. Technical drawings guide the construction of the geometry and the location, numbers and size of reinforcement bars. Bending schedules and cut schedules prescribe the measures for the individual reinforcement bars. Scaffolding and formwork need to be made on-site to cast the concrete slab. These on-site activities make it a labour-intensive construction method. The massive structure leads to a design with a high self-weight compared to the imposed loads acting on the bridge. An important advantage of this bridge type is its low maintenance costs. Since the rise of the prefabrication industry from the seventies is this type of bridge fewer consulted due to the drive delays.



Figure 2.1: Example of a multiple span RC slab bridge, located in Delft constructed in the 1960s, from Google (nd).

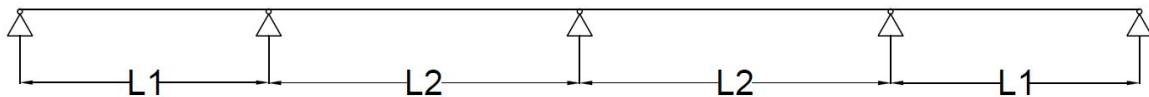


Figure 2.2: Mechanical scheme of a four-span bridge with a continuous beam and end-spans (L1) and mid-spans (L2). The triangles schematise the supports.

### 2.2.1. Classification of jargon

Classification of jargon in civil engineering started with the publication of the first design codes. Symbols are used in civil engineering to communicate and detail the characteristics of an engineering drawing. The classification of symbols has developed through the different design codes. French influence in the early classification of the symbols can be obtained from the GBV codes. The subscript *b* stands for 'béton' which is French for concrete and the *a* stands for 'acier' which is French for steel. In the list of symbols is both the current classification of symbols from the Eurocode and the former classification of symbols from the GBV code obtained.

### 2.2.2. Materials

In the publication of the GBV code, a standard set for construction material contents and properties is prescribed. Through the years the development of construction material properties is expanded, with requirements towards the allowable stress and strain relations. Figure 2.3 shows the development of the strength increment of reinforcement steel and concrete. Plain reinforcement is prescribed to be executed with a steel strength of maximum QR32. However, in practice steel qualities of maximum QR24 are applied (Gantvoort, 1964), so the hatched area in Figure 2.3 indicates plain reinforcement. Higher steel qualities from QR40 are in

general performed with ribbed reinforcement bars. The most applied reinforcement until the 1970's is plain reinforcement with steel quality QR24, see Figure 2.1. The concrete quality is classified with a  $K$ -value, which is the ultimate compressive strength in  $\text{kgf}/\text{cm}^2$ .

Table 2.1: Share in the application of steel qualities from Gantvoort (1964).

Steel type	year		
	1961	1962	1963
high quality steel (>QR24)	19%	24%	28%
QR24	81%	76%	72%

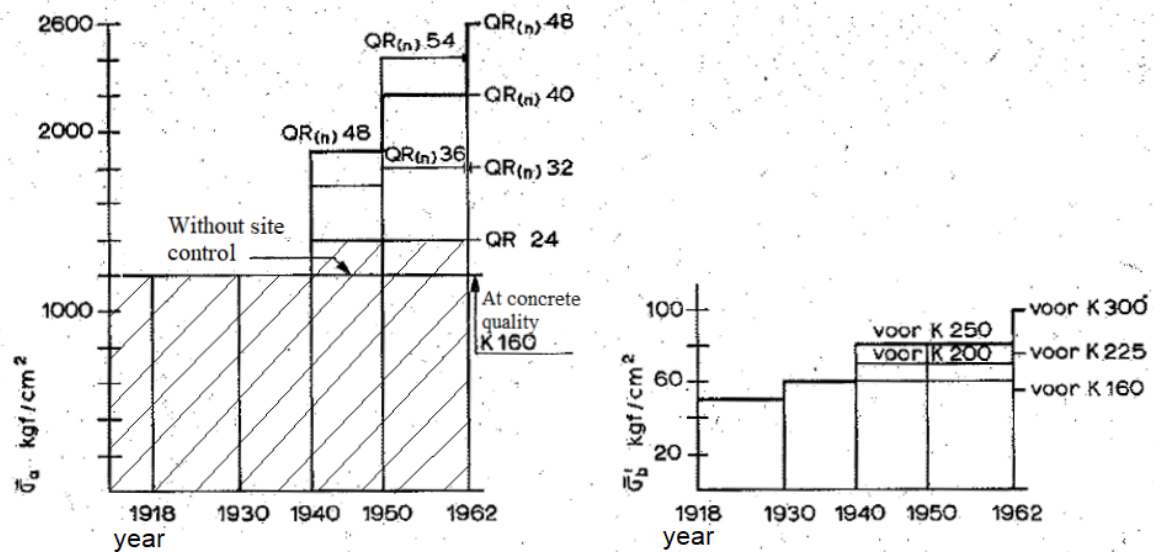


Figure 2.3: Left: development of reinforcing steel, right: development of concrete, from Gantvoort (1964).

### Allowable stresses

The GBV prescribes allowable stresses for concrete and steel for different loading cases. The allowable stresses have a safety function at the capacity side of the construction, leading to an allowable stress design (ASD). Before the GBV1940 allowable stresses for concrete and steel are prescribed based on construction type and loading, and by a ratio ( $n$ ) between the maximum modulus of elasticity of steel and concrete. The GBV 1940 and GBV 1950 use the prerequisite for a site control executed by the engineer, which may lead to higher allowable material stresses. Larger stresses are permitted for concrete in compression and bending, and larger tensile stresses are permitted for reinforcing steel in bending (or in combination with normal force). Larger shear stresses with or without stirrups are permitted. The GBV 1962 expanded the code by depending the allowable steel stresses on the used concrete quality in the particular cross-section. Table 2.2 gives an overview of the allowable stresses according to the GBV1962 for two different load types. where the top bar indicates the allowable stress, the apostrophe the compression stress and without a apostrophe the tensile stress. 10  $\text{kgf}/\text{cm}^2$  is equal to approximately 1MPa.

In case of slabs with a  $h_t \geq 25$  cm and  $b \geq 4 \cdot h_t$ , the allowable concrete compression stresses in bending may be increased with 10  $\text{kgf}/\text{cm}^2$  ( $\approx$  1MPa). In case of slabs with a  $h_t \geq 15$  cm and  $b \geq 4 \cdot h_t$ , the allowable steel tensile stresses in bending may be increased with 100  $\text{kgf}/\text{cm}^2$  ( $\approx$  10MPa). This is only valid for steel types with a yield limit ( $\sigma_e$ ) or an 0.2 strain limit of the steel  $\leq 4000$   $\text{kgf}/\text{cm}^2$  ( $\approx$  400MPa).

### 2.2.3. N-Method

The N-Method is the first developed method to determine the capacity of RC cross-section since the publication of the first GBV code. In a cross-section check, a global safety is encountered by allowable material stresses. Load factors are not taken into account in an allowable stress design. The N-method includes the



Table 2.2: Allowable stresses according to the GBV1962.

Load type	Type of stress	Allowable stress in kgf/cm <sup>2</sup>		
		K 160	K 225	K 300
<i>Bending</i>				
For concrete	$\bar{\sigma}'_b$	55	75	100
For steel types:				
QR 22	$\bar{\sigma}_a \bar{\sigma}'_a$	1200	1300	1300
QR 24	$\bar{\sigma}_a \bar{\sigma}'_a$	1200	1400	1400
QR 32 and QRn 32	$\bar{\sigma}_a \bar{\sigma}'_a$	1200	1800	1800
QR 40 and QRn 40	$\bar{\sigma}_a \bar{\sigma}'_a$	1200	2200	2200
QR 48 and QRn 48	$\bar{\sigma}_a \bar{\sigma}'_a$	1200	2600	2600
<i>Shear force</i>				
Without reinforcement	$\bar{\sigma}_b$	6	7	8
With reinforcement	$\bar{\sigma}_b$	14	17	20

allowable stresses  $\bar{\sigma}'_b$  and  $\bar{\sigma}_a$ , and a ratio ( $n$ ) between the Young's moduli of steel ( $E_s$ ) and concrete ( $E_c$ ). Three basic rules apply for the N-Method: First, the tensile forces are solely sustained by the reinforcing steel. Second, the strain relation is linear for the full cross-section, intersecting the neutral axis. Third, the N-method assumes a proportionate relation of the stresses and shape changes, based on Hooke's law. A linear stress-strain relationship with the allowable stress for steel in tension and concrete in compression are prescribed in the former GBV codes. For the different load methods: (ex)central compression, bending, shear, torsion or the combination of shear and torsion, allowable stress limits are present in the GBV codes. In Figure 2.4 the assumed linear stress and strain relations are drawn for a cross-section loaded in bending. The N-method corresponds with the steel area method (SAM) developed by Shenton et al. (2007) and is reviewed in this section. An alternative procedure to determine the internal bending moment capacity with the material strain as input can be found in Appendix A.1.

Below, the described variables to derive horizontal force equilibrium and the bending moment resistance of the cross-section are presented:

- $h$  = distance between the top of the beam and the reinforcing steel;
- $h_t$  = total depth;
- $X$  = distance of the top of the element and the neutral axis;
- $Z$  = distance between the resulting concrete force  $N'_b$  and the steel tensile force  $N'_a$ ;
- $b$  = element width;
- $c$  = concrete cover;
- $\phi$  = rebar diameter;
- $E_c$  = Young's modulus of concrete;
- $E_s$  = Young's modulus of the reinforcing steel;
- $A_s$  = area of the reinforcing rebar;
- $n = \frac{E_a}{E_b}$  (of a maximum of 15);
- $\sigma'_b$  = allowable compressive stress of the concrete;
- $\sigma_a$  = allowable tensile stresses of the reinforcing steel;
- $\epsilon_b$  = strain of concrete at the top fibre;
- $\epsilon_a$  = tensile strain of rebar.

The resulting concrete compressive force:

$$N'_b = 0.5\sigma'_b bX \quad (2.1)$$

The resulting tensile force in the reinforcing steel is:

$$N_a = A_s\sigma_a \quad (2.2)$$

Horizontal force equilibrium

$$N_a = N'_b \rightarrow 0.5\sigma'_b bX = A_s\sigma_a \quad (2.3)$$

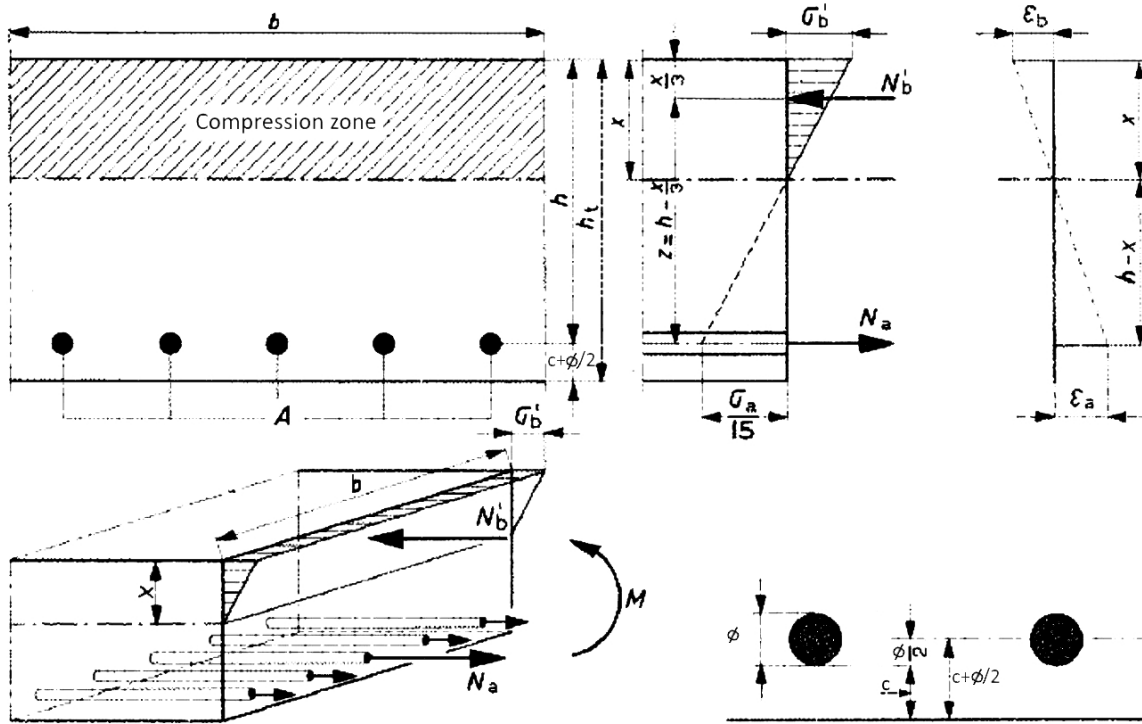


Figure 2.4: The N-Method applied to a cross-section (top-left) with linear stress relation (top-middle) and strain relation (top-right), a 3D cross-section with internal forces and external moment of a slab (bottom-left) and detailing of reinforcement (bottom-right), from Vergoossen (2019).

Required reinforcement

$$A_s = \frac{\sigma'_b}{\sigma_a} \frac{bX}{2} \quad (2.4)$$

Bending moment resistance of the cross-section

$$M = N'_b \cdot z = 0.5\sigma'_b bX \cdot \left(h - \frac{X}{3}\right) \quad \text{or} \quad M = N_a \cdot z = A_s \sigma_a \cdot z \quad (2.5)$$

#### 2.2.4. Crack method ('Breukmethode')

In the GBV1962, the crack method was developed as an alternative for the N-method. The method uses the capacity of the structure at the moment of failure as a starting point. Here a safety factor of  $\gamma=1.8$  is included at the load side of the calculation method. For a structural element solely loaded in bending the calculated cracking moment capacity is described by the following:

$$M_u \geq \gamma M \quad (2.6)$$

In case the yield limit or the 0.2 strain limit of the steel is  $\leq 4000 \text{ kgf/cm}^2$  ( $\approx 400\text{MPa}$ ), the safety factor  $\gamma$  can be reduced with 0.08. This yield limit corresponds with a maximum steel reinforcement quality of QR40.

In the crack method, the concrete stress  $\sigma'_b$  has a parabolic course, see Figure 2.5 and 2.6. The maximum concrete strain  $\epsilon'_u$  is equal to 3.5 ‰ and the maximum concrete compression stress  $\sigma'_u$  is 0.6 times the cubic strength. The strain in steel and concrete have a linear behaviour when loaded in bending. The second-order equation to describe the parabolic shape of the stress/strain behaviour is given in equation 2.7.

$$\sigma'_b = \sigma'_u \cdot \left(1 - \left(1 - \frac{\epsilon_b}{\epsilon'_u}\right)^2\right) \quad (2.7)$$

Below, the required variables to derive the horizontal force equilibrium and the bending moment resistance of the cross-section are:

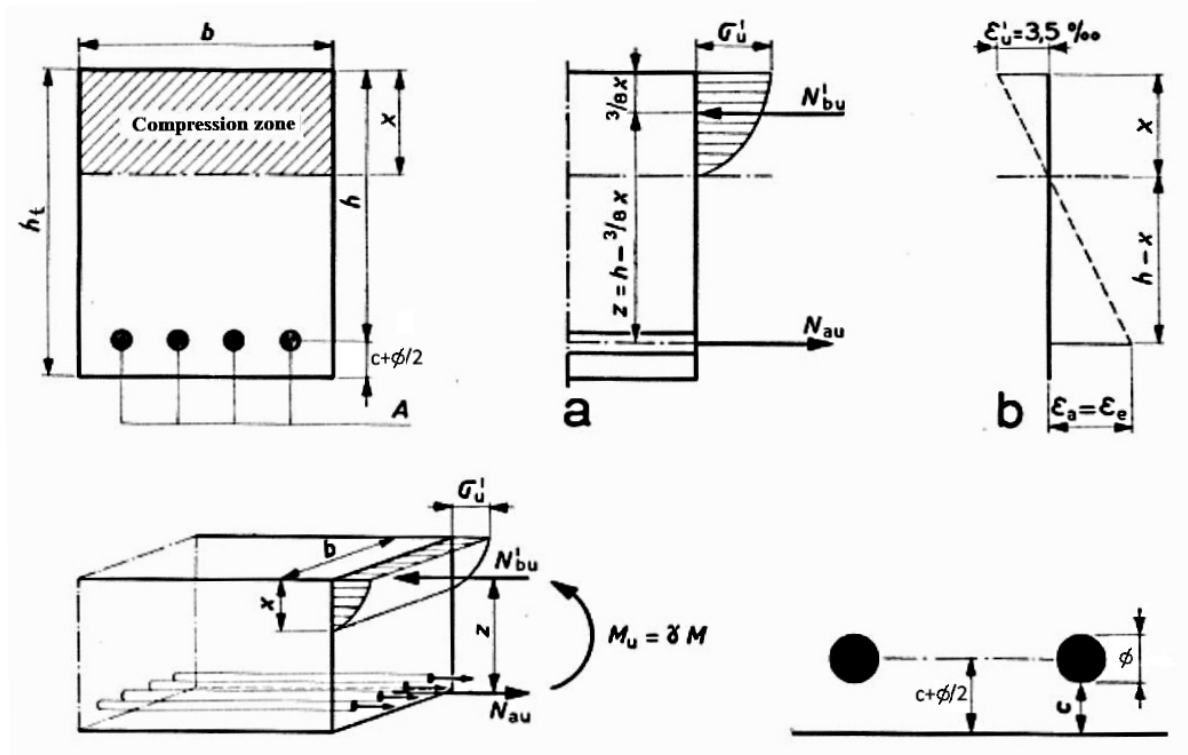


Figure 2.5: The crack method ('Breukmethode') applied to a cross-section (top-left) with parabolic stress relation (top-middle) and linear strain relation (top-right), a 3D cross-section with internal forces of a slab (bottom-left) and detailing of reinforcement (bottom-right), from Franx (1962)

$N'_{bu}$  = ultimate concrete compression force;

$N_{au}$  = ultimate steel tensile force;

$M_u$  = ultimate bending moment at cracking;

$\gamma$  = safety factor;

$\sigma'_u$  = maximum compressive stress in concrete in the cracked situation, which is equal to 0,6 times the cube strength;

$\epsilon'_u$  = maximum strain at cracking of the concrete.

The relation between the steel stress  $\sigma_a$  and the steel strain  $\epsilon_a$  is schematised by a bi-linear function, see Figure 2.6. The first part is starting in the origin and has a slope determined by the modulus of elasticity. The second is a line parallel to the  $\epsilon'_a$ -axis and is determined by the yield line of the material or by the 0.2 strain limit defined in the code. In Figure 2.5 is the parabolic stress course drawn of the concrete in the compression zone.

A construction part solely loaded in bending determined according to the crack-method is explained with the following calculation procedure.

The resulting concrete compressive force:

$$N'_{bu} = 0.67\sigma'_u bX = 0.67 \cdot 0.6KbX \quad \text{Where K is the ultimate concrete cube strength} \quad (2.8)$$

The resulting tensile force in the reinforcing steel is:

$$N_a = A_s \sigma_a = A_s E_a \epsilon_a \quad (2.9)$$

Horizontal force equilibrium

$$N_a = N'_{bu} \rightarrow A_s \sigma_a = 0.67 \cdot 0.6KbX \quad (2.10)$$

Required reinforcement

$$A_s = \frac{0.67 \cdot 0.6KbX}{\sigma_a} \quad (2.11)$$

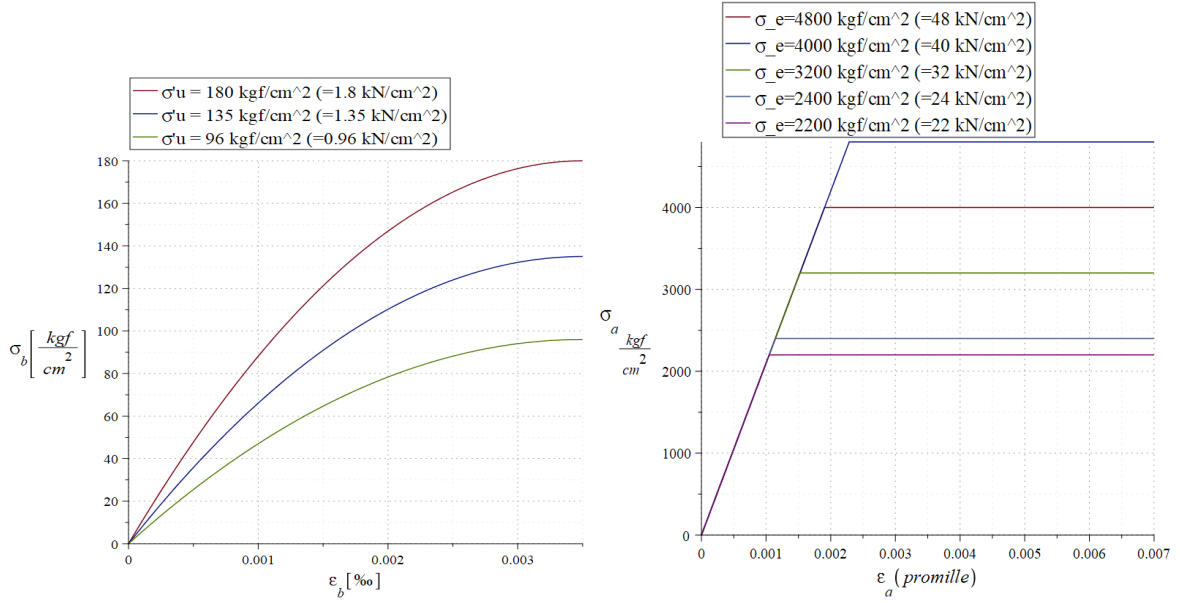


Figure 2.6: The concrete stress/strain relation of the Crack method (left) and the steel stress/strain behaviour in the Crack method ('Breukmethode') (right).

### Bending moment resistance of the cross-section

$$M = N'_b \cdot z = 0.67 \cdot 0.6 K b X \cdot \left(h - \frac{3}{8} X\right) \quad \text{or} \quad M = N_a \cdot z = A_s \sigma_a \cdot z \quad (2.12)$$

$$M_u = \gamma * M \quad (2.13)$$

The height of the concrete compression zone ( $X$ ) cannot be larger than  $0.525h$  in case of a rectangular cross-section. This means that the maximum contribution of tensile reinforcement is determined by:

$$(\omega_0 - \omega'_0) \frac{\sigma_e}{\sigma'_u} \leq 35 \quad (2.14)$$

Where:

$\omega_0$  = the tensile reinforcement in percentage of the effective cross-section, in case of a beam or a plate:

$$\omega_0 = \frac{100 A}{b h} \quad \text{or} \quad \omega_0 = \frac{100 A}{a h}; (n = 1) \quad (2.15)$$

For plates:  $a$  = the bar spacing, so the number of bars ( $n$ ) = 1.

$\omega'_0$  = the compressive reinforcement in percentage of the effective cross-section:

$$\omega'_0 = \frac{100 A'}{b h} \quad (2.16)$$

$\sigma_e$  = the yield strength or 0.2 strain limit of steel.

The required reinforcement ratio ( $\omega_0$ ) can be determined based on the effective bending stress, where the  $k_z$  depends on the concrete compression zone ( $X$ ). The following equation is obtained for internal stress equilibrium:

$$\frac{M_u}{b h^2} = \frac{\omega_0 k_z \sigma_e}{1.8} \quad (2.17)$$

Where:

$$k_z = 1 - \beta X = 1 - \frac{3}{8} X \quad (2.18)$$

$$\omega_0 = 100 \cdot 0.67 \frac{\sigma'_u}{\sigma_e} X \quad (2.19)$$

**Crack width**

In the GBV1962 a limitation is set for the maximum allowed crack width due to imposed loading and self-weight of the structure. The crack width limit is introduced to maintain the durability of the structure along its lifespan. Concrete structures exposed to weather or in connection with soil and water have a crack limit of  $\bar{w} = 0.25\text{mm}$ . Concrete structures exposed to an aggressive environment have a crack limit of  $\bar{w} = 0.20\text{mm}$ . It is allowed for beams and slabs to calculate the largest expected crack width for bending, in case of plain rebars:

$$w_{max} = 0.5\sigma_a \cdot \Delta l \cdot 10^{-6} \text{ cm} \quad (2.20)$$

Or, with the application of prismatic ribbed reinforcement steel:

$$w_{max} = \left[ 0.5\sigma_a \cdot \Delta l - 16 \frac{(\Delta l)^2}{\phi_K} \right] \cdot 10^{-6} \text{ cm} \quad (2.21)$$

Where:

$\bar{\sigma}_a$  = the allowable tensile stress of the reinforcing steel in  $\text{kN}/\text{cm}^2$ . In case of the appliance of the crack method:  $\bar{\sigma}_a = \sigma_e / \gamma$  (the yield strength or 0.2 strain limit of steel divided by the safety factor).

$\Delta l$  = the crack distance in cm:

$$\Delta l = (d_s + 0.3 \cdot \Sigma \phi) \left( 1 + 3 \sqrt{\frac{1}{n \cdot \omega_0}} \right) \quad (2.22)$$

Where:

$d_s$  = the distance between the centre of an outer rebar to the nearest concrete edge;

$\Sigma \phi$  = the sum of all rebar diameters;

$\omega_0$  = as in equation 2.15.

$n$  = the number of rebars per meter slab width.

When the rebar distances and/or rebar diameters are unequal in case of slabs, an average value may be calculated for  $\omega_0$ ,  $\phi$  and  $a$ .

For practical examples of the configuration of bar diameter and bar spacing is the crack width determined with the equations 2.22. Section A.2 elaborates about determined crack widths for different steel qualities QR24 and QR40. The crack limit is set to 0.25 mm advised by the GBV codes, which leads to fulfilling the crack width requirement in case steel quality QR24 is used. This means that former design of RC slab bridges with plain reinforcement where always the steel qualities of QR24 or QR22 is used, is not limited by the crack width limitation. Bridge design with higher steel qualities ( $>QR24$ ) results in a design where crack width can be governing for the dimensioning of reinforcement, as is shown in example two in section A.2.

**Difference between the N-method and Crack-method**

The difference between the required reinforcement amounts according to the N-method and crack-method can be calculated with the following assumption: the steel quality can vary between the low quality of QR22/24 for plain reinforcement and the high quality of  $\geq QR40$  for ribbed reinforcement. The difference between the N-method and crack-method is examined for two steel qualities; QR24 with ultimate stress of  $2400 \text{ kg}/\text{cm}^2$  and allowable stress of  $1400 \text{ kg}/\text{cm}^2$  and QR40 with ultimate stress of  $4000 \text{ kg}/\text{cm}^2$  and allowable stress of  $2200 \text{ kg}/\text{cm}^2$ . For a concrete quality of K300 ( $\sigma_b = 100 \text{ kg}/\text{cm}^2$ ) and a structural width of 100 cm are the results for a variable concrete compressive height 'X' of both methods plotted, see Figure 2.7. Here, the formulae 2.4 and 2.11, and their difference are determined and plotted.

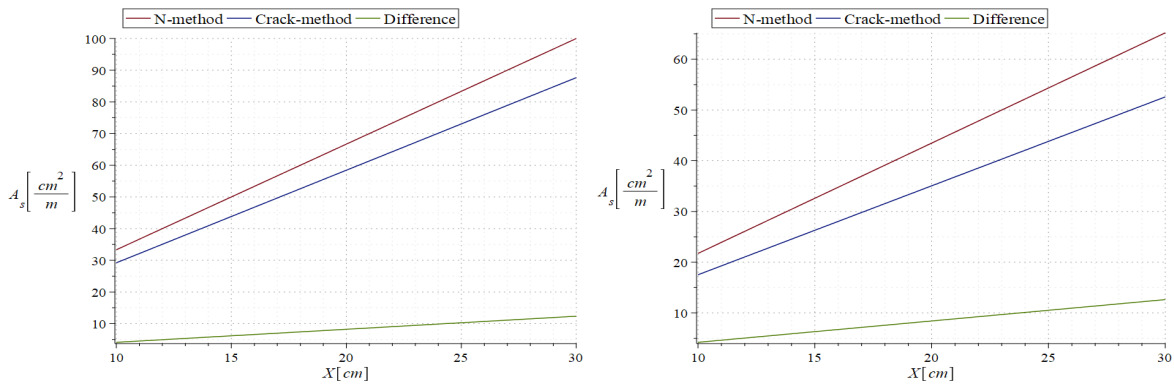


Figure 2.7: The difference in required reinforcement amounts with steel quality QR24 for the comparison of the N-method and Crack-method (left) and for the steel quality QR40 (right), based on the concrete compressive height.

A constant decrease of approximately 12% of required reinforcement for the crack-method compared to the N-method for QR24 is obtained. A constant decrease of approximately 19% of required reinforcement for the crack-method is obtained compared to the N-method for QR40. The decrease in reinforcement percentage for the crack-method compared to the N-method is shown in Figure A.3 in Appendix A. The difference between the required reinforcement percentages for the two steel qualities, lies in the different ratios between the ultimate steel stress and allowable steel stress.

### Shear stress

The shear stress from centric loading and bending is defined with the circle of Mohr. The equation until the GBV1962 to determine the shear stress is equation 2.23. For the substantiation of the determination of the shear stress equation, Appendix A is referred to.

$$\rho = \frac{3}{2} \cdot \frac{D}{F_b} \quad (2.23)$$

Where:

$D$  = acting shear force;

$F_b$  = product of the height and the width of the slab or beam;

$\rho$  = allowable shear stress of the concrete.

In the GBV1962 a second formula to determine the shear stress for a cracked cross-section is developed which is used until the VB1974 was published:

$$\rho = \frac{D}{b \cdot z} \quad (2.24)$$

With  $z$  as the inner arm of the cracked cross-section. The calculated effective shear stress  $\rho$  is checked for the allowable shear stress of the structure. The allowable shear stress in the concrete differs for cross-sections with or without stirrup reinforcement and are presented in Table 2.2 in Section 2.2.2 of this Chapter.

### 2.2.5. Reinforcement

All former design codes have normalised requirements for the reinforcement layout. In the GBV1940, GBV1950 and GBV1962 technical drawings are presented of normalised reinforcement layouts. Besides, multiple versions of the bending schedule (buigstaat) are published at the beginning of the twentieth century, often as an Appendix of the GBV codes. A bending schedule is made from the reinforcement drawings. The bending schedule is the overview of reinforcement bars with their required lengths and shapes, hooks, and positions where to bend the bars. After the bending schedule, the regulations for reinforcement layouts are organised by the National normalisation Institute (NEN). The NEN developed national codes to normalise the layout and technical drawing of reinforcement.

#### Main reinforcement

Main reinforcement is the reinforcement designed to bear the largest tensile forces due to the hogging and sagging moments in a bridge. This means that the main reinforcement is positioned in general at the bottom of the slab in the span and at the top of the slab at the position of supports. The main reinforcement is often



in slab bridges bend from bottom of the slab to the top of the slab, at the transition of span to support. Main reinforcement at mid-span, is often present in one layer for bridges with rectangular cross-sections. Main reinforcement at supports can be present in multiple layers for slab bridges with or without stiff edge beams.

### Type of reinforcement bars

Various types of reinforcement bars are used as main reinforcement in slab bridges since the application of RC. The various types of reinforcement which are not used anymore since the 1960s are shown in Figure 2.8. Difference can be made between plain- and ribbed reinforcement, where the criteria for slip resistance prescribed by the code define the category.

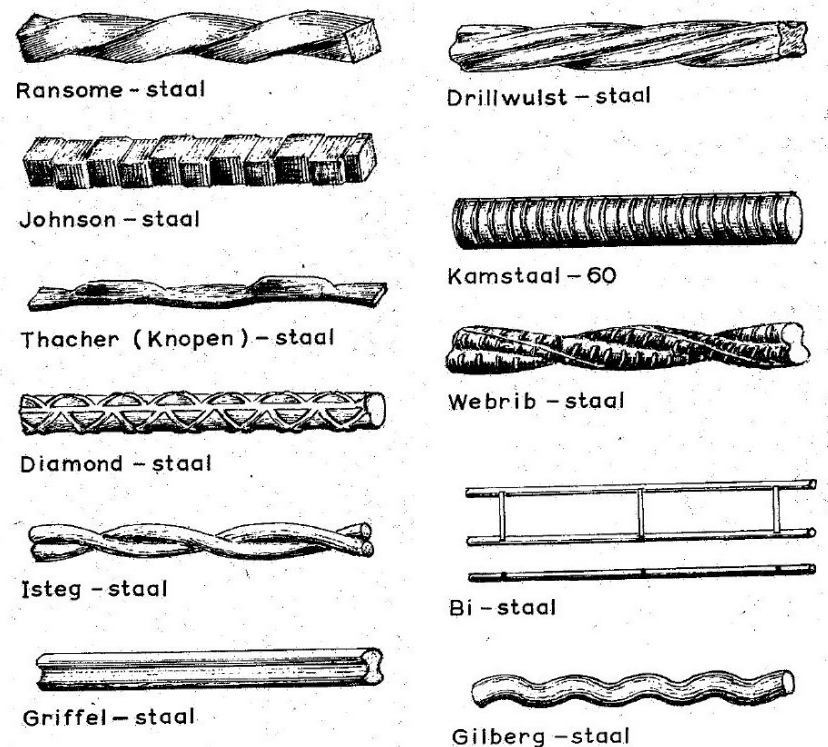


Figure 2.8: Various types of reinforcement bars not used anymore in the Netherlands since the 1960s, illustration from Gantvoort (1964)

### Reinforcement spacing

The GBV codes prescribe the requirements to meet for the reinforcement spacing of slabs and beams. The most important requirements for reinforcing of slabs are schematised in Table 2.3.

Table 2.3: Prescriptions from the GBV codes for reinforcing of slabs.

	Longitudinal reinforcement spacing	Additional prescriptions
GBV1912/ 1918	$S \geq 2.5 \text{ cm}$ $S \leq 25 \text{ cm} \ \& \ \leq 2 \cdot h$	Minimum of 10mm between slab edge and reinforcement
GBV1930	$S \geq 2.5 \text{ cm}$ $S \leq 20 \text{ cm} \ \& \ \leq 2 \cdot h$	Minimal bar diameter of 6 mm
GBV1940/ 1950	$S \geq 2.5 \text{ cm}$ $S \leq 20 \text{ cm} \ \& \ \leq 2 \cdot h$	Minimal bar diameter of 6 mm Slabs loaded vertically need bottom transverse reinforcement
GBV1962	$S \geq 2.5 \text{ cm}$ $S \leq 20 \text{ cm} \ \& \ \leq 2 \cdot h$	Minimal bar diameter of 8 mm slabs thicker than 25cm need a double reinforcement mesh

### Reinforcement hooks, bends and welds

RC bridges constructed with plain reinforcement need always hooks at the end of the bars for anchorage and bends to following the tensile stresses in the slab. Reinforcement subjected to tensile forces needs round or

oblique hooks with an inner diameter of  $\leq 2.5$  the bar diameter and with a connecting straight part of at least four times the bar diameter.

Bending of the longitudinal reinforcement is done by shaping the bars from the bottom of the slab at mid-span to the top of the slab at the support. In this way, the reinforcement is located at the positions where the largest tensile stresses occur. The former design codes prescribe the necessity to design for an accidentally clamping moment at a end-support. The bend reinforcement can be used for this hogging moment. Requirements from the GBV1918-GBV1962 codes say that bending of the bars need to be done with an inner radius of at least five times the bar diameter. The GBV codes prescribe that a minimum of 1/3 of the longitudinal reinforcement should be bend up. In general, reinforcement bars are bend at an angle of approximately 45 degrees. Larger angles can be made in case of beams with a large height and/or a limited span. The mutual distances of the onset of the bends should be less than 50 cm or less than the slab thickness. Figure B.9 shows the visualisation from the GBV codes of the bend reinforcement at an end-support.

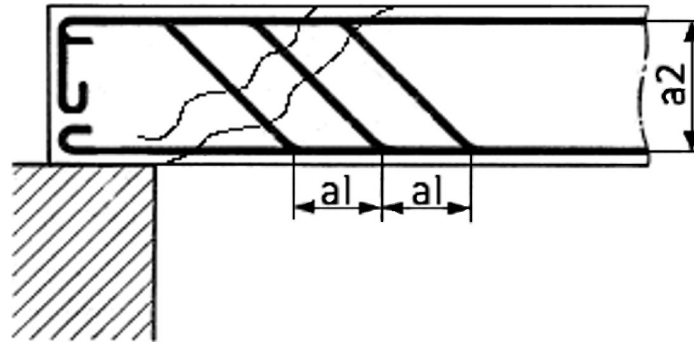


Figure 2.9: Mutual distance of bend reinforcement in a longitudinal cross-section, where  $a_1 \leq a_2$ , with an upper limit of 50cm, according to the GBV1940. Possible shear cracks are illustrated at an angle of  $\approx 90$  degrees compared to the orientation of the bend reinforcement.

The GBV codes prescribe: welding of reinforcement bars needs to be avoided in general and at critical cross-section welding is not allowed at all.

### Anchorage length

According to the GBV the anchorage length should have a minimum of  $l_d$ ;

$$l_d = \frac{1}{4} \phi \cdot \frac{\sigma_a}{\tau_d} \quad (2.25)$$

Where:

$\sigma_a$  = steel stress with a minimum of  $\frac{1}{3} \bar{\sigma}_a$ ;

$\tau_d$  = allowable bond stress along the anchorage length, in case of plain reinforcement bars only depends on the concrete quality, and needs in practice always a hook to secure anchorage.

### Transverse reinforcement

The GBV codes prescribe the necessity of reinforcement in the transverse direction for vertically loaded plates. Plates thicker than 25 cm require a double layered reinforcement in the transverse direction. Transverse reinforcement is also applied to sustain the effects of shrinkage, and temperature changes in the structure. The codes until the GBV1950 have a minimum of three bars prescribed per meter and after a minimum of four bars per meter slab width. Until the appearance of the GBV1962, a so-called transverse distribution reinforcement is required with a minimum of 20% of the coinciding main reinforcement. Since the GBV1940 the code is extended with a distinction between bottom transverse reinforcement and top transverse reinforcement. A distinction is made between the amount of transverse reinforcement at the position of minimum and maximum hogging and sagging bending moments. At these extremes, the tensile forces are consequently minimal and maximal. So in general, at positions of maximum bending moments in longitudinal direction the 20% requirement for the transverse direction counts and at positions of minimum bending moments the requirement can deviate. The GBV1962 changed the code into the requirement of 20% transverse reinforcement of the main reinforcement at any location of the slab.

The transverse bending reinforcement is determined in the GBV1962 utilising an estimated transverse moment  $M_{l2}$ . A transverse bending moment needs to be taken into account in case of  $l_2 < (3 \cdot l_1)$ , where  $l_1$  is

the span length and  $l_2$  the slab width. Within the effective width from concentrated loading, the transverse bending moment is defined by:

$$M_{l_2} = \frac{M_{l_1}}{1 + 4 \frac{b_2}{l_2}} \quad (2.26)$$

And in case  $l_2 > (3 \cdot l_1)$ ,

$$M_{l_2} = \frac{M_{l_1}}{1 + \frac{4b_2}{3l_2}} \quad (2.27)$$

For which  $M_{l_2}$  should be at least 10% of  $M_{l_1}$  at the position of the concentrated load accounted for.

#### Top reinforcement

The GBV1962 states, that in case the effective width reaches the edge of the slab, top transverse reinforcement should be applied over the full length of the slab. This top reinforcement is dimensioned upon the following calculated moment:

$$M_{l_2} = -0,10M_{l_1m} \quad (2.28)$$

Where  $M_{l_1m}$  is the moment at the concentrated load positioned at mid-span.

#### Shear reinforcement

The GBV codes prescribe the necessity of stirrup reinforcement in beams. The stirrups can have a maximum c.t.c. distance of 30 cm. In case of insufficient shear resistance of the concrete beam itself, additional shear reinforcement is required. Shear reinforcement as stirrup reinforcement and/or shear reinforcement as bending of longitudinal reinforcement can be applied. For slabs any prescription towards stirrup reinforcement is vacant. In case the allowable shear stress based on the concrete quality is exceeded, additional shear capacity should be designed for. This shear capacity is reached by bending of bars at an angle of about 45 degrees at the location of maximum shear stresses. However, in none of the available former calculations from the preliminary study, a shear calculation is present for the slab of the bridge. A graphical method is developed by van der Schrier (1938) together with a calculation procedure to determine the required reinforcement to resist the shear stresses. For a combination of concentrated- and distributed loading is the method more complicated and not discussed in the literature. For this reason, the method is not applied in this study. However, the method is briefly demonstrated in Appendix A.

## 2.3. Traffic load

The VOSB1933 forms the basis for the substantiation of design traffic loading on bridges. The design traffic load for normal traffic consists of distributed traffic load and concentrated traffic load. The distributed traffic load is determined by a specific vehicle weight distributed over an assumed vehicle length and by the lane width. The concentrated traffic load is based on the heaviest expected truck with the largest possible axle load, calling the design truck. In the code, overloading of the truck and future traffic load increment are taken into account. The distances between the axles and wheels originate from this specific truck. A reduction to the distributed- and concentrated traffic load from load class A/60 is applied for lower traffic load classes B/45 and C/30. Bridges are classified into load classes based on the expected traffic loading. Load class A/60 defines bridges in the main road network, where diverting of traffic is excluded. Load class B/45 defines bridges in the main road network, where diverting of heavy trucks is possible by class A/60 bridges. Load class C/30 defines bridges prohibited for heavy vehicles.

With the publication of the VOSB1963 the traffic load by normal traffic is revised. The development of the normalisation of traffic load between VOSB1933 and VOSB1963 is visualised with Table 2.4, 2.5 and 2.6 applicable for Figures 2.10, 2.11 and 2.12. In case no value is present in the table, the wheel configuration is not applicable for the specific load class. Class B from the VOSB1933 and VOSB1938 has two possible wheel configurations, visualised in Figures 2.11 and 2.12.

Table 2.4: Traffic load configuration for load class A/60

	a	b	c	d	e	f	g	h	i	j
VOSB	kN	kN	kN/m <sup>2</sup>	cm	cm	cm	cm	cm	cm	cm
1933	200	200	4	150	600	15	20	30	30	-
1938	200	200	4	150	600	15	20	30	30	-
1963	200	200	4 <sup>i</sup>	100	400	32	25	25	50	-

Table 2.5: Traffic load configuration for load class B/45

	a	b	c	d	e	f	g	h	i	j
VOSB	kN	kN	kN/m <sup>2</sup>	cm	cm	cm	cm	cm	cm	cm
1933	100	200	4	150	600	15	20	30	30	150
1938	100	200	4	150	600	15	20	30	30	150
1963	150	150	3 <sup>ii</sup>	100	400	24	25	25	50	-

Table 2.6: Traffic load configuration for load class C/30

	a	b	c	d	e	f	g	h	i	j
VOSB	kN	kN	kN/m <sup>2</sup>	cm	cm	cm	cm	cm	cm	cm
1933	100	0	3.5	500	0	15	20	30	-	150
1938	100	0	3.5	500	0	15	20	30	-	150
1963	100	100	2 <sup>iii</sup>	100	400	16	25	25	50	-

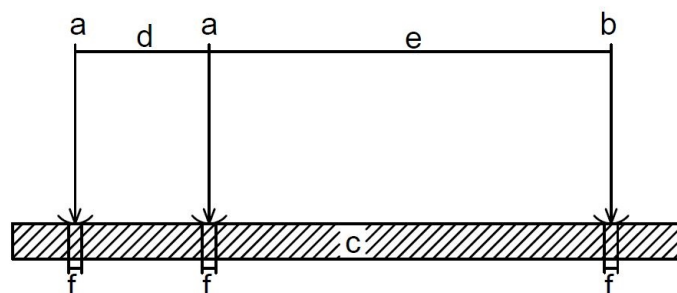


Figure 2.10: Loading scheme of the design truck and uniform distributed traffic load, with the variables from the Tables 2.4, 2.5 and 2.6.

<sup>i</sup> or max 12 kN/m per lane<sup>ii</sup> or max 9 kN/m per lane<sup>iii</sup> or max 6 kN/m per lane

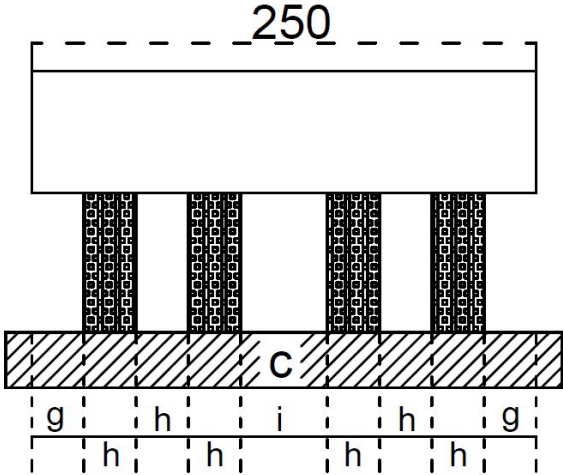


Figure 2.11: Concentrated loading configuration with double wheels from the design truck for load class A/60 and B/45 and 30.

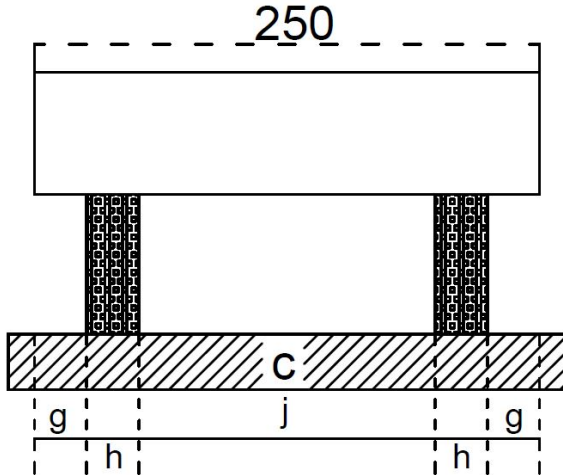


Figure 2.12: Concentrated loading configuration with single wheel from the design truck for load class B/45 and C.

## 2.4. Dynamic amplification factor

Traffic load is modelled as static loading in former bridge design. To define the effect of dynamic loading from actual traffic, a dynamic amplification factor (DAF) is applied to the static traffic load. In the codes before the GBV1940, no distinction is made between the DAF for steel- and concrete bridges. The DAF prescribed by the VOSB1933 for tram- and normal traffic is  $DAF = 1 + 40/(100 + l)$ , with 'l' being the span of the beam or slab. In the GBV1940-1962 an additional DAF is determined for concrete bridges, namely:  $DAF = 1 + 3/(10 + l)$ , with 'l' being the span of the beam or slab. The new formula to determine the DAF is based on the difference between a bridge made of steel with a significant lower self-weight compared to a concrete bridge with a significant high self-weight. A dynamic load has a smaller effect on a bridge with a high self-weight, compared to a bridge with a low(er) self-weight. The two different formulae to determine the DAF and the difference between both formulae ( $DAF_{VOSB} - DAF_{GBV}$ ), are plotted for a span range which can be seen in Figure 2.13.

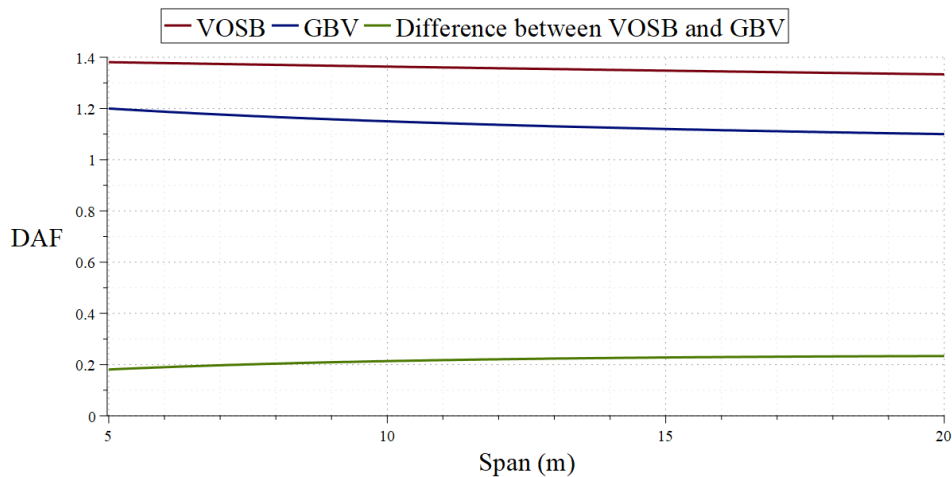


Figure 2.13: DAF determined by the GBV before the GBV1940 and by the GBV1940-GBV1962, and the difference between both formulae.

## 2.5. Concentrated load distribution

Concentrated loading originates in bridge design mainly from wheel loads, where a significant high force is positioned on a small area. To determine the consequential bending moments in the transverse and the longitudinal direction, the concentrated load(s) may be distributed. The concentrated load may be distributed in the longitudinal direction and the transverse direction according to several codes. In this section, the development of methods defining the distribution of concentrated loading is explained.

### The method from the GBV1912-1940

The first wheel-load distribution is defined in the GBV1912 and maintained until the GBV1940. The code prescribes a slab loaded by a concentrated point- or surface load where the load may be distributed over a rectangle. The rectangle has a length in load direction of  $2c + a$  and perpendicular to the load direction  $2c + b + 1/3l$ , see Figure 2.14.

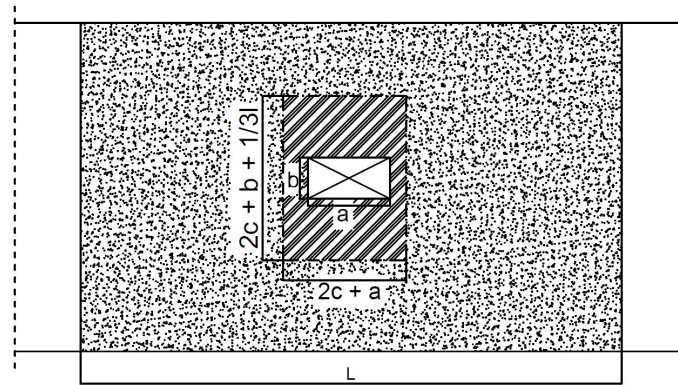


Figure 2.14: Wheel load distribution according to the GBV1912-GBV1940

### The method from the GBV1940-1962

The publication of the GBV1940 led to a modification of the concentrated load distribution. From the GBV1940 until the GBV1962, the load distribution of concentrated point- or surface load is also distributed over a rectangle but with the length 'a' in the load direction and perpendicular to the span an effective load width  $B = \sqrt{(0.75l)^2 + b^2}$ . 'a' and 'b' are presented in Figure 2.15. Here is important that the calculated effective width can not exceed the actual slab width  $b$ . The load distribution in concrete occurs approximately at an angle of 45 degrees and is for simplicity assumed 45 degrees for the load-distributing layer as well.

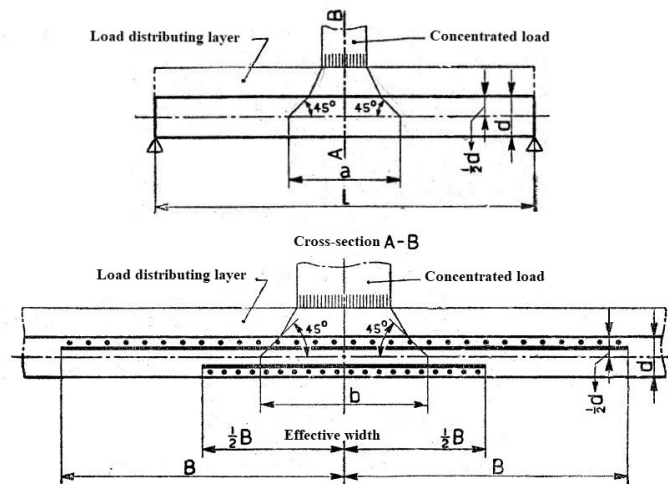


Figure 2.15: Wheel load distribution according to the GBV1940-GBV1962

**CUR16A/B**

In the GBV1962 code, the CUR16A/B is referred to for the distribution of a concentrated load in a slab. In case of rather simple load situations, the load distribution for the calculations of the bending moments can be done according to a simplified and work saving method, stated in the GBV1962. The CUR Report 16B states important differences in results from the method stated in the GBV on one hand, and from the elementary slab theory on the other hand. Here the demand for the more accurate elementary slab theory rises due to increasing traffic loading. However, the method is found time consuming and standardised with in tables.

In the CUR, positions of concentrated loading at the middle of the span, at the free edge of the slab and in-between are described. The ratio between the slab width and the multiplication of the span length ( $l$ ) with the restraint-reduction coefficient ( $r$ ) divides each load case into two parts. This restraint-reduction coefficient  $r$  is called the Sattler coefficient and is defined in the CUR based on the mechanical scheme of the bridge. For a freely supported slab is  $r=1$  and for both sides fixed supported slab is  $r= 0.5$ . In case of partly clamped or continuous slabs  $r$  is determined by applying a load in the middle of the span, after which the points of zero bending moment are determined ( $M_x=0$ ), in the longitudinal direction of the bridge. The length between the points of zero bending moment divided by the total span length divides the coefficient.

Three different load positions are considered in the CUR report: The first is the situation where the load is positioned at the middle of the slab width and is divided into two cases: case 1 where  $b > 3rl$ , and case 2 where  $b < 3rl$ . The second is the situation where the load is positioned at the free edge of the slab and is divided into two cases: case 1 where  $b > rl$  and case 2 where  $b < rl$ . The third situation is where the load is positioned between the middle of the width and at the free edge of the slab.

**Guyon-Massonnet method**

The orthotropic slab behaviour is analysed in 1946 by the French engineer Guyon and further extended by Massonnet in 1950. The method describes the orthotropic behaviour with the input of the slab geometry, material stiffness and flexural- and torsional rigidity  $\theta$  and  $\alpha$ . The fourth-order differential equation 2.29 describes the orthotropic slab behaviour. The method results in an effective width where concentrated loads can be distributed. The following documents from Hofman and van der Vlugt (1956), Brakel (1956) and Ter-moul (2010) are used to analyse the method from Guyon-Massonnet:

$$\rho_{xx} \frac{d^4 w}{dx^4} + 2H \frac{d^4 w}{dx^2 dy^2} + \rho_{yy} \frac{d^4 w}{dy^4} = \rho(x, y) \quad (2.29)$$

Where:

$$2H = 2\alpha \sqrt{\rho_{xx} \rho_{yy}} \quad (2.30)$$

$$\alpha = \frac{\gamma_{xy} + \gamma_{yx} + \nu \rho_{xx} + \rho_{yy}}{2\sqrt{\rho_{xx} \rho_{yy}}} \quad (2.31)$$

$$\theta = \frac{b}{l} \sqrt[4]{\frac{\rho_{xx}}{\rho_{yy}}} \quad (2.32)$$

Or in case of a statically indeterminate structure:

$$\theta = \frac{0.5b}{rl} : \quad r = \text{coefficient of Sattler} \quad (2.33)$$

With:  $\rho_{xx}$  the average bending stiffness per unit width and  $\gamma_{xx}$  the average torsional stiffness per unit width. In general, for (massive) reinforced slabs is  $\alpha=1$  leading to a load distribution independent of the thickness.

In general, two governing load positions of the design truck need to be assessed. The first is a single design truck positioned in practice at a distance  $e$  from the slab edge, and the second is two design trucks placed adjacent to each other in the middle of the slab. For both cases, the design truck(s) are positioned in the middle of the slab oriented in the longitudinal direction, see Figure 2.16 for a visualisation.

The accuracy of the Guyon-Massonnet method is negatively influenced by drawing inaccuracies of the graphs, reading inaccuracies, and the approximation of the surface by making straight lines between the points. In this study, the concentrated load distribution is determined with a programmed Excel sheet. In the sheet the  $K_\alpha$ -values are determined which is called "the principal coefficient of lateral distribution" indicating the non-linear effective part of the slab width. This Excel sheet is obtained from the cooperating company, administrated by R. Vergoossen, and an example is shown in Appendix A.6-A.8.



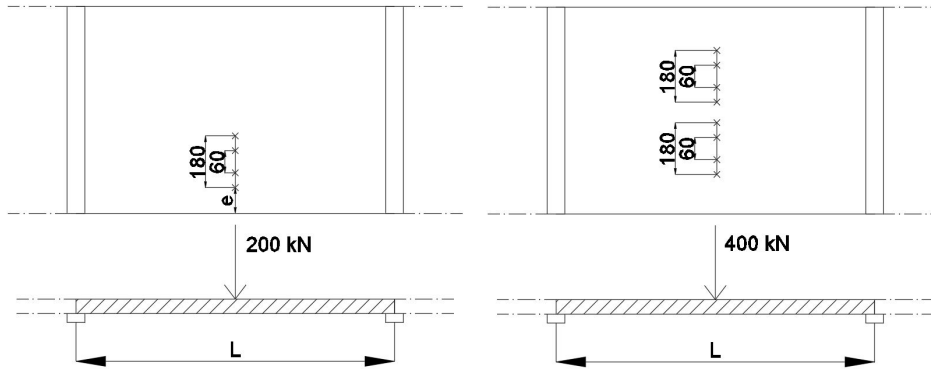


Figure 2.16: Position of design truck(s) leading to the governing load situations.

The contribution of the deck expressed with the  $K_\alpha$ -value is non-uniform over the width of the bridge deck. To determine an effective width for the Guyon-Massonnot method, the following set of formulae are used:

$$P_{eff} = K_\alpha \cdot P \tag{2.34}$$

$$Q_{eff} = \frac{P_{eff}}{B} \tag{2.35}$$

$$B_{eff} = \frac{P}{Q_{eff}} = \frac{P}{\frac{P_{eff}}{B}} = \frac{P}{\frac{K_\alpha \cdot P}{B}} = \frac{B}{K_\alpha} \tag{2.36}$$

The ROBK (op 't Hof, 2006), prescribes a boundary for the use of the Guyon-Massonnet method by limiting the intersection angle of the bridge by 90 gon ( $\approx 81$  degrees). In this study, the limiting angle is stretched to 80 gon ( $\approx 72$  degrees) to be sure that all bridges conform to the scope of this study, will be included. In general, in former bridge design is intended to cross the road or waterway perpendicularly. This approach leads to a bridge with the shortest total span and a constant cross-section of the bridge deck.

**Effect of the different load distribution methods**

The results of the four methods are plotted for a variable span length for one design truck at the edge of the slab in Figure 2.17(left), and two design trucks next to each other in the middle of the slab in Figure 2.17(right). The slenderness of the slab does not influence the method from Guyon-Massonnet, because of equal stiffness in the longitudinal and the transverse direction. The methods of the GBV are plotted for different values of the slenderness. The method from the CUR16 is plotted for a varying width. The extremes in effective widths for both load cases originate both from the GBV1940 and CUR16 methods. The CUR16 method shows the largest deviations in results compared to the average of all methods.

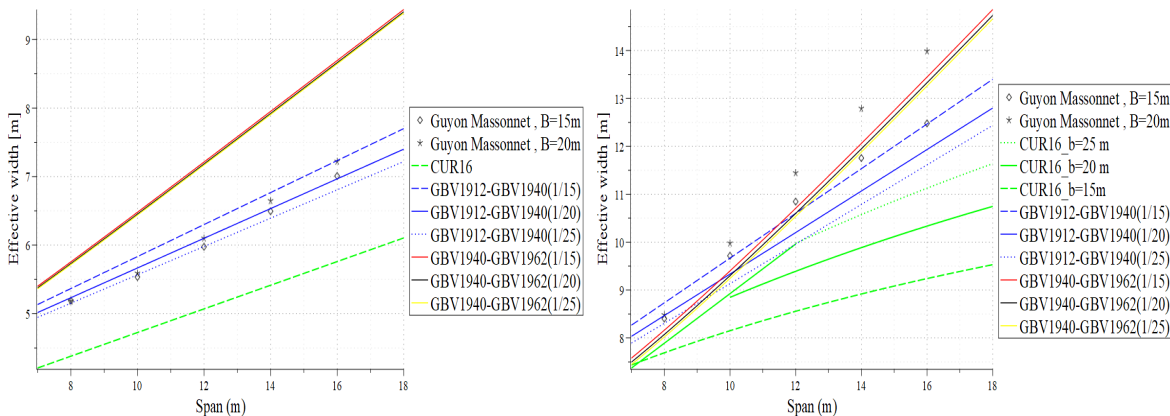


Figure 2.17: The effective width calculated with the different theories, loaded by one design truck of 2 meters width from load class A (left) and loaded by two design trucks of in total 5 meters in width from load class A (right). The width of the bridge deck is mentioned with the letter 'B', or the slenderness between brackets.

### 2.5.1. Shear force distribution

In GBV and VOSB codes, the distribution of shear force is not elaborated for in bridge design. For a beam supported on two or more supports with a distributed load, a reaction force of  $\frac{1}{2}ql$ , and a reaction force of  $\frac{5}{8}ql$  in case of unequally supported beams need to be designed for. In Section 3.3.3 a method is assumed to determine the shear stresses which has the acting shear force as input.

### 2.5.2. Loading in the longitudinal direction

The effect of concentrated loading in the longitudinal direction is described with influence lines since the beginning of design of RC bridges. Influence lines are based on Betti's theorem, also known as Maxwell-Betti reciprocal work theorem, discovered by Enrico Betti in 1872. The most unfavourable loading position of a concentrated load on a structure can be found with the use of influence lines. The unfavourable loading position is defined by the positions and magnitude of the concentrated loads. The VOSB1933 and the VOSB1963 state: "If an influence line shows both positive and negative parts, traffic load only needs to be taken in to account, if positioned only at the positive or only at the negative parts". So, in case the third axle is positioned at a positive influence value and the first and second axles are positioned at negative influence values, the contribution of the third axle should be neglected. Two methods are known to determine the shape of the influence line of a statically indeterminate structure subjected to a concentrated load. The first method is based on shape-deformations (vormveranderingsvergelijkingen). In this method, the beam rotations at the supports by external loading are calculated based on mechanics. The second method to determine the shape of the influence lines is with ordinary differential equations for bending of a beam from the theory of Müller-Breslau. To find the influence line for the bending moment at a specific location, an unit rotation has to be inserted so the force quantity (the bending moment) will produce negative work. In Figure 2.18 the principle of applying an unit rotation of 1.0 defined by  $\phi_1$  and  $\phi_2$  is shown.

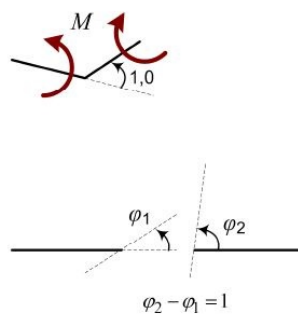


Figure 2.18: Imposing a unit rotation at span, by introducing a nod in the beam, Welleman (2016).

As an example, a multiple span bridge is modelled in four parts each defined by a fourth-order differential equation (ODE) for bending of a beam. To solve these ODE's, sixteen unknown integration constants need to be solved by sixteen boundary- and interface conditions. The total system of sixteen equations and sixteen unknowns is solved with the use of Maple as is shown in Figure B.2 and the influence line from Figure B.1 as a result.

The axles of the design truck should be placed such that the largest sum of; influence factor multiplied by the axle load, of the three axles, is generated. In case of different axle load magnitudes as in load class B/45, the load position of the design truck could differ from the load class A/60 where all axle load magnitudes are equal. In former calculations influence values are determined by hand, and consequently determined by dividing the span usually in ten parts.

To find the influence factor for traffic load on the support, a unit displacement (a shear hinge, no rotation) has to be inserted at the position of the support, see Figure 2.19.

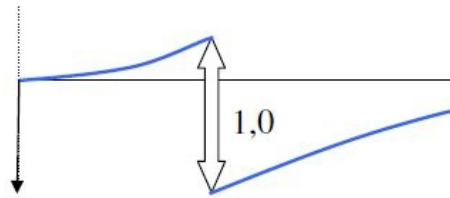


Figure 2.19: Imposing a unit displacement at a support, by introducing a displacement in the beam Welleman (2016).

## 2.6. Force determination

All GBV codes state that the calculations in structural design should serve the rules of mechanics. Empirical rules can not be used for the calculation of a structure. The permanent distributed load (self-weight and additional permanent action) of the structure should always be taken into account. The imposed loads, in this study the traffic loads should always be applied in the most unfavourable situation to find the governing load combination. The GBV states that the calculation of forces should be conducted according to the laws of statics and elasticity. The development in the knowledge of statics caused an increase in rules of the determination of statically determinate and statically indeterminate structures. This can be seen through the development of the GBV codes. Traditional design has a focus on the deck's flexural capacity since bending is the assumed failure mode, according to (G, 2013). The majority of calculations in the GBV is related to the determination of bending moments. This methodology of design was seen as the governing load situation where the reinforcement is to be designed for. In the codes published since the GBV1962, the development in the knowledge of shear force and durability is increased and obtained an important role in design of RC. The GBV codes describe loading by temperature effects by an expansion coefficient for concrete and steel. However, loading by temperature effect is not obtained in former calculations by default. Therefore, is chosen to omit loading by temperature in the RE process, leading to a conservative approach. In the assessment for the ultimate limit state (ULS) thermal loading is not included. In general, thermal loading has limited influence on bridges with short spans.

## 2.7. Former design changes

The increase of knowledge and experience in mechanics and structural design over time, led to development in the design codes. Figure 2.20 shows from the start of the RC design codes and the Traffic load model the successive codes.

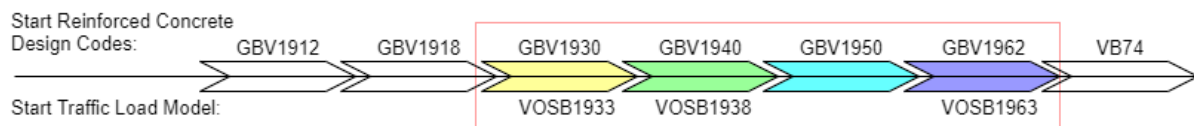


Figure 2.20: Timeline from the start of structural design codes and Traffic load model, with the scope of this research framed in red.

Modifications in the determination of structural design of RC bridges, at the loading- and capacity side, are displayed in Table 2.7. These modifications result in four periods where structural design is constant over time, see the third column in Table 2.7 and visualised in a timeline in Figure 2.21.

Table 2.7: Modification in structural bridge design from 1930 until 1970.

Year of modification	Change of;	Period
1940	DAF and effective width method	1930-1940
1950	effective width method	1940-1950
1962/63	Design code: traffic load, cross-section capacity	1950-1962
Overall	Material strength increase	1930-1970

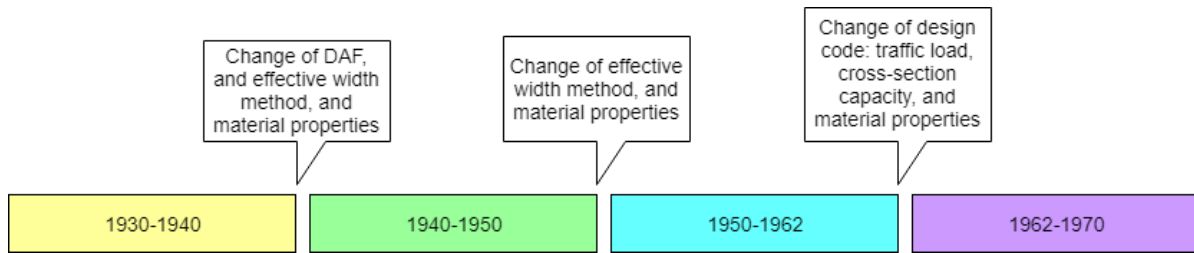


Figure 2.21: Timeline from 1930 until 1970 of the modification in structural design of RC bridges.

## 2.8. Discussion

The development in structural design of RC slab bridges and the traffic load model leads to four periods where structural design is constant over time, see Figure 2.21. The development towards the ultimate capacity of a structure caused an optimisation of the available materials in a cross-section. This can be obtained in the comparison between the required reinforcement amount for the crack-method and the N-method. The crack-method shows a constant decrease of approximately 12 % for steel quality QR24, see Figure A.3, and of approximately 19% for steel quality QR40, see Figure A.3. Together with the assumption made of plain steel having a steel quality of QR24 and the ribbed steel with quality of QR40, this seems to have led to a constant decrease in required reinforcement with the use of the crack-method compared to the N-method.

The change in the DAF for concrete bridges since the GBV1940, led to a lower load factor. The change in load factor leads to a decrease in traffic load of approximately 15% for concrete bridges.

Figure 2.17 shows that for all GBV methods, CUR method and Guyon-Massonnet method the effective width is increasing for an increasing span length. The deviation between the methods is smallest for smaller spans (<12m) compared to larger spans (>12m). The method of the CUR in combination with plain reinforcement is considered to be very unlikely. This is because of publishing the GBV1962, at the transition from plain to ribbed reinforcement and the earlier availability of the Guyon-Massonnet method. The CUR16 method to determine the effective width for concentrated loading is never encountered during this research, and so excluded in the sequel of this study.

The scope of this study focuses on bridges owned by local governments with small spans (<20m). The effective width determined by the different methods shows smaller distribution of concentrated loads for a decreasing span length, leading to a limited influence of the specific methods upon the force distribution due to concentrated loading.

Excluding the CUR16 method in the results leads for the first load case (one design truck) in a distribution of the effective width of 0.5-1.0 meters, which is approximately 10-20% for spans up to 12 meters. The second load case (two design trucks) leads to a distribution in effective width of 0.5-1.0 meters, which is approximate 5-10% for spans up to 12 meters.

A more slender bridge design leads to a smaller load distribution for the GBV1940-GBV1962 method and the GBV1912-GBV1940 method. The CUR16 and Guyon-Massonnet method are independent for the slenderness, in case of a massive slab structure. A larger width will cause a larger load distribution for the Guyon-Massonnet method and CUR16 method, where the methods of the GBV are independent of the width.

# Reverse Engineering by hand calculations

## 3.1. Introduction

A selected list of existing bridges is reverse engineered in this study, and are named not all by their original name but sometimes by location. The reinforcement of the bridges is determined and compared based on their design year, load class and geometry.

The reinforcement dimensioning relies on the assumption that the former calculations and bridge design are performed correctly according to the laws of mechanics and the corresponding design codes. Two different cross-sections are considered: a rectangular-, and rectangular cross-section with edge beams, see Figure 3.1. Rectangular edge beams (including cavities) are assumed for bridges designed with a cross-section. An averaged uniform thickness in the transverse direction of the slab is calculated. In the longitudinal direction the minimum thickness for the sagging bending moments is used, and the thickness at the supports for the hogging bending moments and shear force calculations is used. Loading from maximum two traffic lanes next to each other is taken into account for all RE bridges.

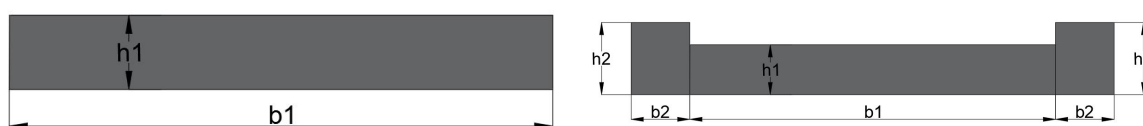


Figure 3.1: The two deck cross-sections of the bridges to be RE. Left: a rectangular deck cross-section with height 'h1' and width 'b1'. Right: a non-rectangular deck cross-section with height 'h1' and width 'b1' of the mid strip and height 'h2' and width 'b2' of the edge beams.

## 3.2. Uniformly distributed load

The GBV codes describe two methods for the calculation of Uniformly distributed loading (UDL) on indeterminate structures. The first is with the use of the shape deformation method, and the second is with hand rules from the GBV codes. In both cases the slab structure is schematised to a beam structure. The UDL is applied with an unit width of 1 meter and can consist of permanent load and distributed traffic load. In this study, the force distributions are determined based on the shape deformation method. ODE's for bending of a beam element are solved for boundary and interface conditions with the use of Maple software. In this way, a parametric approach for the determination of forces can be obtained. A three-span bridge with end-spans(L1) of  $0.8 \cdot \text{mid-span}(L2)$  with an UDL of 10 kN/m at each span, are the bending moment- and shear force line determined, and illustrated in Figure 3.2.

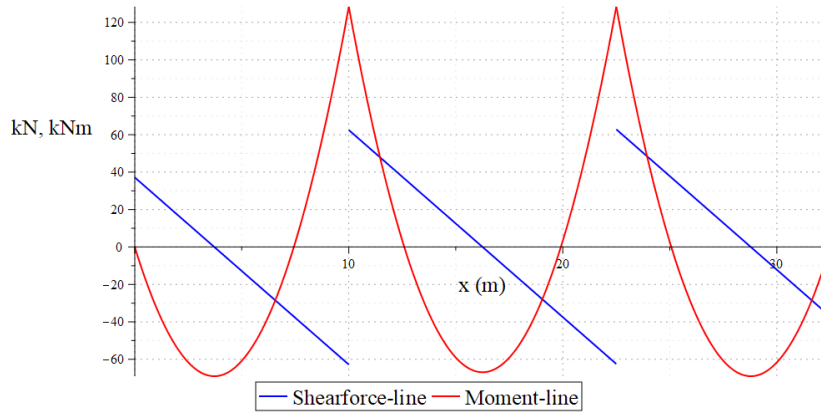


Figure 3.2: Moment- and shear force line of a three-span bridge with an UDL of 10 kN/m.

Since the GBV1940, an appendix is added to the codes to visualise the moment- and shear force coefficients due to UDL and concentrated loading in a schematic overview. The schemes with force coefficients are set up for bridges with equal end- and mid-spans. An example of a schematised tree-span bridge with force coefficients can be seen in Figure 3.3.

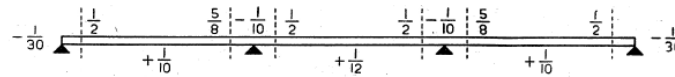


Figure 3.3: Moment- and shear coefficients of a three-span bridge with an UDL, from the GBV1940.

The full overview of bending moment and shear force coefficients due to UDL can be found in Appendix B Figure B.3 from the GBV1940. The formulae from the Maple sheet to calculate the bending moment line and shear force line can be found in Appendix B.1.

In practice, the end-spans ( $L_1$ ) are often designed with a span length of  $\leq 0.8 \cdot$  mid-span ( $L_2$ ), leading to the sagging-moment at mid-span to be the governing moment in the structure. This can simply be proven by multiplying the factor 0.8 times the moment coefficients of the end-spans. It seems in former design that the support-moments are also reduced by this factor, resulting in equal support-moments compared with span-moments. This means that the bending reinforcement at the position of the supports and the bending reinforcement in the end-spans can be based on the bending reinforcement amount calculated for the mid-span. This simplification in bridge design can for several cases be traced back in former calculations. The loading configurations leading to the governing bending moments in the spans due to distributed traffic loading are schematised in Table 3.1. Here, the use of zeroes and ones indicate the loaded span(s). '1' means the distributed traffic load is present and '0' means the traffic load is not present. The governing bending moments at the supports due to distributed traffic loading are schematised in Table 3.2.

Table 3.1: Configurations of the distributed traffic load leading to the governing mid-span bending moments.

Maximum span moment in span 2					
$L_1/L_2 \leq 0.8$	span1	span2	span3	span4	span5
2 span bridge	0	1			
3 span bridge	0	1	0		
4 span bridge	0	1	0	1	
5 span bridge	0	1	0	1	0
Maximum span moment in span 3					
5 span bridge	1	0	1	0	1

Table 3.2: Configurations of the distributed traffic load leading to the governing mid-support bending moments.

Maximum support moment at support B					
$L1/L2 \leq 0.8$	span1	span2	span3	span4	span5
2 span bridge	1	1			
3 span bridge	1	1	0		
4 span bridge	1	1	0	1	
5 span bridge	1	1	0	1	0
Maximum support moment at support C					
4 span bridge	0	1	1	0	
5 span bridge	0	1	1	0	1

### 3.3. Concentrated loads

Each of the VOSB codes prescribes concentrated loading by a design truck. The GBV describes force calculation by the shape deformation method and with hand rules from the GBV, for concentrated loading as for UDL.

The design truck should be placed at the most unfavourable position according to the GBV codes. Influence lines can be drawn to find the location for the design truck causing the maximum span- and support-moments. The maximum influence value in a mid-span is found to be at half the span length. The maximum influence value causing the governing support-moment is by placing the second axle at  $\frac{4}{10}$  of the span length. These governing loading positions are used in former design and so in the hand calculations.

Assessing an existing bridge for the Eurocode traffic model asks for a variable position of the concentrated traffic loading. In a later stage (Chapter 4) influence lines are not used anymore due to the calculation force of the computer. The calculation of the governing support-moments is done with a shape deformation method. By equating the deformed shape equations and solving these equations for boundary conditions, the support-moment(s) due to concentrated loading can be found.

An example of a three-span bridge loaded by a design truck is shown in Figure 3.4. The formulae to determine the support-moments due to concentrated loading from a design truck can be found in Appendix A Figure B.7. In all of the available former calculations, the calculation of support-moments due to concentrated loading is absent.

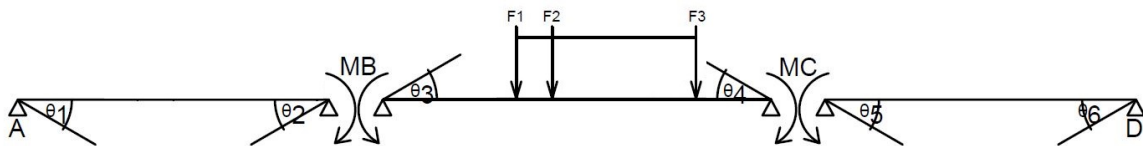


Figure 3.4: Shape deformation method applied for an example multiple span bridge loaded by a design truck.

An example of a three-span bridge with moment- and shear force coefficients is shown in Figure 3.5.

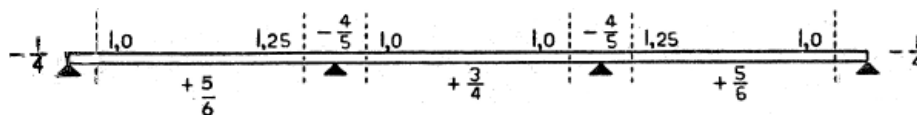


Figure 3.5: Moment- and shear coefficients of a three-span bridge under concentrated loading, from the GBV1940.

### 3.3.1. Edge beam

Bridges constructed with edge beams have a non-uniform cross-section in terms of stiffness and strength. Consequently, the stiffness of the edge beam need to be calculated by determining the beams as slab strips with the same bending stiffness. This makes it possible to schematise the bridge deck by beam elements. The stiffness conversion results in a larger fictitious width ( $b_2^*$ ) of the slab. Figure 3.6 and the following equations show the calculation procedure:

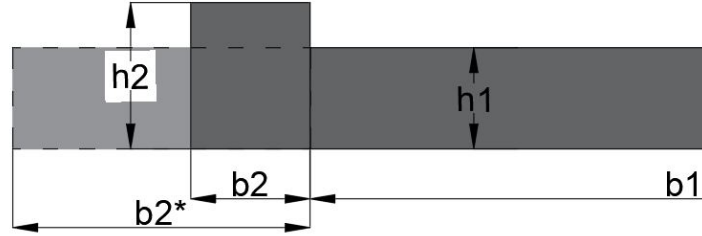


Figure 3.6: Changing the stiff edge beam by a slab strip with the same bending stiffness.

$$I_t = \frac{1}{12} b_2 h_2^3 + a_2^2 A_2 + \frac{1}{12} b_1 h_1^3 + a_1^2 A_1 \quad (3.1)$$

where consequently  $I_t$  should be equal to the total moment of inertia of the new deck cross-section  $I^*$

$$I^* = \frac{1}{12} (b_1 + b_2^*) h_1^3 = I_t \quad (3.2)$$

with  $b_1^*$  as the new width of the edge beam.

Where:

$$z = \frac{b_2 \cdot h_2 \cdot 0.5h_2 + b_1 \cdot h_1 \cdot 0.5h_1}{b_2 \cdot h_2 + b_1 \cdot h_1} \quad \text{Neutral axis} \quad (3.3)$$

$$a_2 = \frac{h_2}{2} - z \quad (3.4)$$

$$a_1 = \frac{h_1}{2} - z \quad (3.5)$$

Or in case the rule of Steiner is left out:

$$b_2^* = \frac{\frac{1}{12} b_2 h_2^3}{\frac{1}{12} h_1^3} \quad (3.6)$$

The concentrated loading is distributed according to the specific method from the design period, described in Section 2.5. The span-moment due to concentrated loading is determined as follows:

1. The concentrated load distribution from the GBV:

$$\text{Moment} = \text{influencevalue} \cdot \frac{\beta \cdot P \cdot DAF}{B^*} \quad (3.7)$$

Where  $B^*$  is determined by the method to calculate the effective width, corresponding with the foundation year of the bridge, as is stated in Section 2.5.  $P$  is the concentrated load and  $\beta$  a load factor.

2. The concentrated load distribution according to the theory of the Guyon-Massonnet method:

$$\text{Moment} = \text{influencevalue} \cdot \frac{K_\alpha \cdot \beta \cdot P \cdot DAF}{B} \quad (3.8)$$



### 3.3.2. Influence lines

Two types of maple sheets are set up to construct influence lines for two different load cases. The first sheet is to construct the influence line for a concentrated load in a span. The second sheet is to make the influence line for a support reaction by concentrated loading. The influence values are determined by solving ODE's for their boundary- and interface conditions, and the theory from Müller-Breslau which is a qualitative approach to find the shape of the influence line based on virtual work.

An example of a maple sheet with the calculation to construct an influence line is shown in Figure B.2, and the shape of the influence line can be seen in Figure B.1. The maple sheets are validated by the comparison of the influence values with a former calculation. It can be seen that the deviation between the calculation of the influence values is equal to or smaller than 5 %, see Table B.1 in Appendix B. Also, the results of the maple sheet are validated by a recalculation of several influence values with the use of Technosoft. This validation can be found in Appendix B.

### 3.3.3. Shear force distribution of concentrated loading

This subsection is meant to find the shear force load distribution of a rectangular deck cross-section with or without edge beams. The French method is assumed for the distribution of the concentrated shear force. The assumption is made that shear forces distribute in a horizontal plane at an angle of 45 degrees to the support, (Lantsoght et al., 2012). The maximum possible occurring shear force caused by the design truck from class A/60 can be found with the mechanical scheme in Figure 3.7. In this load situation, direct force transfer to the substructure is neglected. The maximum shear force due to loading by the design truck from class B/45 is mirrored, with the single axis with the largest magnitude at the support and the two adjacent axes at the span. In case a transverse beam is present at the support, the design truck can be moved from the centre of the support to the edge of the transverse beam.

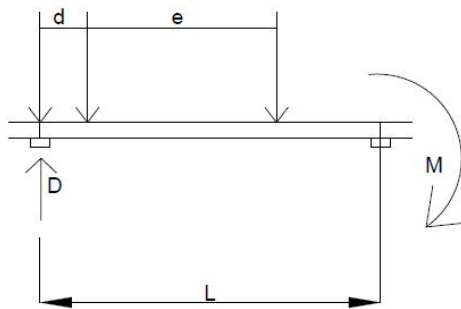


Figure 3.7: Mechanical scheme to determine the maximum shear force (D) in a bridge deck.

The governing load situation to determine the maximum shear force is loading by one design truck. In case of loading by two design trucks positioned next to each other, each axle load is distributed over 5 meters width due to the geometry of the two trucks. This results to a smaller distributed shear load. The assumed distribution of the shear force in the horizontal direction in a bridge deck is drawn in Figure 3.8. Due to the distribution of the shear forces of 45 degrees in the deck, it should be limited to the deck width.

The shear force distribution of a bridge with edge beams differs from a bridge with a rectangular cross-section due to the non-uniform cross-section. The stiff edge beams attract forces, causing a higher effective shear load on the beams. Section 3.6 elaborates on the edge beams in terms of attracting loads due to a larger stiffness.

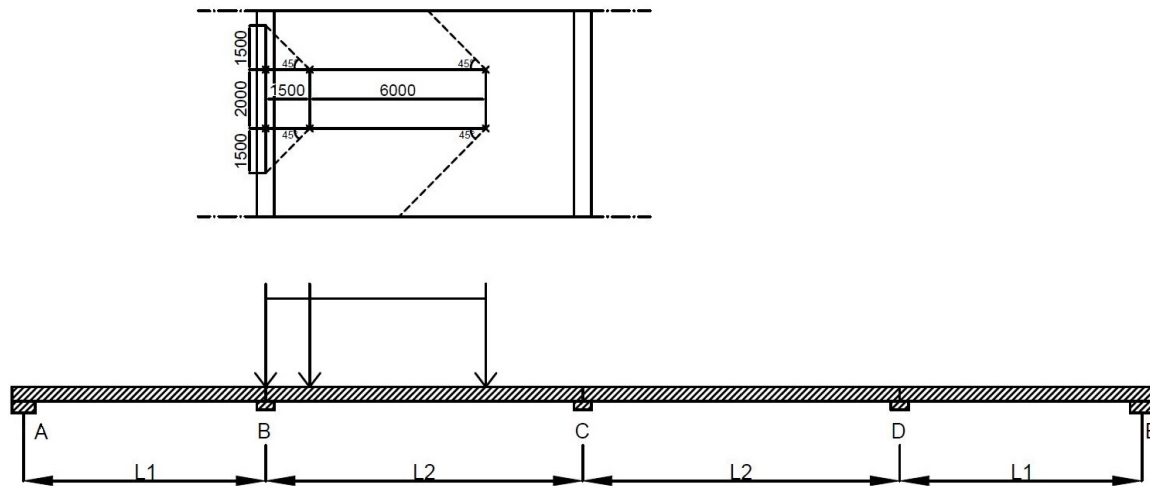


Figure 3.8: Shear force distribution in a bridge deck, top view (above) and side view (below).

### 3.4. Reversed engineered bridges

The list of bridges presented in Table 3.3 is RE. In the table is mentioned which type of information is available for the RE method. If crucial information is missing, assumptions are made based on the design year with corresponding design code, and geometrical matching bridges with known information. In this study, the design year is the year the actual design of the bridge is performed. Meaning that the latest available design codes in the concerning year are consulted for design.

Table 3.3: Available information about the RE bridges.

Bridge	Designyear	Number of spans	L1 (m)	L2 (m)	L1/L2	Slenderness (approx.)	Available information			
							Technical drawings	Former calculation	Load class	Applied material properties
KW7	1964	3	8.65	10.8	0.80	1/18 1/22	yes	yes	yes, 60	steel yes, concrete yes
Ellermansbrug	1949	3	10.5	13.2	0.80	1/20 1/25	yes	no	yes, B	steel no, concrete no
Waalwijk	1958	4	10.1	14.36	0.7	1/17 1/24	yes	no	yes, B	steel no, concrete no
Kw4	1964	4	8.3	10.8	0.77	1/17 1/22	yes	yes	yes, 60	steel yes, concrete yes
Dinkelbrug	1932	4	7	7	1	1/15 1/15	yes	no	no, assumption B	steel no, concrete no
Moergestel	1954	4	10.1	14.36	0.70	1/18 1/25.5	yes	no	yes, B	steel no, concrete no
Ruytenschildtbrug	1962	5	9	9	1	1/15 1/15	yes	no	No, assumption 60	steel yes, concrete no
Heemstedestraatbrug	1960	3	11.4	16.15	0.71	1/20 1/28.5	yes	no	yes, B	steel yes, concrete no

#### Material properties

Table 3.3 shows for a large part of the bridges unknown concrete qualities. In this case, allowable stresses are chosen based on the corresponding design code with the design year. The assumption is made that for all bridges a site control is executed leading to higher allowable material stresses.

#### 3.4.1. Bending capacity

Former design of the cross-sectional bending capacity uses the N-method or the crack-method depending on the design year. Material stresses can be obtained from the corresponding design code or available technical drawings. The concrete compressive height can be determined, when the reinforcement amounts are known, based on a horizontal force equilibrium. So, the bending moment capacity of a specific cross-section can be calculated.

### 3.4.2. Actual reinforcement amounts

The applied reinforcement can be read from the available technical drawings, and be compared with the estimated reinforcement amounts, RE reinforcement amounts. Figure 3.9 shows for the first two spans of each bridge the present reinforcement amounts at mid-span (blue bar) and the support (orange bar). It can be seen that the amount of reinforcement at a support is (almost) always equal or larger than at mid-span, for bridges with unequal span length for end- and mid-spans.

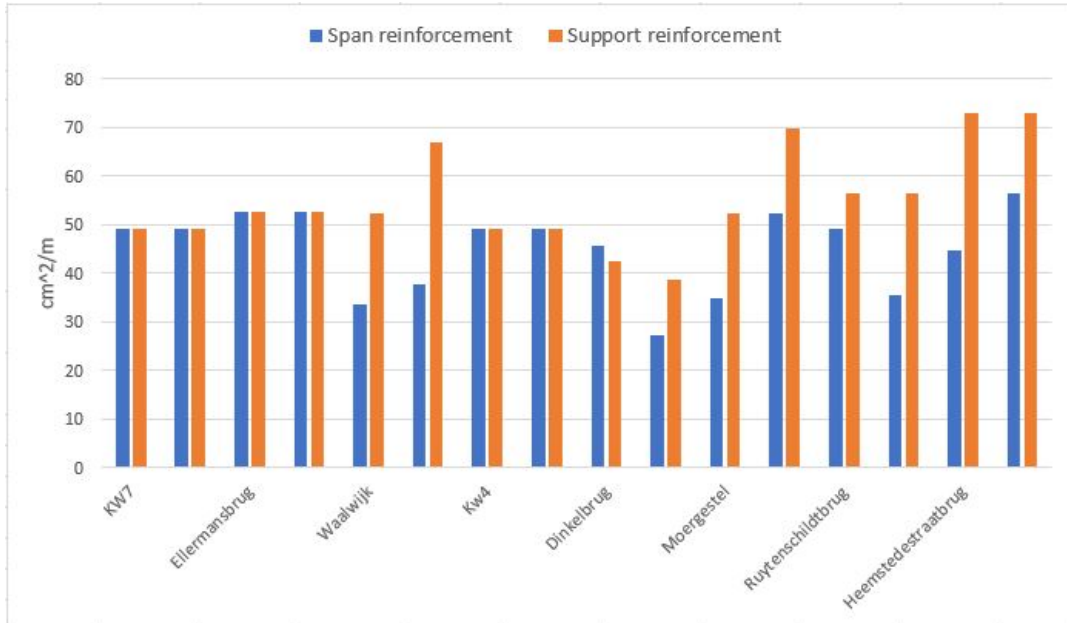


Figure 3.9: Field- and support reinforcement amounts, where the first blue and orange bars are from the first span (end-span) and the support at the right side of the span. The second blue and orange bars are of the second span (mid-span) with adjacent support.

The Unity Checks for bending moment found for the selected list of bridges are presented in Table 3.4, with the locations of the cross-sectional checks illustrated in Figure 3.10. The Unity Checks higher than 0.8 (highlighted) are assumed to be governing and the reinforcement designed for.

Table 3.4: Unity Checks for bending moment, at the location shown in figure 3.10.

Bridge	AB	B1	B2	B3	BC	C1	C2	CD
KW7	0.75	0.66	0.93	-	1.01	0.66	0.93	-
Ellermansbrug	0.69	0.68	0.99	-	0.91	-	-	-
Waalwijk	0.76	0.52	0.95	-	0.89	0.54	1.00	-
Kw4	0.93	1.00	-	-	1.06	1.06	-	-
Dinkelbrug	0.72	-	0.67	0.47	0.96	-	-	-
Moergestel	0.73	0.54	0.92	-	0.78	0.53	0.93	-
Ruytenschildbrug	0.91	0.33	0.64	-	0.88	0.33	0.57	0.81
Heemstedestraatbrug	0.74	0.97	-	-	0.92	-	-	-

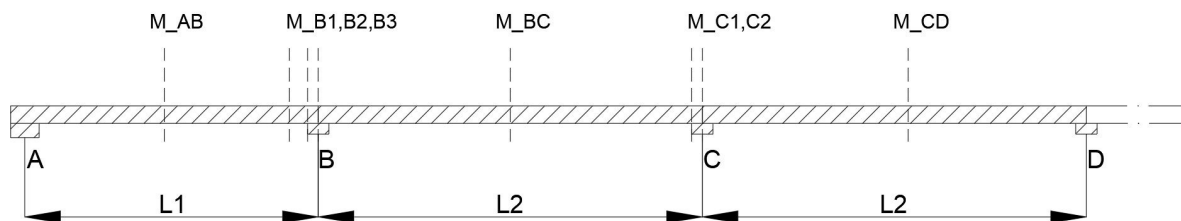


Figure 3.10: Locations of critical cross-sections where the Unity Checks for bending moment are performed.

### 3.5. Estimated required reinforcement

Three bridges have been RE by calculating the required reinforcement amounts in the spans and at the supports. The values of the Unity Checks are aimed for maximum utility ( $UC=1.0$ ) in the cross-sections, see Table 3.5. The estimated required reinforcement to bear the effective bending moments are presented with a bar chart in Figure B.11 in Appendix B. The estimated amounts are compared with the actual amounts from available documents in the next section. The comparison between the estimated reinforcement and present reinforcement shows lower amounts for the present reinforcement for both spans and supports.

Table 3.5: Unity Checks from RE for bending moments, at the location shown in figure 3.10.

Bridge	AB	B1	B2	B3	BC	C1	C2
Dinkelbrug	0.96	0.85	0.61		1.00	0.52	0.65
Ellermansbrug	0.98	0.72	1.03		0.97		
Heemstedestraatbrug	0.70	0.96			0.95		

Important in the comparison between the calculated reinforcement and the applied reinforcement is that the calculated reinforcement should not be larger than the applied reinforcement. In this way, the capacity of the cross-section is not overestimated. The calculated and applied reinforcement are compared in Table 3.6, where can be seen that the calculated reinforcement is never larger than 5% of the applied reinforcement. The RE reinforcement at support B for the Dinkelbrug is significantly lower than the actual applied reinforcement according to the technical drawings. The Dinkelbrug concerns a bridge with equal lengths for the end- and mid-spans, where the largest bending moment occur at the mid-supports. From the technical drawings can be seen that a large part of the reinforcement from the end spans is bend-up to the mid-supports, which might reason for the large amount of applied reinforcement at the end-spans. The reinforcement amount at the end-span (AB) of the Ellermansbrug is in former design equalised to the reinforcement amounts of the adjacent spans and supports. The RE amount of reinforcement is based on the required capacity for the total bending moment in the end-span.

Table 3.6: Comparison of the calculated reinforcement and reinforcement amount from the technical drawings.

	Reverse Engineered (cm <sup>2</sup> )	From technical drawing (cm <sup>2</sup> )	Accuracy
Heemstedestraatbrug	span AB 47.12	44.68	105 %
	support B 73.93	72.95	101 %
	span BC 53.62	56.55	95 %
	support C 73.93	72.95	101 %
Dinkelbrug	span AB 30.41	45.62	67 %
	support B 40.46	42.47	95 %
	span BC 27.15	27.35	99 %
	support C 27.15	31.07	87 %
Ellermansbrug	span AB 35.06	52.59	67 %
	support B 49.42	52.59	94 %
	span BC 49.42	52.59	94 %
	support C 49.42	52.59	94 %

### Transverse reinforcement

Figure 3.11 shows for the first two spans of each bridge the applied percentage of transverse reinforcement of the main reinforcement, at mid-span (blue bar) and at the support (orange bar). It can be seen that at the position of maximum positive and negative bending moments, the transverse reinforcement always meets the requirement from the GBV (red line), which says that the transverse reinforcement should always be at least 20% of the main reinforcement. The variation of the applied transverse reinforcement amount seems to be rather large. The largest amount of transverse reinforcements are found for bridges with non-rectangular cross-section, where the load needs to be transferred to the stiff edge beams.

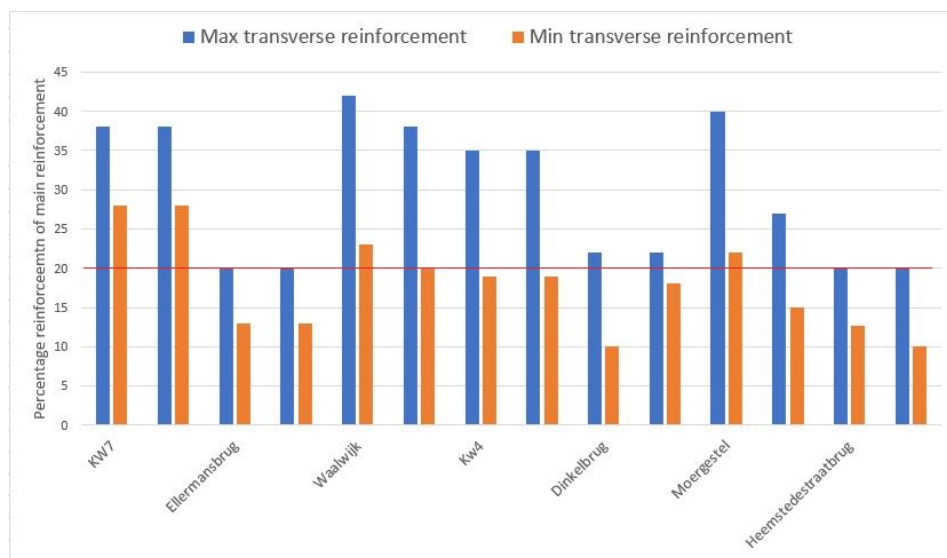


Figure 3.11: Transverse reinforcement amounts, where the first blue and orange bars are of the end-span and the second blue and orange bars are of the adjacent span.

### Reinforcement layout

The reinforcement layout starts with the estimation of the applied bar diameters for the main reinforcement. An overview per bridge of bar diameters and their foundation year can be seen in Figure 3.7.

Examples of bent bars in the beam elements of two different bridges are shown in appendix B in Figure B.8 and B.10. Looking at the distances where the bars are bent, it can be concluded that the graphical method of W. van der Schrier is not consulted. The bent reinforcement just fulfils the requirement from the GBV codes which says that the mutual distance between the bent bars can be maximum 50 cm.

At the location of a support, multiple reinforcement layers could be present. For execution reasons these reinforcement layers are separated with levelling bars, influencing the structural capacity. Regulations towards levelling bars are unknown and from the technical drawings no clarity can be obtained.

Table 3.7: Overview of the applied bar diameters for the main reinforcement of the assessed bridges.

Bridge	Design year	span 1		span 2	
		Bar diameter span (cm)	Bar diameter support (cm)	Bar diameter span (cm)	Bar diameter support (cm)
KW7	1964	25	25	25	
Kw4	1964	25	25	25	25
Heemstedestraatbrug	1960	32	32 36	36	
Ruytenschildtbrug	1962	19 22	22 22	16 22	22 22
Dinkelbrug	1932	22	16 22	16 22	16 22
Ellermansbrug	1949	25	25	25	
Waalwijk	1958	22 25	22 25 32	22 25	22 25 32
Moergestel	1954	24	24 30	24	24 30

### 3.6. Shear capacity

The shear capacity of a slab structure is found by formulae 2.23 mentioned in Chapter 2, where the shear stress ' $\rho$ ' is given in Table 2.2 based on the concrete class. In none of the available former calculations, the shear capacity check is present.

For load class A/60 and B/45 the shear stresses are plotted for a variable span length 'L2' and with four different values of the deck slenderness, see Figure 3.12. Here, the ratio between the end-spans and mid-spans is set to 0.8 and the deck width is set to 10 meters. The shear force is calculated at 0.5 m from the centre of the support. An extra 20% self-weight is added to compensate for permanent loads of asphalt and curbs. In this graph, the shear stress for the individual bridges is determined and plotted with data points.

The shear check for the slab part of all example bridges is executed and it can be seen that the shear capacity is (almost) never exceeded by the shear stress ( $\rho$ ), see Table 3.8, and Figure 3.12. This means that no additional shear reinforcement needs to be applied. Small differences between the plotted graphs and the data points are due to assumptions made for the effective width, self-weight and additional dead weight. Looking at the available reinforcement drawings of the example bridges, the longitudinal reinforcement is bent at the position of a support, resulting in extra shear capacity. For bridge number 4-9, the material properties are unknown and therefore assumed to be according to the values of the corresponding design code. The Dinkelbrug is the only bridge with a Unity Check for shear force higher than 1.0 and is the oldest bridge in the list. Here the suggestion is made that at that stage of structural design, the shear failure mode is not designed for.

<sup>i</sup>Shear force due to self-weight determined by the average weight of the mid strip plus the edge beams.

Table 3.8: Shear check for several example bridges

Bridge	Concrete quality	Load class	$\rho$	Allowable stress	UC	Slenderness
	-	-	kg/cm <sup>2</sup>	kg/cm <sup>2</sup>	-	End-span, mid-span
1 KW4	K350	60	7.82	8.67	0.90	1/17 1/22
2 KW7	K350	60	8.33	8.67	0.96	1/18 1/22
3 Ruytenschildtbrug	K350	45	6.78	8.67	0.78	1/16 1/16
4 Heemstedestraatbrug	K250	B	6.86	7.33	0.94	1/20 1/27
5 Moergestel	K300	B	6.90 <sup>i</sup>	7	0.99	1/18 1/25
6 Waalwijk	K300	B	6.6 <sup>i</sup>	7	0.94	1/17 1/24
7 Ruytenschildtbrug	K350	45	6.78	8.67	0.78	1/16 1/16
8 Ellermansbrug	K250	B	6.61	7	0.94	1/20 1/25
9 Dinkelbrug	K200	B	5.56	5	1.11	1/15 1/15

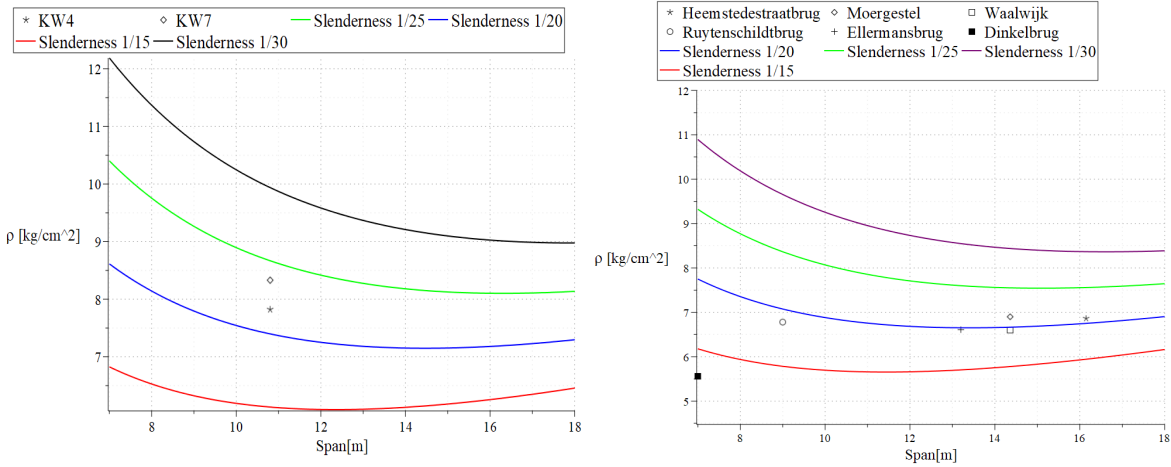


Figure 3.12: Determined shear stress for load class A/60 (left) and for load class B/45 (right), for a variable span length and different deck slenderness ratio's. The shear stress is due to a combination of self-weight, distributed traffic load and concentrated traffic load.

### Shear capacity for bridges with a non-rectangular deck cross-section

The shear capacity of a bridge deck with edge beams deviates from a rectangular cross-section deck. The stiffer edge beams attract more forces than the mid strip. A method to calculate the required shear reinforcement in a beam is developed by van der Schrier (1938) and presented below in formulae 3.9 - 3.12. From the position where the shear stress exceeds the allowable stress  $\sigma'_b$ , shear force reinforcement should be applied, illustrated in Figure 3.13.

$$\rho = \frac{3}{2} \frac{D}{bh_t} \quad \text{or} \quad = \frac{D}{bz} \quad \text{In case of a cracked cross section} \quad (3.9)$$

$$D8 = \bar{\sigma}_b \cdot b \cdot z \quad (3.10)$$

$$y = \frac{D - D8}{q_{total}} \quad (3.11)$$

$$F_{y0} = \frac{\frac{8+\rho}{2} \cdot 100 \cdot y}{\sqrt{2} \cdot \sigma'_a} = A_s \quad (3.12)$$

Where:

D = the applied shear force, caused by permanent- and imposed loads;

b = width of the edge beams;

z = the lever arm of the cracked cross section;

$\rho$  = shear stress;

$\bar{\sigma}_b$  = concrete allowable shear stress;



$\bar{\sigma}_a$  = steel allowable tensile stress;

$q_{total}$  = total distributed load on the structure causing shear stresses. In this case: self-weight, permanent loads, distributed traffic load and concentrated traffic load;

$A_s$  = cross-sectional area of (shear)reinforcement which is required along the length 'y', placed at an angle of about 45 °.

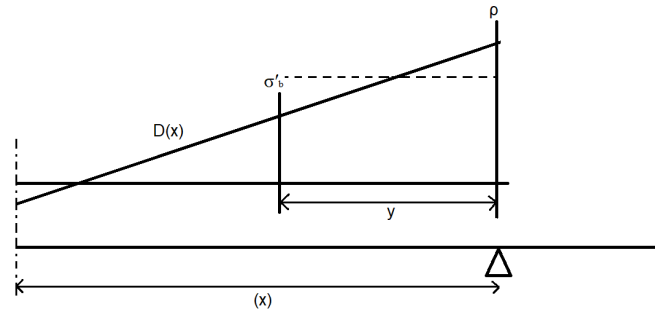


Figure 3.13: Determining the area where extra shear capacity is required.

The GBV codes prescribe the necessity of stirrup reinforcement in beam structures. This means that (a part of) the bent longitudinal reinforcement, is recalculated to stirrup reinforcement. The applied reinforcement in the cross-section is now a combination of the bent rebars  $A_{s1}$  and the stirrup reinforcement  $A_{s2}$ , determined as follows:

$$A_s = A_{s1} + A_{s2} = 2 \cdot \frac{1}{4} \pi d_{s1}^2 + 2 \cdot 2 \cdot \frac{1}{4} \pi d_{s2}^2 \cdot y \cdot \sqrt{2} \quad (3.13)$$

An example of a shear force check for a bridge from Waalwijk can be found at the end of Appendix B. Here, the assumption is made that 100% of the permanent and imposed loading can be transferred to the edge beams and is found plausible.

### 3.7. Discussion

Former bridge design with former available tools and methods has led to a simplified geometry and caused the urge to determine only the necessary. This can be seen in practice by the following examples: Schematising the bridge as a beam structure, calculation of only governing moments in the supports and mid-spans, calculation of one DAF for a bridge with different end- and mid-span lengths, checking of the shear force capacity solely for beam structures, leaving the shear capacity of slab structures to their geometry/slenderness, assuming bending moment to be the governing failure mode.

The comparison of the RE required reinforcement with the present reinforcement, shows conservative results for the estimated reinforcement amount, and so the capacity is (almost) never overestimated.

From RE of former bridge design is obtained that the main reinforcement in many cases is dimensioned based on the governing cross-sections at the mid-spans and the mid-supports. Here is aimed for a Unity Check of 1.0, where structural safety is introduced by allowable material stresses leading to an ASD.

In case a bridge has end-span lengths equal to mid-span lengths, maximum span-moments occur in the end-spans and should therefore be RE.

Safety in former bridge design was solely introduced by the use of allowable stresses in the N-method leading to an ASD. In former bridge design, the amount of support reinforcement is equal or more than the amount of span reinforcement. However, notable is that the bridges KW4 and KW7 designed for load class 60 and the Ellermansbrug designed for load class B, have support reinforcement equal to the span reinforcement.

In former design is obtained that edge beams have an unambiguous structural capacity. A large distribution in transverse reinforcement amounts can be obtained from Figure 3.11. Larger amounts of transverse reinforcements are found for class A/60 bridges, and slab bridges with stiffened edge beams. This can be substantiated by the need for (larger) force transfer. The transverse reinforcement meets in all cases the requirement of 20% transverse reinforcement of the main reinforcement.



### 3.8. Conclusion

From the hand calculations can be concluded that the main reinforcement can be RE for rectangular RC slab bridges. The comparison in reinforcement amounts between the RE reinforcement and the reinforcement from available documents shows an equally conservative approach.

The reinforcement in stiff edge beams in case of a non-rectangular cross-section is designed based on experience. The presumption that the edge beams are designed for 100% of the permanent- and imposed loads from the mid-strip is plausible, but this assumption should be further examined. The layout of the bent bars in the available technical drawings is only limited by the prescription from the GBV code. The distribution in transverse reinforcement amounts is large, and will not be further examined in this study. The restriction of a minimum transverse reinforcement of 20% of the main reinforcement is only recognised in former design.

The next Chapter 4 deals with the question: How does the residual capacity of existing RC slab bridges constructed with plain reinforcement relate to the current traffic loading? This will be examined by constructing a parametric tool to automate the RE method and assess bridges for the current assessment codes.

Chapter 5 tries to elaborate on the reliability of the approach and the effect of uncertainty in input parameters, by a risk analysis. This corresponds with the research question: What are the influences of the engineering factor and the execution factor on the reliability of the reverse engineering method?

# 4

## Reverse Engineering and assessment by coding

### 4.1. Introduction

The hand calculations from Chapter 3 can be automated to reach for an automated and parametric approach for input and output. A computer code enables an in-depth study into the input parameters from former design and the assessment of the RC slab bridges.

The RBK-1-1 (RWS and GPO, 2013) advises through Table 3.1 for several construction types the modelling approach. According to this table, a slab structure is best assessed by modelling with beam elements, with the restriction of an intersection angle of  $> 80$  gon.

The Guyon-Massonnet method is executed with the use of an Excel-file, and is found to be time consuming if needed to be programmed in an other software program. For this reason, coding of a RE-tool needs to be set up in a programming language which can communicate with Excel. The programming language which satisfies all three features of the computer code and is broadly recognised is Python.

The input control of the computer code is divided into two options: Option one is a parametric approach, obtained in the main part of this report and option two is a single case approach, obtained in the Appendix C. The single case approach enables the user to RE and assess a specific case by filling in all input parameters, making a RE-tool.

#### Python

Python is a high-level, interpreted and general-purpose dynamic programming language that focuses on code readability, (Kuhlman, 2011). Python is an object-oriented programming language, meaning that functions, classes, strings and even types are objects in Python. Many functions need to be defined with variables which do not have a fixed type, in order to program dynamically. Python is developed under an OSI-approved open source license, making it freely usable and distributable even for commercial use, (*Welcome to Python.org*, n.d.). Python has extensive support libraries for multiple purposes. The libraries used in coding are Anastruct, Numpy, Openpyxl, xlwings, Matplotlib and Tkinter. AnaStruct is a Python implementation of the 2D Finite Element method for structures. It allows the user to do linear structural analysis of frames. It helps to compute the forces and displacements in the structural elements. Matplotlib is a plotting library for the Python programming language and its numerical mathematics extension NumPy. It provides an object-oriented application programming interface (API) for embedding plots into applications using general-purpose graphical user interface (GUI) toolkits like Tkinter. The Python code is set up parametric for its input, with a specific datatype, leading to a parametric output. The parametric approach makes a group assessment possible for a single variable parameter or even for multiple variable parameters. Python can communicate with Excel with the use of packages Openpyxl and Xlwings.

A schematic flowchart of the computer code is shown in Figures 4.1. The computer code consists of a RE part where the focus lies on the determination of the existing reinforcement, and the assessment part where the focus lies on the assessment of the existing bridge for current loading.

#### Description of the flowchart

The computer code consists of two parts, the first is the RE part (left), and the latter the Assessment (right). The basis of the computer code is a main file (red) linking both parts together, and functions as an input and

output medium. Attached to the main file are modules separating code into parts holding related data and functionality.

Figure 4.1 is imaging the calculation steps in the computer code in a synchronised way.

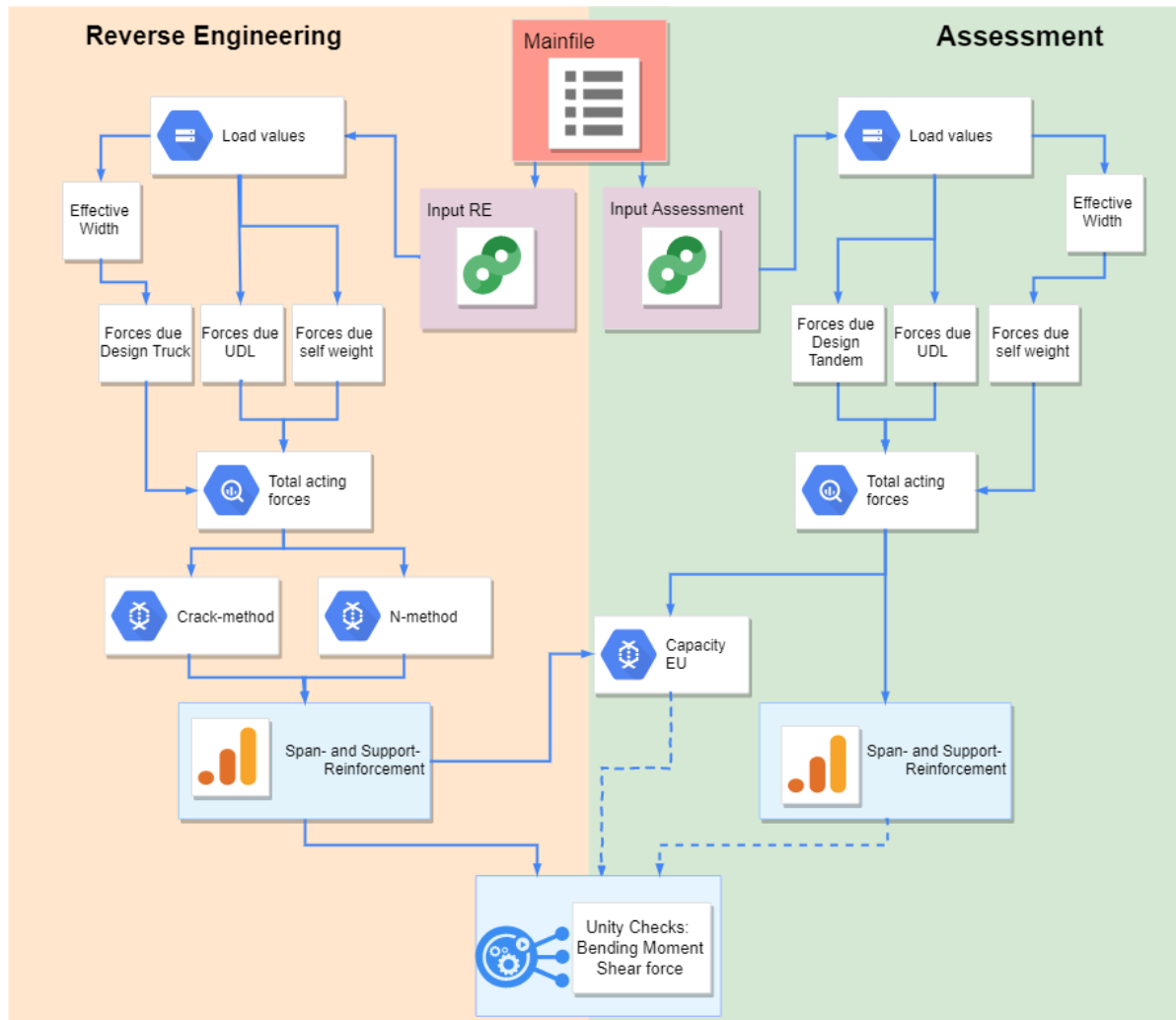


Figure 4.1: Schematic flowchart of the computer code in Python.

The input and output of the computer code are listed in Table C.1 in Appendix C. A graphical user interface (GUI) enables demonstration of the RE-tool for a single case, to interact with the computer code visually. Input as general- and geometrical information, and output as force distributions, required reinforcement and Unity Checks are presented to the user. The presentation of the GUI can be found in Appendix C, Figures C.3 - C.8.

## 4.2. Assumptions

The preliminary study into structural design of RC slab bridges in Chapter 2 led to four design periods, which will be assumed in the parametric study. Within these periods is the RE reinforcement expected to be constant and between the different design periods are differences in applied reinforcement amounts expected. In the parametric study, it is inconvenient to vary all parameters at the same time. Therefore, to show the effect of one or two parameters, all other parameters should be constant. So, assumptions should be made for all parameters held constant during the running of the computer code. Convenient values are chosen based on knowledge from the preliminary study and the hand calculations.

### Geometrical parameters

Symmetry in geometry is used for multiple span bridges as was done in the previous chapter. In the com-

puter code, an asphalt layer with a thickness of 5 cm is used in all former concrete slab bridge design, and for the assessment an additional asphalt layer of 7 cm is taken in to account on top of the former layer. Former calculations from the preliminary study show that additional permanent load is not taken into account. In the assessment, the additional permanent load is left out as well. The most common concrete cover on the outer reinforcement bar in former concrete bridge design is found to be 3 cm. In the parametric study, an example edge distance of 1.0 meter is applied for the positioning of the design truck and design tandem. A slab thickness at the supports is assumed to be 5% larger than at mid-span. A transverse beam of 1.0 meter width is applied at the supports. Available bar diameters for RE of the reinforcement from which the computer code can choose, are obtained from former technical drawings. Former common bar diameters deviate from the currently available bar diameters. The distance between reinforcement layers is a parameter which is difficult to assess. The distance cannot be measured with non-destructive testing and is found unknown, if the documentation is missing. Therefore, a very conservative distance is assumed of 0.0 cm, leading to a lower amount of RE reinforcement compared to a distance of > 0.0 cm. Material qualities have assumed values according to the allowable stresses from the corresponding design codes.

#### **Traffic load**

The traffic load from the Eurocode (EC) consist of an uniformly distributed traffic load and loading by the design tandem. The maximum support moment due to concentrated loading is determined with the shape deformation method with the assumption of equal support stiffness. The deviation of this assumption is assessed in a comparison with a software program Technosoft and is found to be very small and acceptable, see Section C.2 in Appendix C.

The maximum support- and span moments from former design are calculated by searching for the maximum influence value at steps of 1/10 of the span length. Existing former calculations show this method to find the governing load position of the design truck. In contrast, the maximum support moment due to loading from the design tandem can be optimised for its position with the use of the RE-tool.

The governing position of traffic loading in the transverse direction is defined by the combination of the most unfavourable position, and the number of design trucks or -tandems. In the computer code, the contribution of one or two design trucks in former bridge design, and one, two or three design tandems in the assessment are taken into account. In almost all former bridge design until approximately 1970, two carriageways of each 3 meters fit physically on the bridge decks, or just loading from maximum two carriageways is taken into account. The VOSB1963 prescribes loading by a maximum of two design trucks in combination with the distributed traffic load, where the total combination is reduced to 80%. In the assessment the possibility is to either determine traffic loading by the actual carriageway layout or the virtual carriageway layout, wherein the actual carriageway layout the design truck is positioned in the centre of the lane, leading to a slightly larger load distribution of the design tandems compared to the virtual carriageway layout.

In the assessment, the maximum support moment is reduced to the point where the transverse beam ends. An approximation is made by reducing the moment along a linear line between maximum support and maximum span moment. In this way the reduction is never exceeding the actual decrease of force which has a parabolic function, see Figure C.2 in Appendix C for a visual explanation. The maximum shear force is determined at the centre of the support and the capacity at the end of the transverse beam, leading to a conservative approach in terms of concrete shear capacity. Main reinforcement influences the shear capacity of the cross-section, so only the top layer of main reinforcement is taken into account.

### **4.3. Dimensioning of the main reinforcement**

The computer code determines the maximum span and support moments in the structure where the required main reinforcement is designed for. An optimisation function is written where the bending moment capacity is increased until the resulting bending moment from traffic- and permanent loads is exceeded, resulting in an ASD with a Unity Check of < 1.0. The bending moment capacity is increased by increasing the total reinforcement per meter slab width. This reinforcement amount is at the same time determined by the combination of the bar diameter and the stepwise increment of the available bar diameter. The aim of the optimisation is to reach for a Unity Check of < 1.0 meaning that the loading side is equal or smaller than the capacity side. The mutual spacing between the bars is chosen to be an input parameter and set by default to 10 cm.

The minimal required reinforcement amount is determined by two parameters, the bar diameter and the bar spacing. The configuration of bar diameter and bar spacing is variable, where the multiplication has

a limitation of the minimum RE required reinforcement. Hence a reinforcement table is made where the configuration between bar diameter and bar spacing is made, see Figure C.5 in Appendix C. A determined reinforcement amount can be filled in, to find the complying ratios between bar distances and bar diameters.

## 4.4. Assessment for current traffic- and permanent loads

In the problem description in Chapter 1, it is explained that the traffic intensity, as well as the axle, and the average vehicle weight have increased. On the other hand, the structural design codes have changed over the years. Therefore, it is necessary to investigate the safety/reliability of existing structures for the design loads with loading factors from the current codes NEN1990 (2011) and NEN1991 (2011). In the development of the structural design codes is the ASD changed into a Load and Resistance Factor Design (LFRD). In a LFRD structural safety in the ULS is encountered by load factors and material factors. In this chapter are Unity Checks determined by dividing the current loading by the RE capacity.

### 4.4.1. Load reduction factors

The following two load reductions are obtained in the EC load model in the parametric study. First, in case a shorter reference period than 100 years for imposed loads is used, may the vertical loading from normal traffic (LM1 and LM2) be reduced by  $\psi$ -factors according to Table 1 from NEN8701 (2011). Second, a trend-reduction  $\alpha_{trend}$  for the influence of the trend relative to the year 2060 may be applied for the traffic loading from LM1 and LM2, according to Table 2 from the NEN8701 (2011). The parts applicable for this study from Table 1 and 2 from NEN8701 (2011) are presented in Figures C.3 and C.4.

### 4.4.2. Reliability of existing bridges

For the sake of reliability differentiation consequence classes (CC) are defined (from NEN1990 (2011) Appendix B), based on the consequence of failure or malfunction of the structure. For the assessment of the slab bridges CC2 is assumed, with a failure probability of  $3 \cdot 10^{-4}$  and a minimal reference period of 15 years. The decision is substantiated with the fact that existing bridges designed for load class 45/B are assessed.

New bridges to construct with CC2 have a minimum reliability index  $\beta$  of 3.8. However, a reduction of the  $\beta$ -value may be included because the reliability of an existing bridge may be lower than of a new bridge, due to socio-economic consideration of (financial) matters. An existing bridge is more expensive in its maintenance compared to a new bridge.

Existing bridges within the scope are built with a reliability index  $\beta$  of approximately 3.6. This can be substantiated with the fact that the failure probability in the period before 1972 was lower than nowadays. However, a precise average  $\beta$ -value for structures constructed before 1972 is not defined in the literature, (Vrouwenvelder et al., 2012).

The reliability corresponds with the current  $\beta_r$ -value for 'Reconstruction' ('Verbouw') for National roads which is 3.6 as well, from the RBK-1-1. Due to the focus of this thesis upon class B/45 bridges which can be categorised as bridges in local roads, the  $\beta$ -value may be reduced. The reliability index  $\beta_r$  for CC2 according to the NEN8700:2011 from Table B.2 is 3.3, and 3.1 in case the structure has legally been build before 2003 (Bouwbesluit).

A safety level lower than 'Reconstruction' is 'Disapproval' ('Afkeur') with a  $\beta_b$  of 2.5 and functions as the lower limit boundary for the safety of existing structures. A structure allocated with the assessment level 'Disapproval' has a residual lifetime of 1 year.

In the NEN8700:2011 correspond the values between brackets from Table A2.2(B) for 'Reconstruction' with the  $\beta_r$  of 3.1. The partial load factors corresponding to the  $\beta_r$  of 3.1 are presented in Table 4.1. The partial load factors in Table 4.1 differ for equation 6.10a and 6.10b, where for the first equation a high permanent load factor in combination with a transient load factor ( $\psi_1$ ) of 0.8 for the traffic load is used. In the second equation is the transient load factor ( $\psi_1$ ) 1.0 and is often found to be the governing load combination for concrete bridges without large additional permanent loads. The partial load factors for the assessment level 'disapproval' can be found in Appendix C Table C.2 and is also divided by the two equations 6.10a and 6.10b.

Table 4.1: Partial load factors  $\gamma$  for the ULS for the assessment level 'Reconstruction' for CC2 with  $\beta_r = 3.3$  (3.1), from the NEN8700 (2011) Table A2.2(B).

	Permanent load (unfavourable)	Traffic load	$\psi_1$
Load combination (eq. 6.10a)	$\gamma_{Gj,sup}$	$\gamma_{Q,1}$	
Consequence Class 2 (eq. 6.10b)	1.25	1.25 (1.20)	0.8
Consequence Class 2	1.15 (1.10)	1.25 (1.20)	1.0

### Residual lifetime/ Reference period

The safety after assessment must be attuned upon the residual lifetime of the structures, as applies for newly structures. Recommended is to set the minimum residual life time of a structure to 15 years. The reference period for the structural safety can be equal or larger than the residual lifetime. For CC2 must the reference period for imposed loading be at least 15 years, even when the residual lifetime is 1 year according to a strength assessment. A load reduction factor may be applied in case a reference period smaller than 50 years is chosen. However, in the parametric study this reduction factor is not included.

### 4.4.3. Crack width and Fatigue

In the current design of new structures; crack width for concrete, and fatigue for steel and concrete are failure modes to design for. In former design concrete and steel qualities are used with rather low yielding stresses but with high yielding capacity. So, if the structure is loaded for its ULS, the reinforcing steel yields at low stresses leading to small crack widths. For this reason, is it not necessary to calculate the current-, or former crack width control of the former structures designed with plain reinforcement. As an alternative for the crack width control calculations, the structure should visually be inspected, according to the RBK-1-1. In case the inspection leads to uncertainties towards the serviceability of the structure, adequate measures should be implemented. Cracking of the concrete is an important visual sign to focus on during the inspection.

It is also not necessary to check fatigue of steel and concrete due to the low material stresses of concrete and steel. Rather low stress changes occur due to the low yield strength of steel and concrete, by traffic loading. The high self-weight of concrete bridges causes low stress changes as well. In case fatigue calculations are performed a damage factor (schadegetal) of lower than one, or even probably close to zero is to be expected. Also, welding of reinforcement was uncommon in these old structures, and former design codes prescribed to avoid welding of reinforcement in general.

### 4.4.4. Current material properties

The current material properties can be obtained from, former design codes, former calculation and technical drawings, or lab test. In case the material strengths are determined based on lab tests, a factor of  $K_t=0.85$  should be taken in to account according to the RBK-1-1. However, in the RE-tool the material properties are known in general only available through documentation or from the corresponding design code. The assumption that only steel qualities of QR22 and QR24 are used for plain reinforcement results in two possible steel stresses of  $f_{yd}=198 \text{ N/mm}^2$  and  $f_{yd}=209 \text{ N/mm}^2$  respectively, see RBK-1-1 Table 2.6.

The RBK-1-1 prescribes two methods to obtain the current concrete strength. The first method determines the current concrete strength based on the design year and the corresponding design code. The second method focuses on bridge assessment with unknown material properties. It states that research led to a minimum concrete strength of  $f_{cd}=18 \text{ N/mm}^2$  for bridges constructed before 1976, due to time effect causing ongoing hydration and strength increase. In case material properties are present from documentation or lab test, the highest values from the two methods may be used.

## 4.5. Current capacity based on assessment codes

### 4.5.1. Bending moment capacity

The bending moment capacity is to be determined by performing a horizontal force equilibrium and moment equilibrium in a cross-section. Therefore, the current material strengths are used, so the required amount of reinforcement can be calculated. The partial material factors for concrete (1.5) and steel (1.15) need to be

taken into account for the ultimate limit state (ULS). The bending moment capacity is determined by two methods, one with the RE reinforcement (equation 4.1), and one with the required reinforcement (capacity) for current loading when is optimised for a Unity Check of 1.0. In this chapter both methods are used for the parametric study.

$$M_{rd} = A_{SRE} \cdot f_{yd} \cdot Z \quad (4.1)$$

With:

$A_{SRE}$  = the amount of RE reinforcement;

$f_{yd}$  = the current design strength of the former steel qualities, according to the RBK-1-1;

$Z$  = the lever arm.

### 4.5.2. Shear Capacity

The RBK-1-1 prescribes two formulae 4.2 and 4.3 to determine the shear capacity for a rectangular concrete cross-section. The maximum of these two formulae may be used for the shear capacity of the cross-section.

$$V_{Rd,c} = \left[ 0,12k_{cap} \cdot k(100\rho_l f_{ck})^{\frac{1}{3}} + 0,15\sigma_{cp} \right] b_{wgem} d \quad (4.2)$$

$$V_{Rd,c} = \left[ v_{min} + 0,15\sigma_{cp} \right] b_{wgem} d \quad (4.3)$$

For massive reinforced slabs:  $k_{cap} = 1,2$ ;

$k = 1 + \sqrt{\frac{200}{d}} \leq 2,0$  with  $d$  in mm.

For non-prestressed massive reinforced slabs and beams may  $v_{min}$  be determined with:

$$v_{min} = 0,83 \cdot k_p^{\frac{3}{2}} \cdot k^{\frac{3}{2}} \cdot f_{ck}^{\frac{1}{2}} / f_{yk}^{\frac{1}{2}} \quad (4.4)$$

With:

$b_{wgem}$  = the average width (for the attributable area);

$d$  = the average height of the centre of the tensile reinforcement in the outer layer until the bottom, or top of the slab;

$\rho_l$  = the amount of bending tensile reinforcement, located in the effective width ( $b_{eff}$ ), in this study a conservative approach is chosen where only the reinforcement in the upper layer at a support is taken into account;

$\sigma_{cp}$  = the average concrete compression stress, due to the design value of the normal force, in this research left out due to the absence of prestressing.

## 4.6. Reinforcement amounts based on former- and current structural design

The required reinforcement is determined according to the former design codes, and according to the assessment with the Eurocode: Load model 1 (LM1) and load model 2 (LM2) with load factors from the NEN8700 (2011). The required reinforcement amounts for different load models are determined for a variable mid-span length and variable slenderness. At the position of the maximum span moment and at the position of the maximum support moment with the lowest capacity, the required reinforcement amounts can be determined. The two determined reinforcement amounts can be expressed in a reinforcement difference ratio to clarify the development in required reinforcement amounts over the span length for different bridge slenderness. The slenderness of existing RC slab bridges is examined with a database from the Dutch Directorate-General for Public Works and Water Management (Rijkswaterstaat) which includes mainly class A/60 bridges. It can be expected that existing bridges designed for class B/45 have the same slenderness or are more slender due to a reduced load model.

### 4.6.1. Span reinforcement

The formulae below 4.5 to 4.7 express the calculation steps for the executed calculations. Here, the  $S$  stands for the load side determined for a specific load model and the  $R$  for the resistance according to a specific code. Figure 4.2 and the Figures C.11, C.12 and C.13 in Appendix C show the determined reinforcement amounts at mid-span. In each case the reinforcement amounts are compared by dividing the required amount for the EC with the RE amount, giving an indication of the development of reinforcement amounts in the design periods from Table 2.7. From the results of each design period turn out that the periods 1940-1950 and 1950-1962 are most critically designed. In the period 1940-1950 is the (new) DAF (Section 2.4) introduced in the GBV1940 for concrete bridges assumed, the traffic load class A/B from the VOSB1933 (Section 2.3), the N-method (Section 2.2.3) to determine the cross section capacity and the effective width method from the GBV1940 (Section 2.5). In the period 1950-1962 are the same methods as for the period 1940-1950 assumed, only the the Guyon Massonnet method (Section 2.5) is assumed instead of the method from the GBV1940.

$$\frac{S_{RE}}{R_{RE}} \quad \text{optimised for} \quad UC = 1.0 \quad (4.5)$$

$$\frac{S_{EC}}{R_{EC}} \quad \text{optimised for} \quad UC = 1.0 \quad (4.6)$$

$$\frac{R_{RE}}{R_{EC}} \Rightarrow \frac{AS_{RE}}{AS_{EC}} = \text{Reinforcement difference ratio} \quad (4.7)$$

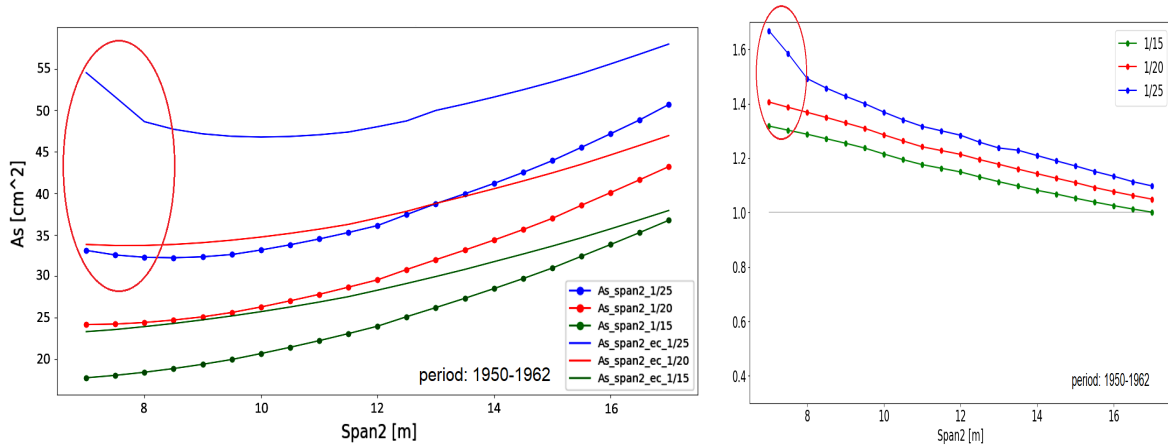


Figure 4.2: RE reinforcement at mid-span for load class B and the EC (left) and the reinforcement difference ratio (right) for the period 1950-1962, for a variable mid-span length for three slenderness' 1/15, 1/20 and 1/25. The effect of the slenderness on small spans highlighted with the red ovals.

From the RE reinforcement amount graphs and the reinforcement difference ratio graphs is obtained that the slenderness has large influence on short-span bridges, indicated with the red oval in Figure 4.2. Therefore, a minimum slab thickness is included in the computer code of 400 mm, which can be substantiated by the technical drawings from the preliminary study. The minimum thickness found is approximately 450 mm, so a spacious lower limit is chosen.

### Unity Checks

The RE reinforcement can be used to determine the current capacity. By dividing the current load from the EC with the current capacity with RE reinforcement, a Unity Check can be determined, see formulae 4.8 to 4.10. Figures 4.3 show the Unity Checks for RE reinforcement for the bending moment at mid-span for all design periods, with a minimum slab thickness of 400 mm.

$$\frac{S_{RE}}{R_{RE}} \quad \text{optimised for} \quad UC = 1.0 \quad (4.8)$$

$$R_{RE} \Rightarrow AS_{RE} \Rightarrow R_{EC} \quad (4.9)$$



$$\frac{S_{EC}}{R_{EC}} = UC \quad (4.10)$$

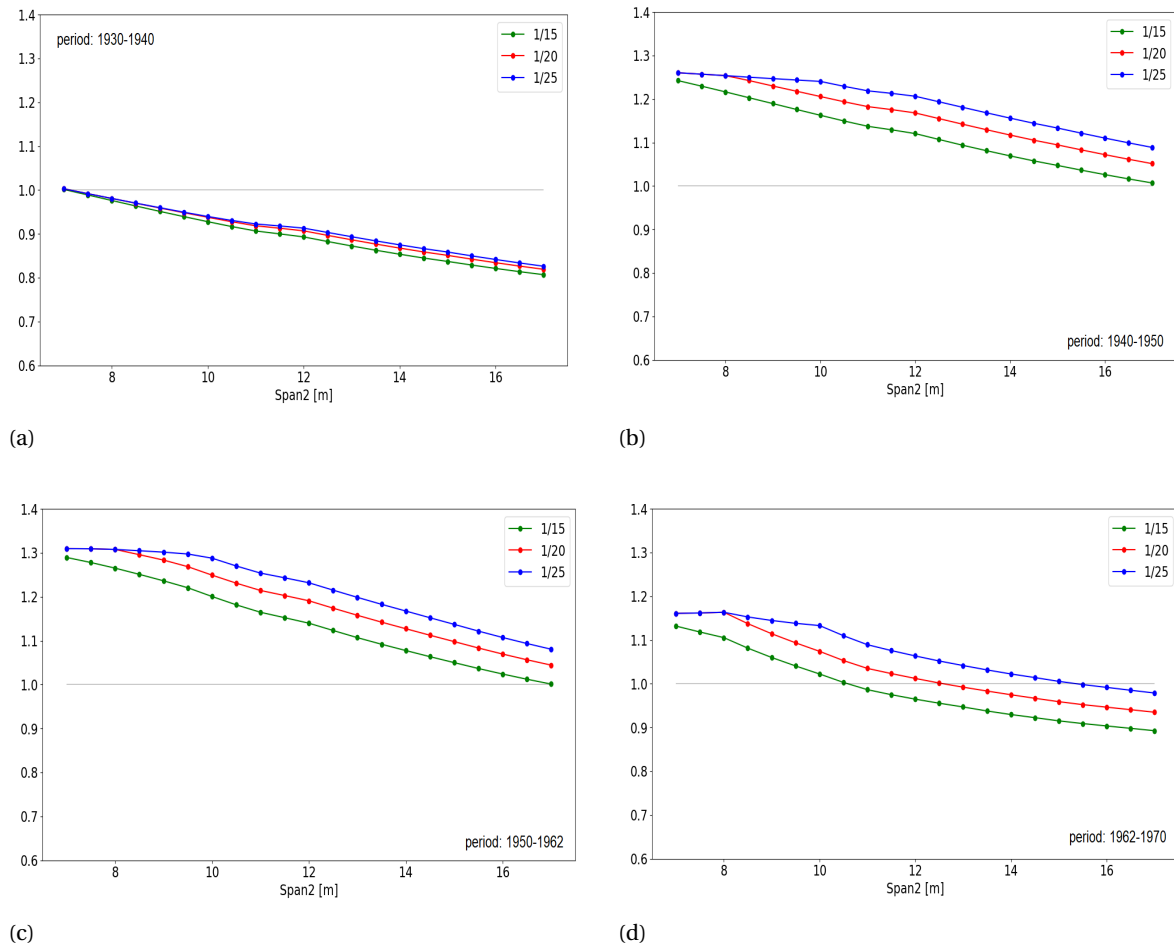


Figure 4.3: Determined Unity Checks for bending moment at mid-span, for the periods 1930-1940(a), 1940-1950(b), 1950-1962(c) and 1962-1970(d) for a variable mid-span length for three slenderness' 1/15, 1/20 and 1/25, and a minimum slab thickness of 400mm.

The period from 1950-1962 is found to be the most critical period in structural design of the bending moment capacity of RC slab bridges. Therefore, this period is focused on in the next sections, and the other periods can be found in the Appendix C or are only contemplatively discussed in comparison to the critical period.

#### 4.6.2. Support reinforcement

In case a transverse beam is present no advantage is obtained for the structural capacity in former design. However, in the assessment a reduction is taken into account in case a transverse beam is present, see Figure C.2 in Appendix C. This reduction is determined by assuming a linear decrease between hogging and sagging moment, over the distance centre-to-edge of the transverse beam. For the support are also the Unity Checks determined, according to formulae 4.8 to 4.10. Figure 4.4 shows the RE reinforcement and the Unity Checks for RE reinforcement for the bending moment at the support. For the design periods 1930-1940, 1940-1950 and 1962-1970 is referred to Appendix C, Figures C.14, C.15 and C.16.

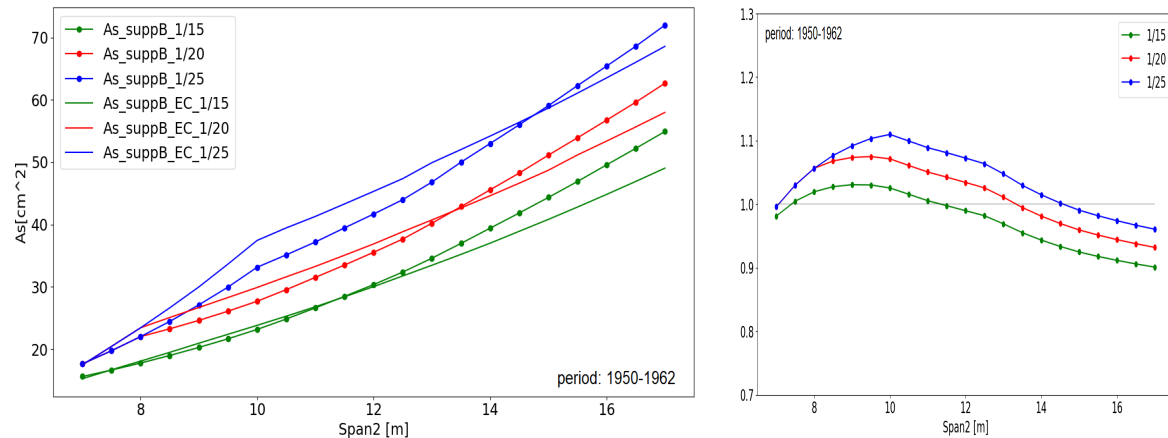


Figure 4.4: RE reinforcement at a mid-support for load class B and the EC (left) and Unity Checks (right) for the period 1950-1962, for a variable mid-span length for three slenderness' 1/15, 1/20 and 1/25, with a minimum slab thickness of 400mm.

#### 4.6.3. reinforcement difference ratio support/span

The amount of main reinforcement in the mid-support and at mid-span are both RE with the computer code. The difference between these amounts (support/span) is visualised in Figure 4.5 for bridges design with load class B/45. The reinforcement difference ratio support/span of bridges designed with load class A/60 is shown in Appendix C Figure C.20. However, in several former design the amount of support reinforcement and span reinforcement are equal, for bridges with span ratio  $L1/L2 \leq 0.8$ .

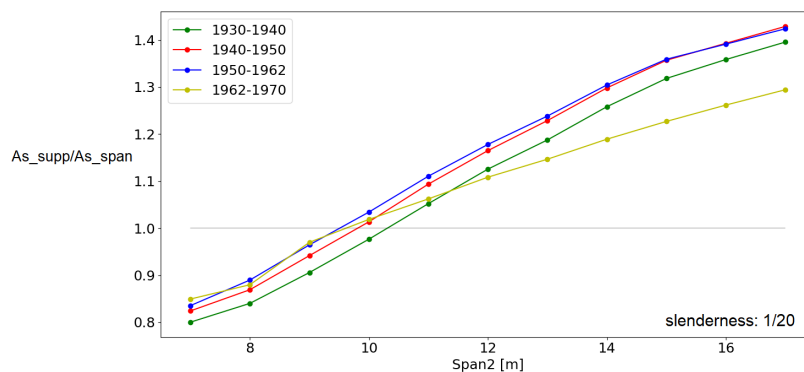


Figure 4.5: reinforcement difference ratio between the RE support reinforcement and the RE span reinforcement for load class B/45 for  $L1/L2 \leq 0.8$ , a slenderness of 1/20 and a minimum slab thickness of 400mm.

For the periods 1950-1962 the support reinforcement amount is based on the determined RE span reinforcement and the effect presented with Unity Checks at the support, see Figure 4.6. Consequently, the number of reinforcement layers at the support is limited to one. A constant decrease of about  $20\text{cm}^2$  RE reinforcement for all slenderness can be seen. The Unity Check is defined by the bending moment due to loading according to the EC, divided by the bending moment capacity of the support with the RE amount of reinforcement from mid-span. Here, self-weight has an increasing significant influence on the support bending moment. This can be seen in the change in: bridges with low slenderness have higher Unity Checks, than bridges with high slenderness have lower Unity Checks. The assumption of applying less RE reinforcement from span effects the thicker bridges more due to the constant decrease of  $20\text{cm}^2$ .

### 4.7. Decentralised traffic load model

Recent research from TNO (Steenbergen et al., 2018) in cooperation with the municipality of Rotterdam, about traffic loading in the local road network, led to new traffic load factors and resulted in the Decentralised traffic load model (DC Load model). Bridges with less than 125 000 crossing vehicles of  $>3.5$  ton a year ( $N_{obs} \leq 125\ 000$ ) approximately 625 per working day, and with an influence length of maximum 20 me-

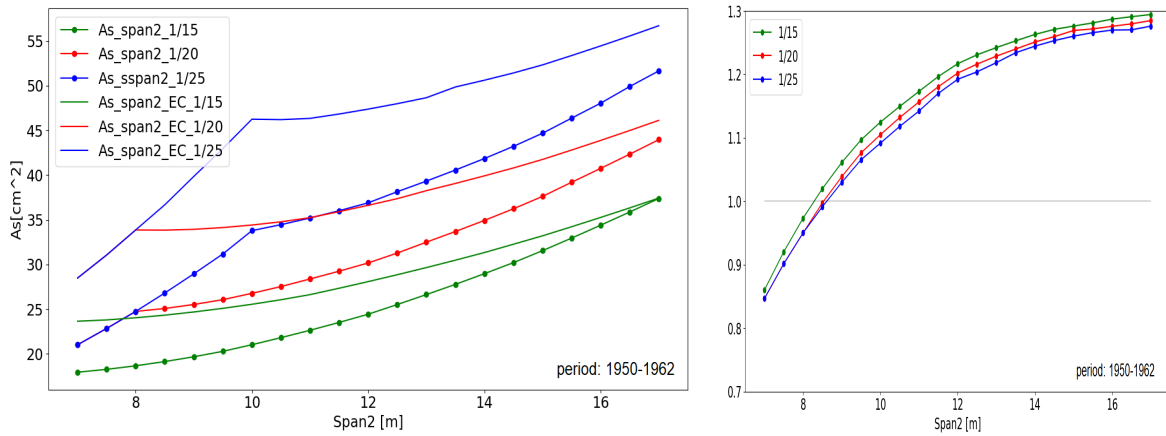


Figure 4.6: Determined support reinforcement amount based on the RE span reinforcement and in the assessment based on the maximum support moment due to EC (a). Corresponding Unity Check (b) for the period 1950-1962 according to the assessment calculations, for a variable mid-span length for three slenderness' 1/15, 1/20 and 1/25, and with a minimum slab thickness of 400mm.

ters, and without an annual exception for trucks heavier than 60ton, can have deviating traffic load factors according to Steenbergen et al. (2018). Measurements of actual traffic loading by the municipality of Rotterdam in the local road network show the abundance of the vehicles reaching the upper load limit. Here for, the load factor for concentrated traffic loading ( $\alpha_Q$ ) can be reduced to 0.8 and the load factor for distributed traffic load ( $\alpha_q$ ) in the heavy lane increased to 1.35. The number of crossing vehicles of >3.5 ton influences the load rating on the bridge. In case  $N_{obs}$  is even less than 125 000 reduction factors are defined by TNO. For  $N_{obs} = 50\ 000$  the factor is 0.98 and for  $N_{obs} = 5\ 000$  the factor is 0.93. The modified load factors are in addition to the NEN 8700, prescribing consequence classes, reference periods and partial factors. As a result, the DC load model includes trend- and reference period factors.

The required reinforcement amounts according to the assessment with the DC load model decreased due to the traffic load factor modifications, see Figure 4.7. Compared to the results from the EC are the Unity Checks in the new situation for the most critical period 1950-1960 now below 1.0. The same calculations are executed for the three remaining periods and presented in Appendix C part C.6.

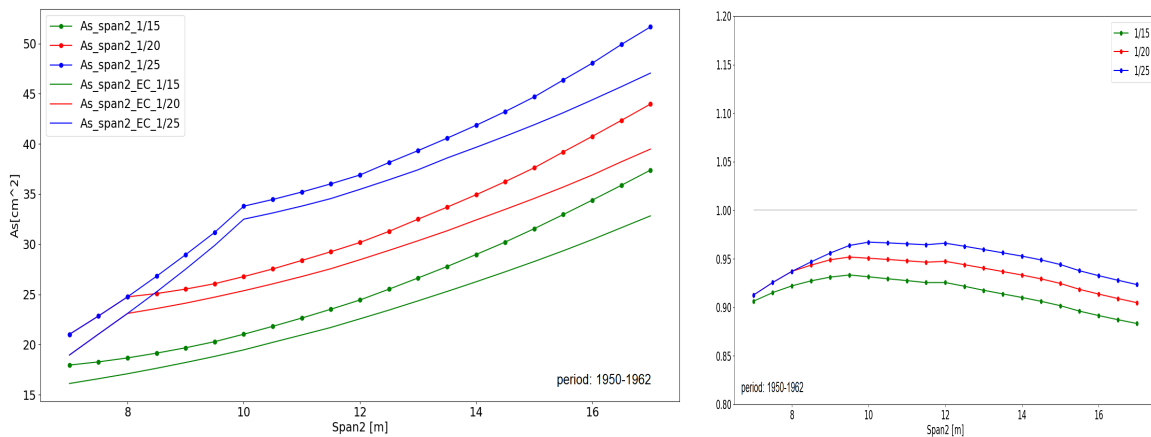


Figure 4.7: Determined span reinforcement amount for bending moment according to the former design code and assessed according to the DC load model (a). Corresponding Unity Checks (b) for the period 1950-1962, for a variable mid-span length for three slenderness' 1/15, 1/20 and 1/25, and minimum slab thickness of 400mm.

The Unity Checks for the bending moments of the support are determined with the DC load model as well. Compared to the results from the EC the Unity Checks in the new situation for the most critical period 1950-1960 are now below 1.0, see Figure 4.8.

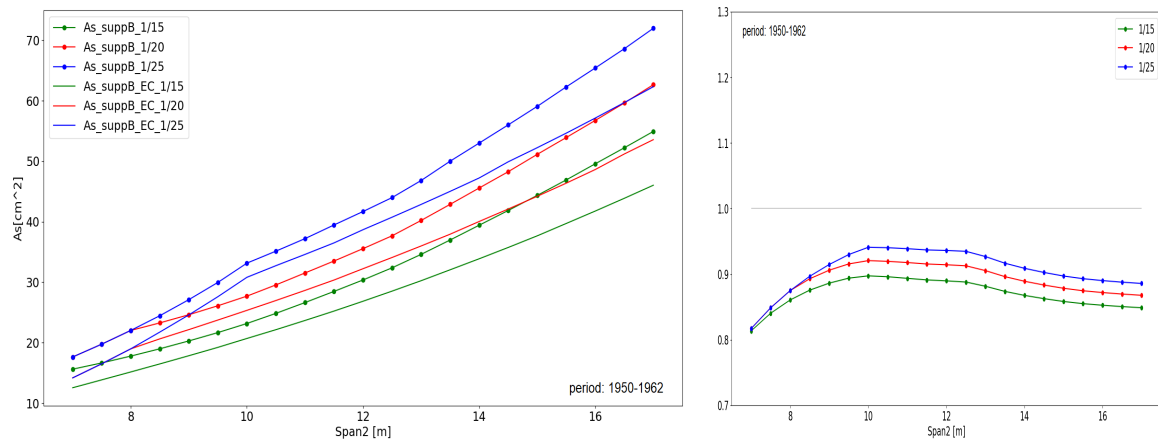


Figure 4.8: Determined support reinforcement amount for bending moment according to the former design code and assessed according to the DC load model (a). Corresponding Unity Checks (b) for the period 1950-1962, for a variable mid-span length for three slenderness' 1/15, 1/20 and 1/25, and minimum slab thickness of 400mm.

### Support with reinforcement from span for the DC load model

The Unity Checks for the support with the RE reinforcement amounts from span is determined with the DC load model. For all four periods are the graphs with Unity Checks shown, in Figures 4.9 and 4.10. Compared to the results from the EC are the Unity Checks in the new situation for the most critical period 1950-1962 now lower and shifted the boundary of Unity Check  $>1.0$  from 8 meters span to 10.5 meters span length, see Figure 4.9. Here, self-weight has significant influence on the support bending moment, as was stated in 4.6.3. Again, the switch of bridges with low slenderness having a higher Unity Checks than bridges with a high slenderness occurs.

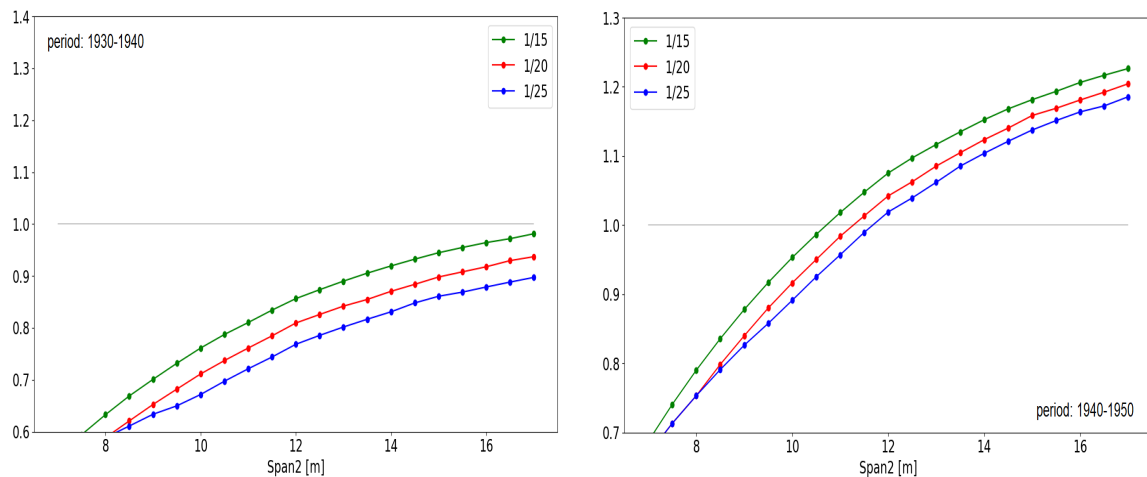


Figure 4.9: Determined Unity Checks for the bending moment at the mid-support for the DC load model with RE reinforcement from mid-span. Assessed for the period 1930-1940 and 1940-1950 with the amount of RE reinforcement from span, and according to the assessment calculation with DC load model, for a variable mid-span length for three slenderness' 1/15, 1/20 and 1/25, and minimum slab thickness of 400mm.

## 4.8. Shear control

A shear check is performed for RC slab bridges for the same design periods of Table 2.7. The capacity of the cross-section at the mid-support is determined based on the RE reinforcement for bending. The acting shear force in this cross-section is determined as an effect of the permanent loads, and the traffic loads from the EC. The face-to-face distance between axle and cross-beam is  $2.5d_l$ , which is the critical position for shear failure (Lantsoght et al., 2013). The shear force is distributed in the horizontal plane towards the support at an angle of 45 degrees, as was assumed in Section 3.3. Again, the same load factors for the assessment level

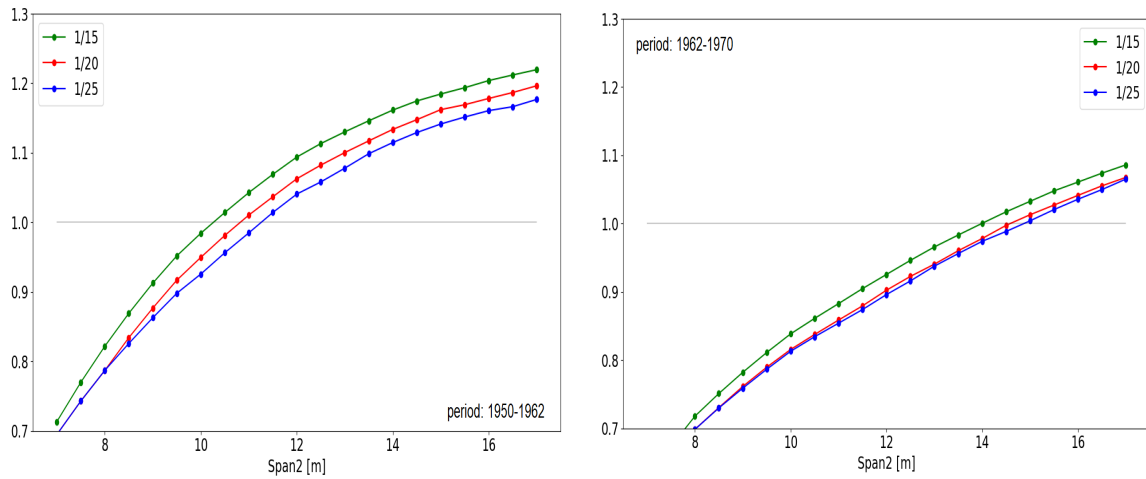


Figure 4.10: Determined Unity Checks for the bending moment at the mid-support for the DC load model with RE reinforcement from mid-span. Assessed for the period 1950-1962 and 1962-1970 with the amount of RE reinforcement from span, and according to the assessment calculation with DC load model, for a variable mid-span length for three slenderness' 1/15, 1/20 and 1/25, and minimum slab thickness of 400mm

'Reconstruction' ('Verbouw') are applied. The resulting Unity Checks are presented in Figures 4.11.

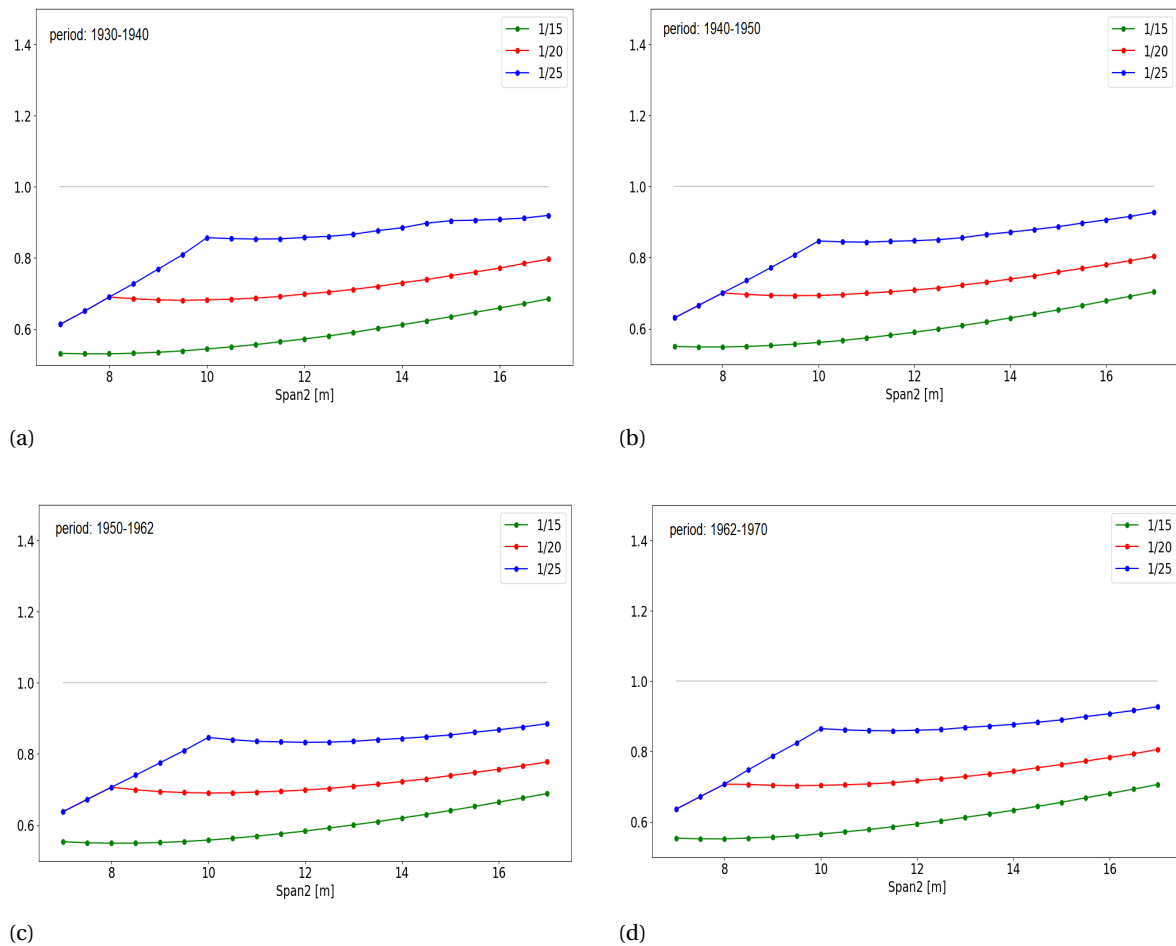


Figure 4.11: Determined Unity Check for shear force, for the period 1930-1940(a), 1940-1950(b), 1950-1962(c) and 1962-1970(d) for a variable mid-span length for three slenderness' 1/15, 1/20 and 1/25, and a minimum slab thickness of 400mm.

The Unity Checks for shear force are also determined with the use of the load factors defined by the research from TNO, see Figure 4.12. Applying here the RE amount of span reinforcement at the support, has a negligible effect on the shear capacity due to limited contribution of the reinforcement compared to the concrete, in the formulae from the RBK-1-1.

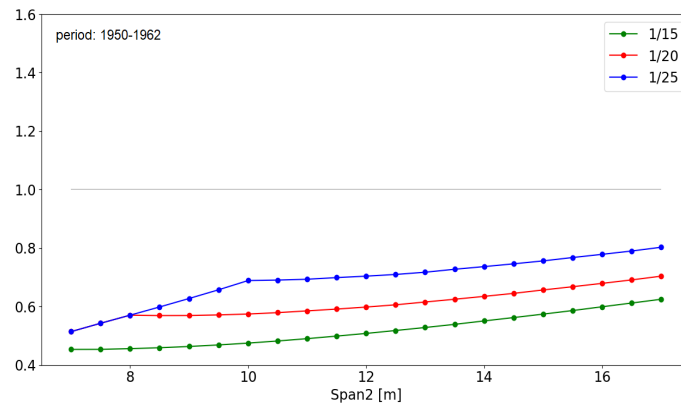


Figure 4.12: Unity Checks for shear force according to the former design code and assessed according with DC load model, for bridges design in the period 1950-1962.

## 4.9. Summary of the results

The Unity Checks of class B bridges designed in the period 1950-1962 are presented in table 4.2. Unity Checks of the bending moment capacity at the mid-span and at the mid-support and of the shear force capacity for the different load models are included. The Unity Checks of class A bridges designed in the period 1950-1962 are presented in Table C.6 in Appendix C.

Table 4.2: Overview of the Unity Checks from bending moment and shear force results for RE class B bridges, designed in the period 1950-1962.

Unity Checks for 1950-1962	EC	EC, with span reinforcement	DC load model	DC load model, with span reinforcement
Span	1.0 - 1.30		0.85 - 0.95	
Support	0.9 - 1.15	0.85 - 1.30	0.75 - 0.90	0.7 - 1.2
Shear force	0.55 - 0.90		0.45 - 0.80	- <sup>i</sup>

## 4.10. Validation

Verification and validation of the computer code are conducted during the development of the code with the ultimate goal of producing an accurate and credible tool, (Banks et al., 2010). Validation is concerned with checking that the system meets the actual needs and is performed in accordance, while verification is concerned with whether the system is well-engineered and error-free. The Verification is performed with the use of available documentation of existing bridges, functioning as controllable results of the computer code. The example bridges from Chapter 3, with known reinforcement amounts from technical drawings are used to verify the RE part of the computer code. The Table below 4.3 presents an overview of the RE reinforcement amounts of the computer code, compared with the reinforcement amounts from the technical drawings. The comparison between the RE reinforcement and the reinforcement from the technical drawings results in the accuracy of the computer code. Here is obtained that the RE reinforcement is almost never overestimated. This means that the computer code probably contains no type- or thinking errors. The gap in reinforcement amounts between the RE reinforcement and from the technical drawings shows rounding up of the reinforcement amounts in former design. The rounding up could be due to safety reasons, execution,

<sup>i</sup>The Unity Checks of shear force in combination with RE reinforcement from span and the DC load model is not determined, because the influence of the reinforcement amount is limited for shear compared to the share of concrete.

manufacture or financial reasons. The validation concludes the computer code has sufficient robustness for the RE method and can be used appropriate for the assessment of an existing RC slab bridge.

Table 4.3: Comparison of the RE reinforcement and reinforcement amount from the technical drawings.

	Required reinforcement (cm <sup>2</sup> )		From technical drawing (cm <sup>2</sup> )	Accuracy
Kw4	span BC	45.5	49.1	93 %
	support C	45.9	49.1	93 %
KW7	span BC	44.1	49.1	90 %
	support C	43.8	49.1	89 %
Heemstedestraatbrug	span BC	51.8	56.55	92 %
	support C	28.3 + 43.1 = 71.4	28.3 + 44.7 = 73.0	98 %
Dinkelbrug	span BC	27.73	8.0 + 19.0 = 27.0	103 %
	support C	26.1	12.1 + 19.0 = 31.1	84 %
Ellermansbrug	span BC	43.0	52.59	82 %
	support C	50.32	52.59	96 %
Ruytenschildtbrug	span BC	32.0	36.5	88 %
	support C	38.0	56.32	67%

The computational accuracy of the numerical methods used in coding and in the mechanical models is elaborated in Appendix C.7.

#### 4.1.1. Limitations of the computer code

The most important assumption in the RE approach is the structural schematisation of the bridge with beam elements. Until the appearance of the computer, bridge design was done with 1d beam element models. This leads to the limitation in RE of bridges designed with plate type computer programs. Plate type structures can be designed with a skewness and/or if larger spans are required prestressing can be applied.

The focus of the computer code lies on existing RC slab bridges with a span ratio  $L1/L2 \leq 0.8$ . With this ratio, the governing bending moments and shear forces occur at the mid-spans. Bridges with a span ratio  $> 0.8$  can have governing forces at the end-spans, leading to larger required reinforcement amounts. So, the end-spans of these bridges are not correctly RE. In case of one and two-span bridges, the governing span is determined correct, so for more than two-span bridges with a span ratio  $> 0.8$  is the computer code inadequate.

The computer code is limited at former bridge design where the crack method is used in the cross section calculation. The required reinforcement according to the crack method can be calculated with the safety factor ( $\gamma$ ) in the crack method ('breukmethode') from strength calculations. Consequently if the crack width calculation is governing for dimensioning of the reinforcement, the safety factor ( $\gamma$ ) increases but the crack width control calculations are not repeated with this new safety factor. Dimensioning of the required main plain reinforcement is expected not to be influenced by the crack width limitation. The crack width limitation has influence on the configuration of the bar diameter and bar spacing of reinforcement with a higher steel quality than QR24. A brief example of crack width results are shown in the Figures A.4 and A.5. Since the publication of the VB in 1974 the development in knowledge of shear force is increased, which might have influenced the slenderness of RC slab bridges.

Local strengthening of a bridge deck as edge beams, voids, or local increment of reinforcement amounts cannot be included in the structural calculations of the computer code. However, the computer code including its limitations can be ensured to be fit-for-purpose, used appropriately and is producing reliable and defendable results.

#### 4.1.2. Discussion

The focus in this chapter lies on RE of the required support- and span reinforcement due to the maximum support- and span moment. The maximum bending moments occur in multiple span bridges with  $L1/L2 \leq 0.8$  always in the mid-span(s) and the mid-support(s). These locations are assumed to be the governing locations where the bending moment reinforcement is designed for. In several former bridge designs is obtained that the amount of support reinforcement and span reinforcement is equal. However, bridge design for load class B/45 exceeds the 1.0 support/span reinforcement difference ratio for a mid-span length of  $>10\text{m}$ , see

Figure 4.5. Bridge design for load class A/60 exceeds the ratio of 1.0 for mid-span lengths of  $>11\text{m}$ , see Figure C.20. In case the mid-span lengths in former bridge design exceed these values for the specific former load classes, and the reinforcement amounts at span and support are equal, the amounts should be designed for the maximum support moment. In case the mid-span lengths are less than these values and the reinforcement amount at span and support are equal, the amounts can be designed for the maximum span moment. Figure 3.9 shows that for some bridges the amount of span reinforcement in the end-spans is lower than for the mid-spans. So, applying the mid-span reinforcement to the end-spans would overestimate the capacity of the end-spans.

A significant difference in the EC and DC load model can be seen from the results (Unity Checks), summarised in Table 4.2. This means the reduction in concentrated traffic loading has a large positive influence on the current structural capacity. In case the support reinforcement and span reinforcement are individually designed, the assessment with the DC load model for the most critical period 1950-1962 results in sufficient capacity regarding the Unity Checks. Assessment with the EC for existing bridge design in the critical period 1950-1962 does not show sufficient structural capacity instantly regarding the Unity Checks.

The results from both the EC and the DC load model assessments show the governance of bending moment failure upon shear force failure in terms of Unity Checks. So, based on the slenderness the governing failure mode between these two can be obtained and consequently be assessed or inspected for. Only for bridges with a mid-span length of  $>14\text{m}$  and with a slenderness higher than  $1/25$  assessed for the EC, the shear capacity can be governing above the bending moment capacity.

Higher Unity Checks for bending moment are obtained for bridges designed for load class B/45 compared to load class A/60 due to less required reinforcement in former design and equal loading in the assessment according to EC. The small decrease in load factors for bridges in the local road network compared to bridges in the National road network has a limited effect on structural safety. This makes bridge design for load class B/45 and lower classes more critical for bending moment failure compared to bridges designed for load class A/60 when exposed to the same traffic load model. Despite bridges designed for load class A/60 have in general more reinforcement, the shear capacity is hardly influenced by the reinforcement. Results in Table C.6 show for the assessment with the EC similar Unity Checks values for bending moment and shear force.

Bridges designed for load class B and with the DAF from the VOSB1933 assessed for the EC, result in Unity Checks below 1.0 for bending moment and shear force. Meaning that RC slab bridges conform the previous conditions which are parametrically assessed, have sufficient structural safety.

The shear control Section 4.8 shows for the assessment according to the EC for all design periods that all the Unity Checks result below 1.0. Here, the assumption of a minimal slab thickness of 400mm has large influence on the shorter spans ( $<10\text{m}$ ) leading to a safe design for shear loading. The assessment according to the DC load model decreases the Unity Checks for shear force even more below 1.0. Last ten years, research from Lantsoght et al. (2013) and Lantsoght et al. (2012) had already constraint the shear failure risk of existing RC slab bridges constructed without shear reinforcement.

In case a bridge width increased edge beams is assessed, the extra stiffness from the edge beams cannot be taken into account in the computer code. Most likely the span and support reinforcement in the mid-strip will be overestimated to compensate for the capacity of the edge beams.

The results from the assessment are Unity Checks, defined by the ratio between current loading and the current capacity with RE reinforcement. The question that arises from these results is: What are the influences of the engineering factor and the execution factor on the Unity Checks of the reverse engineering method? This question is dealt with in the next Chapter 5 Sensitivity Analysis.



# Sensitivity Analysis

## 5.1. Introduction

The chapter starts with the effect of the assumptions for the design year, former load class and geometry on the RE reinforcement in the parametric study.

Thereafter, a sensitivity analysis to see the effect of uncertainty in the input on the Unity Checks is performed. The sensitivity analysis aims to quantify capacity regions based on Unity Checks for uncertainty in the input parameters during an assessment. Furthermore, based on a proposed capacity prioritisation is the assessment of existing RC slab bridges guided by a drafted protocol.

### Effect of the design year

In the parametric study are boundaries set for different former design periods. Hereby, hard transitions are introduced between these design periods. In case the actual design year is uncertain, the applied design methods are uncertain. Figure 5.1 shows for an unchanged bridge design the required span reinforcement over time. In this graph modifications in structural bridge design from 1930-1970 can be seen, as was illustrated before in Table 2.7. These transitions at the capacity and/or at the load side lead to modifications in required reinforcement. Bridge design around these transitions has uncertainty in input parameters in case of unknown documentation, leading to the possibility of assessing with wrong conditions. Overestimation of the capacity side and/or underestimation of the loading side falsifies the assessment. Bridges designed in the middle of the design periods have the lowest chance of interfering with a design transition, so the chance of using the wrong parameter is minimal in these cases.

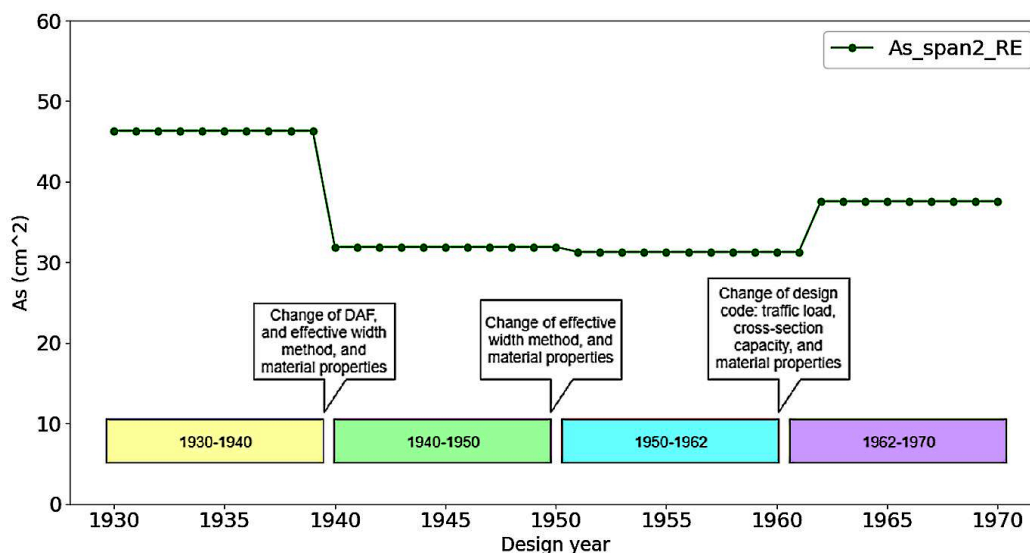


Figure 5.1: RE span reinforcement for constant bridge design over time.

### Effect of the load class

Each bridge in former bridge design is classified into a specific load class based on their expected traffic

loading, as was elaborated in Section 2.3 Traffic load. In Figure 4.2 and in Figure C.17 in Appendix C.6 is observed that the difference in required reinforcement between load class A/60 and load class B/45 is significant. Classifying a bridge in a higher load class than designed for, overestimates the capacity and endangers the current structural safety. Classifying a bridge in a lower load class underestimates the capacity and impedes the assessment. The results from the parametric RE study, show an increase of the RE reinforcement of approximately 25% for a class A bridge from the period 1950-1962 classified as a class B bridge. Conversely, a decrease of the RE reinforcement of 25% for a class B bridge classified as a class A bridge. The same situation for a class 60 bridge considered as a class 45 bridge, increases the RE reinforcement with approximately 15%. And a class 45 bridge considered as a class 60 bridge, decreases unjustified the RE reinforcement with approximately 15%.

#### **Effect of the assumptions for the geometry**

In the parametric study is an extra *slab thickness* of 5% assumed at the supports. This effect on the RE required reinforcement amounts is examined by omitting the extra thickness at the support. Figure D.1 shows that omitting the extra slab thickness at the support leads to slightly higher required RE reinforcement amounts. The same effect is expected at mid-span because a larger lever arm leads to a decrease in required RE reinforcement.

The effect of the *transverse beam* has influence on the RE required reinforcement amount at a support. In case the transverse beam is absent, the extra slab thickness can not be used in the calculation of the capacity. Figure D.2 shows a small increase of required reinforcement in case the transverse beam is absent and consequently the capacity in the centre of the support is determined.

The *distance between the reinforcement layers at a support* has influence on the amount of reinforcement in the second layer. Bridges where the required reinforcement does not fit in one layer, can have a second layer of reinforcement. The distance between the layers has influence on the contribution of the second layer of reinforcement on the total bending moment capacity. Running the computer code with an example layer distance of 2.0cm leads to higher RE required reinforcement amounts, see Figure D.3.

The *concrete cover* has an influence on the amount of RE reinforcement at span and support. Running the computer code with a lower concrete cover of 2.0cm leads to lower RE required reinforcement amounts, which can be seen in Figure D.5.

In the parametric study is the *permanent load* defined only by the self-weight of the structure. No additional dead-load is included. In Figure D.4 the effect of including 1 kN/m dead-load in the RE-tool is shown. The required reinforcement needs to increase in order to compensate for the increased loading on the bridge. This can be observed in Figure D.4 where the required reinforcement increases.

The assumption for a *slab width* of 15 meters in the parametric study is examined in Appendix D. The graphs show a constant distribution of the resulting Unity Checks from 10 meters slab width. An increase of 0.2 UC can be obtained for a slab width smaller than 10 meters.

#### **Remaining assumptions**

The application of the CUR16A/B for bridge design since the publication of the GBV1962 is omitted in this study. The application of the CUR16A/B leads to a much smaller effective width, which leads to higher forces and consequently larger amounts of RE reinforcement in calculations. So, when during an assessment the design year and load class are known, and the RE reinforcement is much less than the actual or measured reinforcement the CUR16A/B might be consultant during former design.

Assumed *material properties* will have a small effect on the RE reinforcement because the material properties can be obtained from the former design code. These prescribed material qualities function as lower limit boundaries in former design and so in the RE method. Due to the standard low material qualities in bridge design with plain reinforcement, is the influence on the RE process limited as well.

A hard transitions between the different methods to determine the effective width for the distribution of concentrated loading is assumed. The consequences of assuming the wrong method need to be dealt with at

two periods in time: the first transition between the two GBV methods around 1940 and the second when the Guyon-Massonnet method is introduced around 1950. The difference in the resulting effective width between the two GBV methods is -10% for the load case with one design truck at the edge of the slab. For the load case with two design trucks in the middle of the slab is the resulting difference +/-5% between the GBV methods. The difference in the resulting effective width between the GBV method and the Guyon-Massonnet method differs between -10% and +15% for both load cases, see Figure C.9 and C.10.

Table 5.1 shows an overview of the effect of the individual assumptions on the RE method. A large increase of RE reinforcement due to assumption is indicated with (++), a small increase of RE reinforcement with (+), a large decrease of RE reinforcement with (-) and a small decrease of RE reinforcement (-).

Table 5.1: Effect of the assumptions made for the input parameters in response to the RE reinforcement amounts in the parametric study.

Assumption	Conservative	Unconservative	Modification	Effect on the RE required reinforcement amount
Design year	RE for 1940-1962	RE for 1930-1940 or 1962-1970	-	++ (at support and span)
Load class	RE class A/60 as class B/45 <sup>i</sup>	RE class B/45 as class A/60 <sup>i</sup>	-	++ (at support and span)
Slab thickness at support +5%	x		+0%	+ (at support)
Width transverse beam 1.0 m	x		0.0 m	+ (at support)
Distance between reinforcement layers 0 cm	x		2.5 cm	+ for span >14m (at support)
Concrete cover 3cm		x	2cm	- (at support and span)
Zero additional permanent load	x		1 kN/m	+ (at support and span)
Slab width	x		variable slab width	+ for slab width < 10m (at span)

## 5.2. Sensitivity analysis

Bridge design from technical drawings can deviate from the actual design made on site, or deviate from the as-built drawings made from site. Here, may be expected that the structural capacity is not negatively influenced by decisions made during construction. The uncertainty in geometry, possibly introduced during fabrication, construction, execution and/or during the lifetime of a structure is examined.

To include uncertainty in the assessment, the input parameters can be allocated using a normal distribution (ND). The value found from a technical drawing or measurements outside can function as the mean ( $\mu$ ) of the ND, where after a standard derivation (SD) is to be decided for. In this study, the SD is decided based on expert judgement but in practise the magnitude of the SD can be quantified by the accuracy of the method to define the input parameter. The following parameters are allocated to a ND: design year (Figure 5.2), span lengths (Figure 5.3), slab thicknesses (Figure 5.2), slab width, edge distance, asphalt thickness, concrete cover (Figure 5.3), width of the transverse beam, the distance between reinforcement layers, the new edge distance and the second asphalt layer. Uncertainty in the load class is limited to two times two sides: the side of the highest load classes A/60 and lower load classes B/45, and the side of load class A or 60, or load class B or 45. Where the first mentioned side is based on the expected traffic loading and the second based on the application of the VOSB1933 or VOSB1963.

The self-weight and additional permanent load, material qualities, and the bar distance are not defined by a ND and are given a constant value.

The method used in this thesis approaches Monte Carlo simulations (level III) due to the high number of variable (n), but without the calculation of an actual failure probability. The outcome of the method are Unity Checks with a ND. The load is based on the EC with the partial coefficients ( $\gamma$ 's) concept, belonging to a level I method. The level I and III reliability methods are elaborated in Appendix D.

<sup>i</sup>Here can be stated that a lower load class than load class B/45 should be more conservative, but is found unlikely to appear for the larger group of existing bridges in the road network.

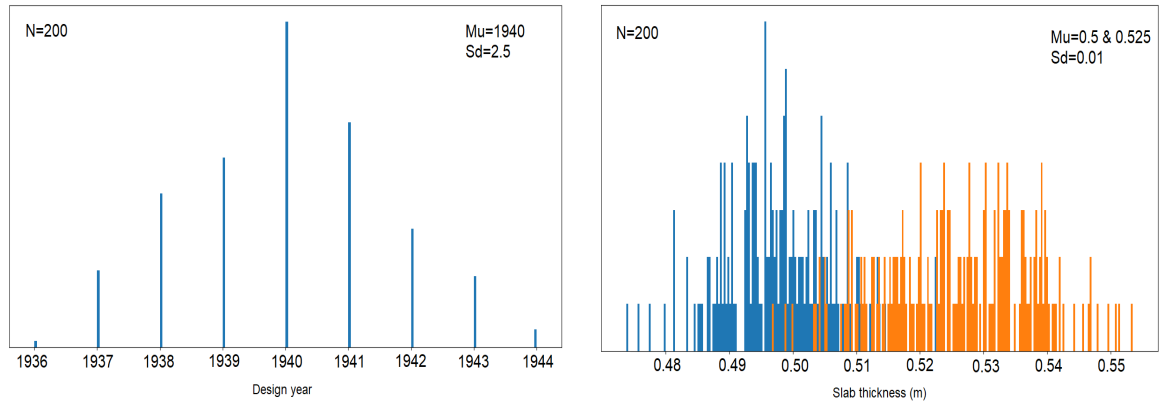


Figure 5.2: ND of the design year with a Mu of 1940 and a SD of 2.5 (left) and of the slab thicknesses (right) at span (blue) and the support (orange) with a Mu of 0.5 and 0.525, and a SD of 0.01. Both graph are formed with 200 samples (N=200)

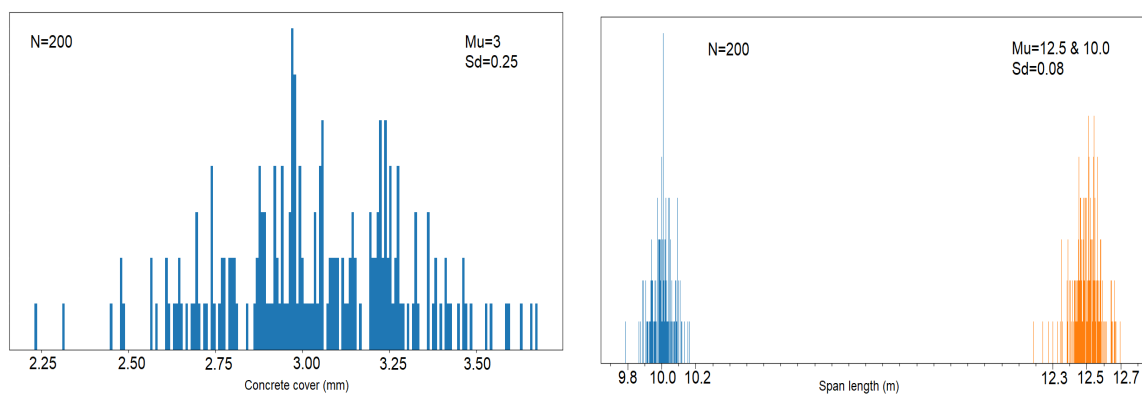


Figure 5.3: ND of the concrete cover with a Mu of 3 and a SD of 0.25 (left) and the span lengths (right) the mid-span (orange) and the end-span (blue) with a Mu of 12.5 and 10.0, and a SD of 0.08. Both graph are formed with 200 samples (N=200)

Table 5.2: Overview of input parameters with a Normal Distribution

Input parameter	Mean	Standard derivation
Design year	1940/1962	1.2
Load class	A/B, 45/60, B/45 or A/60(coin toss)	
Midspan length	12.5	0.5
Endspan length	10.0	0.5
Slab thickness at support	$1/19 \cdot \text{spanlength}$	0.01
Slab thickness at span	$1/20 \cdot \text{spanlength}$	0.01
Slab width	15	0.1
Edge distance	1.0	0.1
Concrete cover	3.0	0.25
Asphalt thickness	5.0	0.002
Width transverse beam	1.0	0.1
Reinforcement layer distance	2.0	0.8
Edge distance in the assessment	1.0	0.1
Extra asphalt layer in the assessment	7.0	0.002

By distributing the input parameters with a ND, the results (Unity Checks) will have a distribution. The mean value in the distribution of the Unity Checks originates from the measurements or technical drawings filled in the computer code. The scatter in the resulting Unity Checks represents the uncertainty in the input parameters and the possible non-linearity in the RC cross-section. Here, the possibilities of picking very conservative parameters, until the possibility of picking very critical parameters are included. The sensitivity analysis is

performed by assessing for the EC- and DC Load model.

In Figure 5.4, the *load class* is kept constant and is for the EC and the DC load model a bridge design one hundred (N=100) times determined with the input parameters having a ND. So, the effect of uncertainty in geometry and the design year can be obtained. In Figure 5.5, the *design year* is kept constant and is for the EC and the DC Load model a bridge design one hundred (N=100) times determined with the input parameters having a ND. So, the effect of uncertainty in geometry and in the load class can be obtained. In case the uncertainty of the design year fits within a design period and the load class is known, the scatter can be related to the uncertainty in geometry only, as can be seen in Figure D.8.

The analysis exhibits the largest scatter due to uncertainty in design year and load class approximately 0.2-0.35 UC, because two different clouds of scattered results can be obtained. Especially uncertainty in the design year around 1940 and load class A/B show the largest scatter. The analysis exhibits a relative small scatter for geometrical uncertainties, as can be obtained when the design year or load class are constant. In such cases is the relative scatter in a cloud of results, approximately 0.05 UC from the mean.

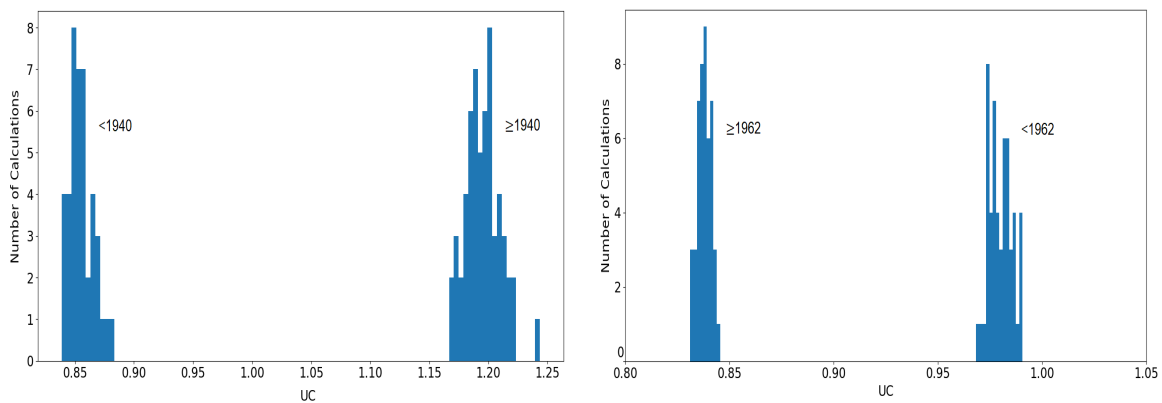


Figure 5.4: Histogram showing the effect of a ND design year and geometry on the Unity Checks at mid-span with RE reinforcement. The left graph is a class B bridge, assessed for the EC with a ND design year of 1940 and the right graph is a class B/45 bridge, assessed for the DC load model with a ND design year of 1962. The number of samples is: N=100.

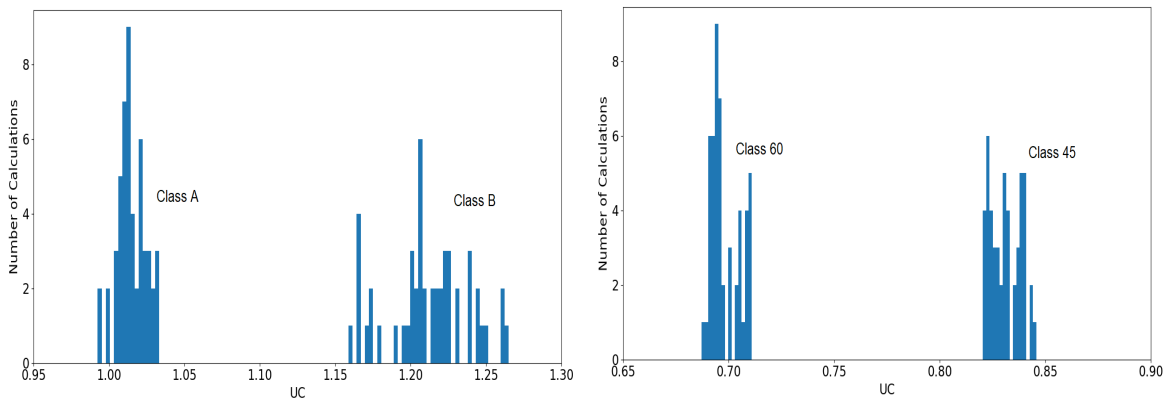


Figure 5.5: Histogram showing the effect of a ND load class and geometry on the Unity Checks at mid-span with RE reinforcement. The left graph is a class A or B bridge, assessed for the EC with a design year of 1945 and the right graph is a class 60 or 45 bridge, assessed for the DC load model with a design year of 1964. The number of samples is: N=100.

### 5.3. Prioritisation of existing RC slab bridges for current traffic loading

Three groups of bridges from all existing RC slab bridges with plain reinforcement can be point out as most critical after assessment. First, the group (with unknown size) of bridges with support reinforcement based on the span reinforcement. Second, is the group of bridges designed in 1940-1962 for load class B with  $N_{obs} > 125\,000$  or span length  $>20\text{m}$  or maximum vehicle load of  $>60\text{ton}$ . Third, the group of bridges with unknown design year and/or load class.

This results in a prioritisation of the existing RC slab bridges based on capacity margins, and can be visualised in a risk triangle illustrated in Figure 5.6:

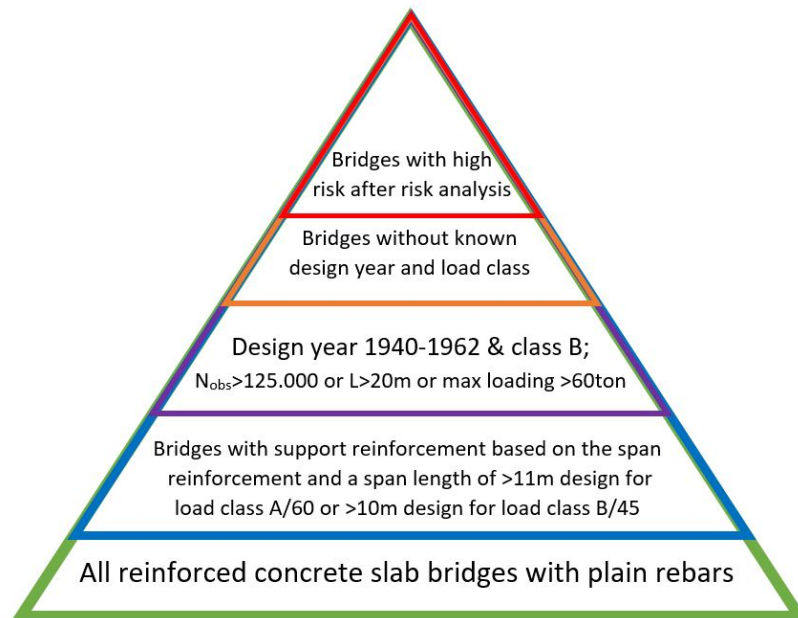


Figure 5.6: Schematic view of collection of RC slab bridges with plain reinforcement, where for no assessment is required (green), provisional no assessment (blue) if the structural reliability can legally be proven, an assessment on moment- and shear capacity (purple), an assessment for bending moment capacity with scanned reinforcement of the bridge layout (orange), and urgent measures indicated by the protocol Figure D.9 (red).

#### 5.3.1. Risk quantified

Capacity regions can quantify the risk of existing RC slab bridges, based on the resulting Unity Checks from the sensitivity analysis. The uncertainty of the input parameters and consequently the sensitivity of the results from this uncertainty can be quantified. Risk in the structural capacity can be quantified by categorising the Unity Checks into three regions: 'Safe' ( $UC \leq 0.95$ ), 'Low risk' ( $0.95 > UC < 1.3$ ) and 'High risk' ( $UC \geq 1.3$ ), as is illustrated in Figure 5.7. The boundary for the region quantified as 'Safe' with a UC of 0.95 is substantiated due to the uncertainty in geometry leading to a deviation of 0.05 UC; theoretically a safe UC of 0.95 can turn into a Unity Check of 1.0. This includes the possibility of picking all geometrical parameters negatively in correspondence to the capacity, as was elaborated in Section 5.2. The boundary of the region quantified as 'Low risk' with a Unity Check of  $< 1.30$  is substantiated due to the possibility of an incorrect load class or design year, the Unity Check can exceed the critical boundary of  $UC=1.0$ . So, more research is required to track down if the actual load class and design year are applied. In case the load class and design year are substantiated by documentation, additional analysis is required until legal safety can be assured and visual inspection of the bridge should be performed. The boundary for the region 'High risk' with a Unity Check of  $\geq 1.30$ , suspects a direct risk toward structural safety. However, if the design year and load class are both unknown and cannot be tracked down for the assessment of the existing bridge, the structural safety is questionable in general.

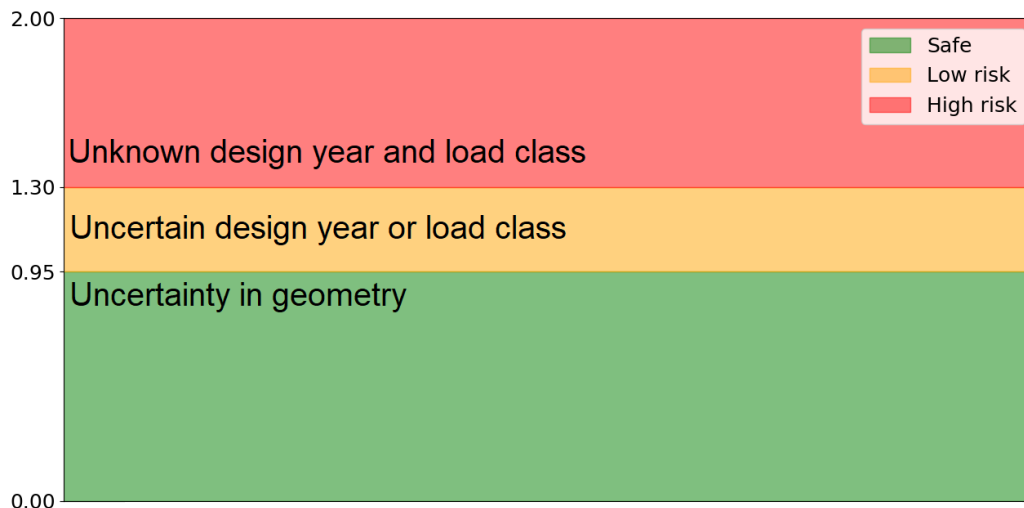


Figure 5.7: Capacity regions in terms of Unity Checks to quantify risk from the assessment.

### 5.3.2. Possible extra capacity

The parametric analysis provides a global insight into the structural capacity of RC slab bridges. Assessing individual cases can have influence on the input parameters and consequently on the capacity of the structure. Extra bending moment- and/or shear force capacity might be found with more detailed calculations. For an individual case, the conservative assumptions during the parametric study can be omitted. In former design, engineers might have rounded up the reinforcement amounts for practical reasons, because higher reinforcement amounts are obtained from the technical drawings compared to the RE amounts, see the accuracy in the validation Table 4.3. Furthermore, the actual material properties can be obtained by lab tests and the actual reinforcement can be scanned. The assumption of leaving out additional permanent load in RE the reinforcement of the bridge and (the same amount) in the assessment of the RE bridge is negatively influencing the capacity of the structure. This is due to the overall safety factor in former ASD which accounts for permanent load too, wherein the assessment a lower load factor is valid for permanent load. Redistribution of maximum 20% of the bending moments between the span and the supports is allowed, when reinforcement with a high ductility is applied. Ductility classes are defined in the RWS and GPO (2013) where plain reinforcement with the qualities QR22 and QR24 have sufficient ductility for force redistribution.

A full probabilistic analysis with all parameters allocated to a probability density distribution can be seen as the most accurate approach of bridge assessment. Actual reliability indices can be determined to reach for a reliability relative to newly build structures.

### 5.3.3. Possible reduced loading

Assumptions (from Section 4.2) towards the determination of the governing bending moments and shear forces, lead to slightly larger forces than actually are occurring. These resulting forces can be determined with more precision. The Guyon-Massonnet method to distribute concentrated loading compared to a 2D finite plate analysis results in general in slightly higher bending moments, as was stated by de Boon (2018) in Section C.7. In addition, the use of a 2D finite plate analysis can result in more accurate shear forces. Measuring the traffic weight crossing the bridge can be used to determine the actual traffic loading for the assessment.

#### Proceeding measurements

Proceedings to perform an assessment are exemplified in a protocol, Figure D.3 in Appendix D with additional explanation in Section D.3. The methods from the previous Sections 5.3.2 and 5.3.3 are obtained in the protocol.

# 6

## Conclusion

The thesis aims to examine the possibility of Reverse Engineering (RE) of existing planless reinforced concrete (RC) slab bridges constructed with plain reinforcement. Consequently, the RE bridges are assessed with current assessment codes to examine the capacity margin. The main research question is: *How can the main reinforcement of existing reinforced concrete slab bridges constructed with plain reinforcement be estimated, and what is the margin in structural capacity of the reverse engineered bridges according to the current assessment codes?*

Research started with a preliminary study into former structural design to be able to perform hand calculations to RE reinforcement. The hand calculations exhibited the reinforcement in stiff edge beams in case of a non-rectangular cross-section is designed based on experience. The presumption that the edge beams are designed for 100% of the permanent- and imposed loads from the mid-strip is plausible, but this assumption should be further examined.

Subsequently, the hand calculations are automated in order to do a parametric study to existing RC slab bridges. The reinforcement of an existing RC slab bridge can be RE with sufficient robustness if the design year, former load class and the geometry are known. A single bridge can be RE by hand-calculations or with a computer code (RE-tool). Besides, the RE-tool is able to do a parametric study to reach for a group assessment of these existing bridges. Table 4.3 shows sufficient accuracy of the RE reinforcement compared to the actual reinforcement from the technical drawings. The reinforcement amounts are in general underestimated which leads to a reliable method where the capacity of the bridge is not overestimated. At the same time, the actual applied reinforcement will influence the results. This concludes that the RE-tool makes it possible to determine the span- and support reinforcement with sufficient robustness.

The engineering- and execution factor can influence the accuracy of RE the reinforcement and consequently the assessment with the current assessment codes. The effect of uncertainty in the input parameters upon the capacity margin is examined. The computer code is run with the input parameters having a normal distribution. The uncertainty in the *geometry* results into a scatter for the resulting Unity Checks (load/capacity) with a deviation of approximately 0.05 UC from the mean value. The uncertainty in the *design year* and *load class* have the largest influence on the RE reinforcement and therefore on the resulting Unity Checks (approximately 0.2-0.35 UC), making the design year and load class the most important input parameters in an assessment.

Significant bending capacity margins are obtained in structural design of RC slab bridges in the period 1930-1970, see Figures 5.1 and 4.3. The main contribution of this research is that bridges designed between 1940 and 1962 show the most critical Unity Checks for bending in the assessed period. It can be concluded that these bridges with RE reinforcement are found to be legally unsafe for bending moment failure according to the parametric assessment with the EC. In the period 1940-1962 account the following former design methods: The dynamic amplification factor (Section 2.4) introduced in the GBV1940 for concrete bridges, the traffic load class from the VOSB1933 (Section 2.3), the N-method to determine the cross-section capacity (Section 2.2.3), and the effective width method from the GBV1940 (Section 2.5) and from the Guyon Massonnet method (Section 2.5).

The capacity margin for shear is found to be almost independent of the design period, see figures 4.11. Here can be concluded that the slenderness of the deck slab in RC slab bridge design with low material qualities is the main contribution in the shear capacity.

Bridges designed in the period 1940-1962 with the support reinforcement based on the span reinforcement



and with mid-span lengths >10m designed for load class B/45 (Figure 4.5), or with mid-span lengths >11m designed for load class A/60 (Figure C.20), form the group with the most critical bending capacity in the assessment. However, the size of the group of former bridges designed according to these conditions is unknown.

Bending is found to be the governing ductile failure mode above the non-ductile shear failure mode for RC slab bridges designed for load class B/45 constructed with plain reinforcement, see Table 4.2. The bending moment capacity is determined with RE reinforcement and the shear force capacity including the material qualities determined according to the NEN8700/NEN8701 and the RBK-1-1. The assessment of RC slab bridges designed for load class A/60 constructed with plain reinforcement shows that the capacity margin for bending moment and shear force are more alike, due to a larger amount of required reinforcement for bending, see Table C.6.

The focus within literature was mainly on the shear capacity of existing RC bridges rather than on the bending capacity. The shear capacity was expected to be governing above the bending capacity of the existing RC slab bridges. This research showed the governing failure mode for RC slab bridges designed for load class B/45 constructed with plain reinforcement is bending according to the parametric study. This means that these structures, and especially the structures designed between 1940-1962, have in general a ductile failure mode where redistribution of forces occurs to avoid brittle fracture modes. Continuously, in the ductile failure mode of a RC slab bridge, failure is initiated by yielding of the reinforcement and cracking of the concrete in the tensile stress area. Relating this conclusion to insufficient capacity during the assessment of an existing bridge, substantiation with visual inspection for cracks is evidential.

# Recommendations

## 7.1. Recommendations for Reverse Engineering

This study shows that Unity Checks for bending moment result above 1.0 from the parametric study, which is legally unsafe. However, the CROW (2019) states: In case an assessment of a bridge results in Unity Checks larger than 1.0, it means not by definition that the structure is unsafe. In this study, regions indicated with 'low risk' and 'high risk' are defined which can be acted upon. More research can be performed to reach for a more detailed examination of the capacity margin of the bridge, for example by defining the actual material strengths by lab tests, scanning of the reinforcement, or exposing the bridge to a load test. When a structural assessment of an existing bridge is performed, visual inspection for damage and degradation of the existing structure should always be executed.

The assessment of a group of bridges can be performed in a parametric way by ranking bridges based on the capacity margin, as is elaborated in Chapter 5. In this way, a capacity-based prioritisation for the assessment of existing RC slab bridges can be obtained. Large risk origins regularly from a lack of information of the existing structure.

The application of the DC load model, from Steenbergen et al. (2018) decreases the Unity Checks for bending moment towards a legally safe level of the existing RC slab bridges for all design periods according to the parametric study. Therefore, it is recommended to aim for an assessment with the DC load model in case the bridge satisfies the requirements.

The group of bridges with the amount of support reinforcement based on the amount of span reinforcement with mid-span lengths >11m designed for load class A/60, or with mid-span lengths >10m designed for load class B/45 should be searched for. It is recommended to assess these bridges with the current codes thereafter visual inspection has to be performed.

## 7.2. Recommendations for future research

Chapter 1 explained that this research is subjected to a larger goal where assessment of existing concrete bridges with a wide scope of bridge types is aimed for. This larger goal of automated assessment of existing bridges, can be seen as the ultimate goal in research of the existing infrastructure.

It would be recommended to assess existing structures in general with a parametric approach, mainly because of the large number of structures constructed in the '60 and '70 and older, which need to be assessed due to the descending structural lifetime. A capacity-based prioritisation from a parametric assessment reduces the amount of work and focuses on the most critical structures.

The reliability index of existing RC slab bridges build before approximately 1970, is unknown. Another recommendation for future research is restructuring and expanding of the computer code to perform a reliability analysis to determine a relative failure probability ( $\beta$ -value) of existing RC slab bridges. The reliability index of former bridges will be relative to the reliability of current structural design of bridges. To perform such an analysis, all parameters at the load side and capacity side need a probability distribution, whom is unknown for former material qualities.

Furthermore, following research could expand the RE-tool for the RE and assessment of bridges with end-spans equal to mid-spans, to find the required reinforcement in the end-spans. Examine bridge design of cross-sections with stiff edge beams and consequently add them in the computer code. The model could also be expanded for bridge design after 1962, when bridge design influence by the development in knowledge in crack width and shear force. In case existing bridges are designed with 2D FE-software, the computer code is not applicable.

Finally, further research could look into increment of the speed of the RE-tool to decrease the run-time for the parametric study and probabilistic analysis by making smart decisions for data types and find a solution to program the Guyon Massonnet method in Python. Substantiate the date of the introduction of Guyon Massonnet method by research into data to make a more accurate assumption.

# Bibliography

- Banks, J., Carson, J., Nelson, B. and Nicol, D. (2010), *Discrete-Event System Simulation*, fifth edn, Upper Saddle River, Pearson Education.
- Brakel, J. (1956), *Appendix E: Bepaling van de belastingspreiding in balkroosters en orthotrope plaatbruggen met de methode Guyon-Massonnet.*, publisher unknown.
- CROW (2019), Constructieve veiligheid bestaande bruggen en viaducten van decentrale overheden, Technical report, CROW.
- Cuaron, A., Jáuregui, D. and Weldon, B. (2016), 'Invited student paper - a procedure for load rating reinforced concrete slab bridges', *Transportation Research Board (TRB) 2017 Annual Meeting*. New Mexico State University, Department of Civil Engineering.
- de Boon, J. (2018), Quick scan methode voor t-liggers, Master's thesis, Delft University of Technology. Graduation company/organisation: Rijkswaterstaat.
- Dieteren, G. (2012), 'Beoordelen bestaande bouw, betonnen bruggen en viaducten', Presentation: Centraal overleg Bouwconstructies. TNO.
- Directie van Waterstaat (1933), Voorschriften voor het ontwerpen van stalen bruggen (vosb1933), Technical report, Ministerie van Waterstaat.
- Franx, C. (1962), *de breuk methode & volgens de G.B.V. 1962*, Mouton & Co.N.V. 'S.-Gravenhage.
- G, E. (2013), *Bridge design and evaluation LFRD and LRFR*, Wiley.
- Gantvoort, G. (1964), 'Betonstaal, overzicht van maten en eigenschappen', *Cement XVI no. 10*, 638–647. T.H.Delft, afdeling Weg-en Waterbouw.
- Google (nd), 'Google maps, street view'.  
**URL:** <https://www.google.com/maps>
- Harris, D., Ozbulut, O., Alipour, M., Kassner, B. and Usmani, S. (2015), Implications of load rating bridges in virginia with limited design or as-built details, University of Virginia – Charlottesville, VA, USA, and Virginia Department of Transportation- Charlottesville, VA, USA, SHMII 2015 - 7th International Conference on Structural Health Monitoring of Intelligent Infrastructure - At Torino, Italy.
- Hofman, J. and van der Vlugt, B. (1956), 'Berekening van balkrooster- en plaatbruggen', *Cement 8, Nr. 19-20*.
- Jonkman, S., Steenbergen, R., Morales-Nápoles, O., Vrouwenvelder, A. and Vrijling, J. (2017), *Probabilistic Design: Risk and Reliability Analysis in Civil Engineering*, Delft University of Technology.
- Koninklijk Instituut van Ingenieurs (1912), *Gewapend Beton Voorschriften (GBV1912)*, Afdeling Bouw- en Waterbouwkunde.
- Kuhlman, D. (2011), *A Python Book: Beginning Python, Advanced Python, and Python Exercises*, Platypus Global Media.
- Lantsoght, E., van der Veen, C., de Boer, A. and Walraven, J. (2012), Shear assessment of solid slab bridges, Delft University of Technology, Conference: ICCRRR 2012, 3rd International Conference on Concrete Repair, Rehabilitation and Retrofitting.
- Lantsoght, E., van der Veen, C., de Boer, A. and Walraven, J. (2013), 'Recommendations for the shear assessment of reinforced concrete slab bridges from experiments', *IABSE International Association for Bridge and Structural Engineering*. 1016-8664.

- LYNCH, D. (2019), 'How to construct a mohr's circle'.  
**URL:** <https://blog.prepineer.com/how-to-construct-a-mohrs-circle/>
- Mulder, R. (2015), 'Onderzoek gemeentelijke bruggen', *Bouwend Nederland* pp. 1–15. Bouwend Nederland, de vereniging van bouw- en infrabedrijven.
- NEN1990 (2011), *Eurocode: Grondslagen van het constructief ontwerp.*, Normcommissie 351001 "Technische Grondslagen voor Bouwconstructies".
- NEN1991 (2011), *Nationale bijlage bij NEN-EN 1991-2+C1: Eurocode 1: Belastingen op constructies – Deel 2: Verkeersbelasting op bruggen.*, Normcommissie 351001 "Technische Grondslagen voor Bouwconstructies".
- NEN8700 (2011), *Assessment of existing structures in case of reconstruction and disapproval - Basis Rules*, Normcommissie 351001 "Technische Grondslagen voor Bouwconstructies".
- NEN8701 (2011), *Assessment of existing structures in case of reconstruction and disapproval - Actions*, Normcommissie 351001 "Technische Grondslagen voor Bouwconstructies".
- op 't Hof, M. (2006), *Richtlijnen voor het Ontwerpen van Betonnen Kunstwerken (ROBK)*, number 6 in '1', Rijkswaterstaat Bouwdienst, Afdeling Civiele Techniek.
- RWS and GPO (2013), *Richtlijnen Beoordeling Kunstwerken (RBK), Beoordeling van de constructieve veiligheid van een bestaand kunstwerk bij verbouw, gebruik en afkeur.*, Utrecht : RWS, GPO.
- Shenton, H., Chajes, M. and Huang, J. (2007), Load rating of bridges without plans, Technical report, Department of Civil and Environmental Engineering, University of Delaware. Sponsored by: Delaware Center for Transportation and prepared in cooperation with: Delaware Department of Transportation.
- Steenbergen, R., Allaix, D., la Gasse, L. and Vervuurt, A. (2018), Verkeersbelastingmodel voor wegverkeersbruggen in het onderliggend wegennet zonder jaarontheffingen, Technical report, De Nederlandse Organisatie voor toegepast-natuurwetenschappelijk onderzoek (TNO). TNO-R10614.
- Termoul, T. (2010), La methode de guyon-massonet-bares, Technical report, Ecole Nationale Polytechnique departement du genie civil.
- van der Schrier, W. (1938), *Bouwen in gewapend beton*, Argus, Amsterdam.
- Vergoossen, R. (2015), Examining and conserving existing structures; the dutch way, Delft University of Technology.
- Vergoossen, R. (2019), 'Bestaande bruggen algemeen (presentation)'.  
**URL:** <https://www.pythons.org/about>
- Vrouwenvelder, A., Scholten, N. and Steenbergen, R. (2012), Veiligheidsbeoordeling bestaande bouw, (tno-060-dtm-2011-03086) achtergrondrapport bij nen 8700, Technical report, De Nederlandse Organisatie voor toegepast-natuurwetenschappelijk onderzoek (TNO). Client: Rijkswaterstaat, NEN.
- Vrouwenvelder, A., Waarts, P. and Wit, M. (2000), De algemene veiligheidsbeschouwing en modellering van wegverkeersbelasting voor brugconstructies, tno rapport 98-con-r1813, Technical report, De Nederlandse Organisatie voor toegepast-natuurwetenschappelijk onderzoek (TNO).
- Welcome to Python.org (n.d.). Accessed: 2019-09-18.  
**URL:** <https://www.python.org/about>
- Welleman, H. (2016), *Work, energy methods & influence lines. Capita Selecta in engineering mechanics*, Bouwen met Staal.

# List of Figures

2.1	Example of a multiple span RC slab bridge, located in Delft constructed in the 1960s, from Google (nd). . . . .	5
2.2	Mechanical scheme of a four-span bridge with a continuous beam and end-spans (L1) and mid-spans (L2). The triangles schematise the supports. . . . .	5
2.3	Left: development of reinforcing steel, right: development of concrete, from Gantvoort (1964). . . . .	6
2.4	The N-Method applied to a cross-section (top-left) with linear stress relation (top-middle) and strain relation (top-right), a 3D cross-section with internal forces and external moment of a slab (bottom-left) and detailing of reinforcement (bottom-right), from Vergoossen (2019). . . . .	8
2.5	The crack method ('Breukmethode') applied to a cross-section (top-left) with parabolic stress relation (top-middle) and linear strain relation (top-right), a 3D cross-section with internal forces of a slab (bottom-left) and detailing of reinforcement (bottom-right), from Franx (1962) . . . . .	9
2.6	The concrete stress/strain relation of the Crack method (left) and the steel stress/strain behaviour in the Crack method ('Breukmethode') (right). . . . .	10
2.7	The difference in required reinforcement amounts with steel quality QR24 for the comparison of the N-method and Crack-method (left) and for the steel quality QR40 (right), based on the concrete compressive height. . . . .	12
2.8	Various types of reinforcement bars not used anymore in the Netherlands since the 1960s, illustration from Gantvoort (1964) . . . . .	13
2.9	Mutual distance of bend reinforcement in a longitudinal cross-section, where $a_1 \leq a_2$ , with an upper limit of 50cm, according to the GBV1940. Possible shear cracks are illustrated at an angle of $\approx 90$ degrees compared to the orientation of the bend reinforcement. . . . .	14
2.10	Loading scheme of the design truck and uniform distributed traffic load, with the variables from the Tables 2.4, 2.5 and 2.6. . . . .	16
2.11	Concentrated loading configuration with double wheels from the design truck for load class A/60 and B/45 and 30. . . . .	17
2.12	Concentrated loading configuration with single wheel from the design truck for load class B/45 and C. . . . .	17
2.13	DAF determined by the GBV before the GBV1940 and by the GBV1940-GBV1962, and the difference between both formulae. . . . .	18
2.14	Wheel load distribution according to the GBV1912-GBV1940 . . . . .	19
2.15	Wheel load distribution according to the GBV1940-GBV1962 . . . . .	19
2.16	Position of design truck(s) leading to the governing load situations. . . . .	21
2.17	The effective width calculated with the different theories, loaded by one design truck of 2 meters width from load class A (left) and loaded by two design trucks of in total 5 meters in width from load class A (right). The width of the bridge deck is mentioned with the letter 'B', or the slenderness between brackets. . . . .	21
2.18	Imposing a unit rotation at span, by introducing a nod in the beam, Welleman (2016). . . . .	22
2.19	Imposing a unit displacement at a support, by introducing a displacement in the beam Welleman (2016). . . . .	23
2.20	Timeline from the start of structural design codes and Traffic load model, with the scope of this research framed in red. . . . .	23
2.21	Timeline from 1930 until 1970 of the modification in structural design of RC bridges. . . . .	24
3.1	The two deck cross-sections of the bridges to be RE. Left: a rectangular deck cross-section with height 'h1' and width 'b1'. Right: a non-rectangular deck cross-section with height 'h1' and width 'b1' of the mid strip and height 'h2' and width 'b2' of the edge beams. . . . .	25
3.2	Moment- and shear force line of a three-span bridge with an UDL of 10 kN/m. . . . .	26
3.3	Moment- and shear coefficients of a three-span bridge with an UDL, from the GBV1940. . . . .	26

3.4	Shape deformation method applied for an example multiple span bridge loaded by a design truck. . . . .	27
3.5	Moment- and shear coefficients of a three-span bridge under concentrated loading, from the GBV1940. . . . .	27
3.6	Changing the stiff edge beam by a slab strip with the same bending stiffness. . . . .	28
3.7	Mechanical scheme to determine the maximum shear force (D) in a bridge deck. . . . .	29
3.8	Shear force distribution in a bridge deck, top view (above) and side view (below). . . . .	30
3.9	Field- and support reinforcement amounts, where the first blue and orange bars are from the first span (end-span) and the support at the right side of the span. The second blue and orange bars are of the second span (mid-span) with adjacent support. . . . .	31
3.10	Locations of critical cross-sections where the Unity Checks for bending moment are performed. . . . .	32
3.11	Transverse reinforcement amounts, where the first blue and orange bars are of the end-span and the second blue and orange bars are of the adjacent span. . . . .	33
3.12	Determined shear stress for load class A/60 (left) and for load class B/45 (right), for a variable span length and different deck slenderness ratio's. The shear stress is due to a combination of self-weight, distributed traffic load and concentrated traffic load. . . . .	35
3.13	Determining the area where extra shear capacity is required. . . . .	36
4.1	Schematic flowchart of the computer code in Python. . . . .	39
4.2	RE reinforcement at mid-span for load class B and the EC (left) and the reinforcement difference ratio (right) for the period 1950-1962, for a variable mid-span length for three slenderness' 1/15, 1/20 and 1/25. The effect of the slenderness on small spans highlighted with the red ovals. . . . .	44
4.3	Determined Unity Checks for bending moment at mid-span, for the periods 1930-1940(a), 1940-1950(b), 1950-1962(c) and 1962-1970(d) for a variable mid-span length for three slenderness' 1/15, 1/20 and 1/25, and a minimum slab thickness of 400mm. . . . .	45
4.4	RE reinforcement at a mid-support for load class B and the EC (left) and Unity Checks (right) for the period 1950-1962, for a variable mid-span length for three slenderness' 1/15, 1/20 and 1/25, with a minimum slab thickness of 400mm. . . . .	46
4.5	reinforcement difference ratio between the RE support reinforcement and the RE span reinforcement for load class B/45 for $L1/L2 \leq 0.8$ , a slenderness of 1/20 and a minimum slab thickness of 400mm. . . . .	46
4.6	Determined support reinforcement amount based on the RE span reinforcement and in the assessment based on the maximum support moment due to EC (a). Corresponding Unity Check (b) for the period 1950-1962 according to the assessment calculations, for a variable mid-span length for three slenderness' 1/15, 1/20 and 1/25, and with a minimum slab thickness of 400mm. . . . .	47
4.7	Determined span reinforcement amount for bending moment according to the former design code and assessed according to the DC load model (a). Corresponding Unity Checks (b) for the period 1950-1962, for a variable mid-span length for three slenderness' 1/15, 1/20 and 1/25, and minimum slab thickness of 400mm. . . . .	47
4.8	Determined support reinforcement amount for bending moment according to the former design code and assessed according to the DC load model (a). Corresponding Unity Checks (b) for the period 1950-1962, for a variable mid-span length for three slenderness' 1/15, 1/20 and 1/25, and minimum slab thickness of 400mm. . . . .	48
4.9	Determined Unity Checks for the bending moment at the mid-support for the DC load model with RE reinforcement from mid-span. Assessed for the period 1930-1940 and 1940-1950 with the amount of RE reinforcement from span, and according to the assessment calculation with DC load model, for a variable mid-span length for three slenderness' 1/15, 1/20 and 1/25, and minimum slab thickness of 400mm. . . . .	48
4.10	Determined Unity Checks for the bending moment at the mid-support for the DC load model with RE reinforcement from mid-span. Assessed for the period 1950-1962 and 1962-1970 with the amount of RE reinforcement from span, and according to the assessment calculation with DC load model, for a variable mid-span length for three slenderness' 1/15, 1/20 and 1/25, and minimum slab thickness of 400mm . . . . .	49
4.11	Determined Unity Check for shear force, for the period 1930-1940(a), 1940-1950(b), 1950-1962(c) and 1962-1970(d) for a variable mid-span length for three slenderness' 1/15, 1/20 and 1/25, and a minimum slab thickness of 400mm. . . . .	49

4.12	Unity Checks for shear force according to the former design code and assessed according with DC load model, for bridges design in the period 1950-1962. . . . .	50
5.1	RE span reinforcement for constant bridge design over time. . . . .	53
5.2	ND of the design year with a Mu of 1940 and a SD of 2.5 (left) and of the slab thicknesses (right) at span (blue) and the support (orange) with a Mu of 0.5 and 0.525, and a SD of 0.01. Both graph are formed with 200 samples (N=200) . . . . .	56
5.3	ND of the concrete cover with a Mu of 3 and a SD of 0.25 (left) and the span lengths (right) the mid-span (orange) and the end-span (blue) with a Mu of 12.5 and 100, and a SD of 0.8. Both graph are formed with 200 samples (N=200) . . . . .	56
5.4	Histogram showing the effect of a ND design year and geometry on the Unity Checks at mid-span with RE reinforcement. The left graph is a class B bridge, assessed for the EC with a ND design year of 1940 and the right graph is a class B/45 bridge, assessed for the DC load model with a ND design year of 1962. The number of samples is: N=100. . . . .	57
5.5	Histogram showing the effect of a ND load class and geometry on the Unity Checks at mid-span with RE reinforcement. The left graph is a class A or B bridge, assessed for the EC with a design year of 1945 and the right graph is a class 60 or 45 bridge, assessed for the DC load model with a design year of 1964. The number of samples is: N=100. . . . .	57
5.6	Schematic view of collection of RC slab bridges with plain reinforcement, where for no assessment is required (green), provisional no assessment (blue) if the structural reliability can legally be proven, an assessment on moment- and shear capacity (purple), an assessment for bending moment capacity with scanned reinforcement of the bridge layout (orange), and urgent measures indicated by the protocol Figure D.9 (red). . . . .	58
5.7	Capacity regions in terms of Unity Checks to quantify risk from the assessment. . . . .	59
A.1	Mohr's circle, (LYNCH, 2019) . . . . .	73
A.2	2D stress element with indicated principal stresses, (LYNCH, 2019) . . . . .	73
A.3	Decrease in percentage (approx. 12%) of reinforcement (QR24) and decrease in percentage (approx. 19%) of reinforcement (QR40), for Crack-method compared with the N-method. . . . .	74
A.4	Minimal required reinforcement (QR24) in red based on strength with the right-hand y-axis and the configuration of bar diameter and mutual bar spacing in blue to fulfil the crack width limitation with the left-hand y-axis. . . . .	75
A.5	Minimal required reinforcement (QR40) in red based on strength with the right-hand y-axis and the configuration of bar diameter and mutual bar spacing in blue to fulfil the crack width limitation with the left-hand y-axis. . . . .	75
A.6	Excel sheet (1/3). . . . .	76
A.7	Excel sheet (2/3). . . . .	77
A.8	Excel sheet (3/3). . . . .	77
A.9	Graphical method to determine the position of the bent reinforcement, from 'Bouwen in gewapend beton' (van der Schrier, 1938) . . . . .	78
B.1	Illustration of the influence line for a wheel load schematised to a point load at span 2, leading to the maximum influence value. . . . .	79
B.2	Calculation procedure of the influence line for a point load at span 2. . . . .	79
B.3	Schematic overview of the coefficients of bending moments and shear forces for distributed loads. . . . .	81
B.4	Schematic overview of the coefficients of bending moments and shear forces for the design truck. . . . .	82
B.5	Ordinary differential equations with boundary- and interface conditions . . . . .	83
B.6	Resulting bending moment-line and shear force line. . . . .	83
B.7	Formulae to determine the support-moment due to concentrated loading from the design truck. . . . .	84
B.8	Detailing of shear reinforcement at a support. . . . .	84
B.9	Longitudinal cross-section of a RC bridge deck to overview the reinforcement, and unity checks for shear force, leading to no need for additional shear capacity from reinforcement for the end-supports. . . . .	84
B.10	Two figures showing the bend reinforcement and their mutual distances. . . . .	84

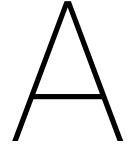


B.11	Field- and support reinforcement amounts RE, where the first blue and orange bars are from the first span and the support at the right side of the span. The second blue and orange bars are of the second span and the support at the right side of the span. . . . .	85
C.1	Bending moment line as a consequence of a concentrated load in span two, determined with the use of Technosoft. . . . .	87
C.2	The reduction of the support moment in case of the presence of a transverse beam is shown with the linear green line. . . . .	87
C.3	Input sheet of the GUI. . . . .	88
C.4	Pop-up screens of force lines from the AnaStruct package. Left: example of a structure loaded by a design truck and right: Corresponding maximum sagging bending moment line . . . . .	89
C.5	Pop-up screen of force lines from the AnaStruct package. Left: example of a structure loaded by a self-weight and right: corresponding bending moment line. . . . .	89
C.6	Pop-up screen of force lines from the AnaStruct package. Left: example of a structure loaded by a distributed traffic load and right: corresponding bending moment line. . . . .	89
C.7	Pop-up screen of force lines from the AnaStruct package. Left: example of a structure loaded by a distributed traffic loading and right: corresponding bending moment line with maximum sagging bending moment. . . . .	90
C.8	Output screen of the GUI. . . . .	90
C.9	Comparison of the determined effective width for loading by one design truck at the edge of the slab, the left figure determined with the RE-tool and the right figure with calculations in Maple. . . . .	92
C.10	Comparison of the determined effective width for loading by two design trucks in the middle of a slab, the left figure determined with the RE-tool and the right figure with calculations in Maple. . . . .	92
C.11	RE reinforcement amounts at mid-span for load class B and the EC (left) and reinforcement difference ratio (right) for the period 1930-1940, for a variable mid-span length for three slenderness' 1/15, 1/20 and 1/25. . . . .	93
C.12	RE reinforcement amounts at mid-span for load class B and the EC (left) and reinforcement difference ratio (right) for the period 1940-1950, for a variable mid-span length for three slenderness' 1/15, 1/20 and 1/25. . . . .	93
C.13	RE reinforcement amounts at mid-span for load class 45 and the EC (left) and reinforcement difference ratio (right) for the period 1962-1970, for a variable mid-span length for three slenderness' 1/15, 1/20 and 1/25. . . . .	94
C.14	RE support reinforcement amounts at a mid-support for load class B and the EC (left) and corresponding Unity Checks (right) for the period 1930-1940, for a variable mid-span length for three slenderness' 1/15, 1/20 and 1/25. . . . .	95
C.15	RE support reinforcement amounts at a mid-support for load class B and the EC (left) and corresponding Unity Checks (right) for the period 1940-1950, for a variable mid-span length for three slenderness' 1/15, 1/20 and 1/25. . . . .	95
C.16	RE support reinforcement amounts at a mid-support for load class 45 and the EC (left) and corresponding Unity Checks (right) for the period 1962-1970, for a variable mid-span length for three slenderness' 1/15, 1/20 and 1/25. . . . .	96
C.17	RE span reinforcement amount at a mid-span for load class 60 and the EC (left) and corresponding Unity Check (right) for the period 1950-1962 for class A, and according the assessment calculations, for a variable mid-span length for three slenderness' 1/15, 1/20 and 1/25. . . . .	96
C.18	RE support reinforcement amount at a mid-support for load class 60 and the EC (left) and corresponding Unity Check (right) for the period 1950-1962 for class A, and according the assessment calculations, for a variable mid-span length for three slenderness' 1/15, 1/20 and 1/25. . . . .	97
C.19	Unity Check for the shear force for period 1950-1962 for load class A, assessed for the EC. Geometry with a variable mid-span length for three slenderness' 1/15, 1/20 and 1/25. . . . .	97
C.20	Reinforcement ratio between the RE support reinforcement and the RE span reinforcement for load class A/60 for $L1/L2 \leq 0.8$ , a slenderness of 1/20 and a minimum slab thickness of 400mm. . . . .	97
C.21	RE span reinforcement amounts for bending according to load class B and assessed according to the DC load model (right) and corresponding Unity Checks (b) for the period 1930-1940, for a variable mid-span length for three slenderness' 1/15, 1/20 and 1/25, and minimum slab thickness of 400mm. . . . .	98

C.22 RE span reinforcement amounts for bending according to load class B and assessed according to the DC load model (right) and corresponding Unity Checks (b) for the period 1940-1950, for a variable mid-span length for three slenderness' 1/15, 1/20 and 1/25, and minimum slab thickness of 400mm. . . . .	98
C.23 RE span reinforcement amounts for bending according to load class B and assessed according to the DC load model (right) and corresponding Unity Checks (b) for the period 1962-1970, for a variable mid-span length for three slenderness' 1/15, 1/20 and 1/25, and minimum slab thickness of 400mm. . . . .	99
D.1 Effect of the removal of the extra slab thickness on the RE required reinforcement amounts at the support. . . . .	101
D.2 Effect of the removal of the transverse beam on the RE required reinforcement amounts at the support. . . . .	102
D.3 Effect of the addition of the reinforcement layer distance of 2.0cm on the RE required reinforcement amounts at the support. . . . .	102
D.4 Effect of the addition of extra dead load on the RE required reinforcement amounts at the support (left) and span (right). . . . .	103
D.5 Effect of a lower concrete cover 2.0cm relative to 3.0cm on the RE required reinforcement amounts at the support (left) and span (right). . . . .	103
D.6 Unity check for the midspan reinforcement for a bridge with variable width and span length of 10, 12 and 14m. Design in the period 1930-1940 (a), 1940-1950 (b), 1950-1962(c) and 1962-1970 (d) for load class 45. . . . .	104
D.7 Unity check for the midspan reinforcement for a bridge with variable width and span length of 10, 12 and 14m. Design in the period 1930-1940 (a), 1940-1950 (b), 1950-1962(c) and 1962-1970 (d) for load class 45. . . . .	105
D.8 Scatter plot of the Unity Checks for bending moment at midspan, with RE reinforcement designed for load class B, assessed for the DC load model with a ND design year of 1955. . . . .	106
D.9 Protocol for the assessment of existing RC slab bridges. . . . .	107

# List of Tables

2.1	Share in the application of steel qualities from Gantvoort (1964).	6
2.2	Allowable stresses according to the GBV1962.	7
2.3	Prescriptions from the GBV codes for reinforcing of slabs.	13
2.4	Traffic load configuration for load class A/60	16
2.5	Traffic load configuration for load class B/45	16
2.6	Traffic load configuration for load class C/30	16
2.7	Modification in structural bridge design from 1930 until 1970.	23
3.1	Configurations of the distributed traffic load leading to the governing mid-span bending moments.	26
3.2	Configurations of the distributed traffic load leading to the governing mid-support bending moments.	27
3.3	Available information about the RE bridges.	30
3.4	Unity Checks for bending moment, at the location shown in figure 3.10.	31
3.5	Unity Checks from RE for bending moments, at the location shown in figure 3.10.	32
3.6	Comparison of the calculated reinforcement and reinforcement amount from the technical drawings.	33
3.7	Overview of the applied bar diameters for the main reinforcement of the assessed bridges.	34
3.8	Shear check for several example bridges	35
4.1	Partial load factors $\gamma$ for the ULS for the assessment level 'Reconstruction' for CC2 with $\beta_r = 3.3$ (3.1), from the NEN8700 (2011) Table A2.2(B).	42
4.2	Overview of the Unity Checks from bending moment and shear force results for RE class B bridges, designed in the period 1950-1962.	50
4.3	Comparison of the RE reinforcement and reinforcement amount from the technical drawings.	51
5.1	Effect of the assumptions made for the input parameters in response to the RE reinforcement amounts in the parametric study.	55
5.2	Overview of input parameters with a Normal Distribution	56
B.1	Calculation and comparison of the influence values for KW7.	80
B.2	List of shear forces and distributed loading at the Waalwijk bridge.	85
C.1	Overview of the input and output from the computer model.	86
C.2	Partial load factors $\gamma$ for the ULS for the assessment level 'Disapproval' for CC2 with $\beta_b = 2.5$ , from the (NEN8700, 2011) Table A2.2(C).	87
C.3	$\psi$ -factors for shorter reference periods.	88
C.4	Reduction factor $\alpha_{trend}$ for the influence of the trend related to the year 2060, for the traffic loads from LM1 and LM2.	88
C.5	The reinforcement table with possible configurations of bar distance times bar diameter, filled in for an example required reinforcement amount.	91
C.6	Overview of the Unity Checks from bending moment and shear force results for RE class A bridges, designed in the period 1950-1962.	99



## Appendix - Chapter 2: Literature

### A.1. Cross-sectional forces and stresses

#### Bending moment

From (Shenton et al., 2007), the calculation for the internal bending moment follows from equation 2.1 and 2.2 from Chapter 2 giving:

$$\frac{\sigma_a}{\sigma_b} = \frac{bX}{2A_s} \quad (\text{A.1})$$

From the two assumptions that the linear strain relationship stands across the transverse section and that stress is proportional to strain, they yield

$$\frac{\epsilon_a}{\epsilon_b} = \frac{h-X}{X} \quad (\text{A.2})$$

$$\frac{\sigma_a}{\sigma_b} = \frac{E_a \epsilon_a}{E_b \epsilon_b} = n \frac{h-X}{X} \quad (\text{A.3})$$

The following equation for the neutral axis can be obtained by equating A.2 and A.3:

$$\frac{bX^2}{2} = nA_s(h-X) \quad (\text{A.4})$$

The internal moment is given by the following equation, where the steel strain can be test encountered.

$$M = A_s E_a \epsilon_a \left(h - \frac{X}{3}\right) \quad (\text{A.5})$$

Where after the internal moment can be checked for the external moment.

#### Shear stress

The circle of Mohr is defined by the following formulae, and drawn in figure A.1.

$$\sigma_1 = \sqrt{(0.5 \cdot (\sigma_x - \sigma_y))^2 + \tau_{xy}^2} - 0.5 \cdot (\sigma_x - \sigma_y) \leq f_{ctd} \quad (\text{A.6})$$

Where the corner  $\theta$  defining the direction of the shear force is determined by dividing the shear stress  $\tau_{xy}$  by the compressive stress  $\sigma_x$ .

$$\tan(\theta) = \frac{\tau_{xy}}{\sigma_x} \quad (\text{A.7})$$

The compressive stress in a cross-section is defined by to normal stress due to the normal force, and compressive stress due to bending moment:

$$\sigma_x = \frac{N}{A} + \frac{M \cdot z}{I} \quad (\text{A.8})$$

The force equilibrium of the shear stresses  $\tau_{xy}$  and  $\tau_{yx}$  shown in figure A.2, results in the following equation:

$$\tau_{xy} = \tau_{yx} = \frac{V \cdot S}{b \cdot I} \quad (\text{A.9})$$

With S being the shear modulus.

$$S = \frac{1}{8} b h^2 \quad (\text{A.10})$$

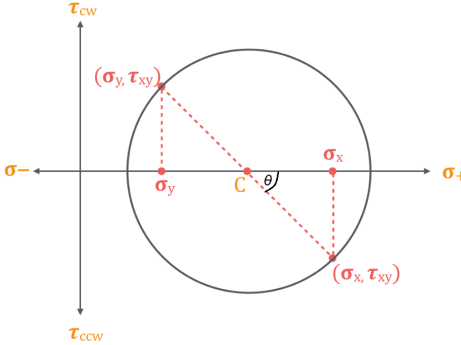


Figure A.1: Mohr's circle, (LYNCH, 2019)

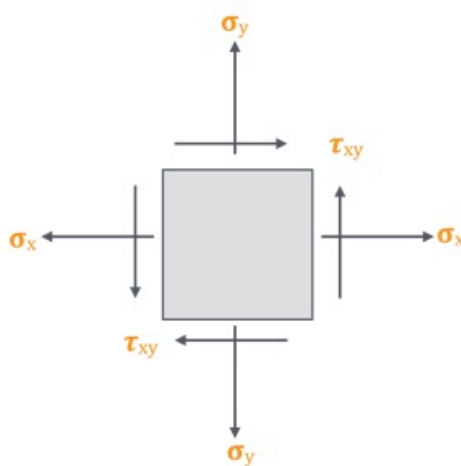


Figure A.2: 2D stress element with indicated principal stresses, (LYNCH, 2019)

With I the moment of inertia.

$$I = \frac{1}{12}bh^3 \tag{A.11}$$

Results in the following formulae to determine the shear stress:

$$\tau_{xy} = \tau_{yx} = \frac{V \cdot S}{b \cdot I} = \frac{3}{2} \frac{V}{bh} \tag{A.12}$$

**N-method compared to the crack-method**

The constant decrease in reinforcement percentage for the crack-method compared to the N-method for two different types of reinforcement qualities.

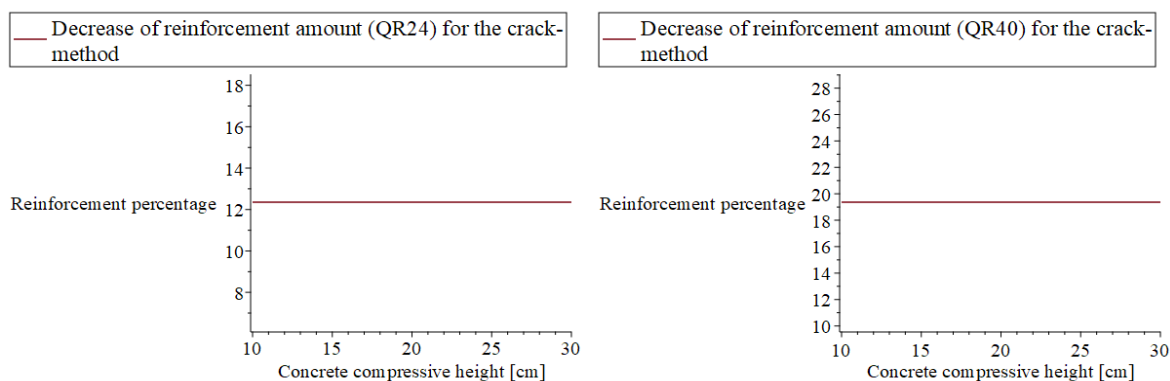


Figure A.3: Decrease in percentage (approx. 12%) of reinforcement (QR24) and decrease in percentage (approx. 19%) of reinforcement (QR40), for Crack-method compared with the N-method.

## A.2. Crack width control

The crack width control, introduced in the GBV1962, is an additional check after the required reinforcement for strength is determined. The configuration of bar diameter and mutual bar spacing fulfilling the crack width limitation is searched for. The steel stress in the ULS is used in the crack width formulae and divided by the safety factor  $\gamma$ . In case a larger reinforcement amount is required to fulfil the crack width limitation, the reinforcement is dimensioned based on crack width. This increases the safety factor ( $\gamma$ ) for the strength calculations. The safety factor ( $\gamma$ ) is an input parameter for the crack width calculation, which leads to an iterative calculation procedure. In the two examples below is the crack width check performed at mid-span. In former RC slab bridge design, the same amount or more reinforcement is applied at the support so the governing occurring crack width is expected at mid-span.

### Example class B bridge with steel quality QR24

A class B bridge from 1965 is RE with the GBV1962 so including the crack-method. It is assumed that ribbed reinforcement with steel quality QR24 is applied in former design. From the strength calculation results a minimal required reinforcement amount at span of  $39 \text{ cm}^2$ . This amount is also a boundary for the crack width control. Figure A.4 shows with the horizontal blue line the crack limit (0.025cm) and in blue the expected crack width depending on the configuration of the bar diameter and mutual bar spacing. The horizontal red line is the minimal required reinforcement amount based on strength ( $39 \text{ cm}^2$ ) and the red line (nonlinear) line the applied reinforcement based on the bar diameter and mutual bar spacing. Here, the crack width limit does not influence the required reinforcement configuration, which is expected in case low steel qualities are used (QR<40).

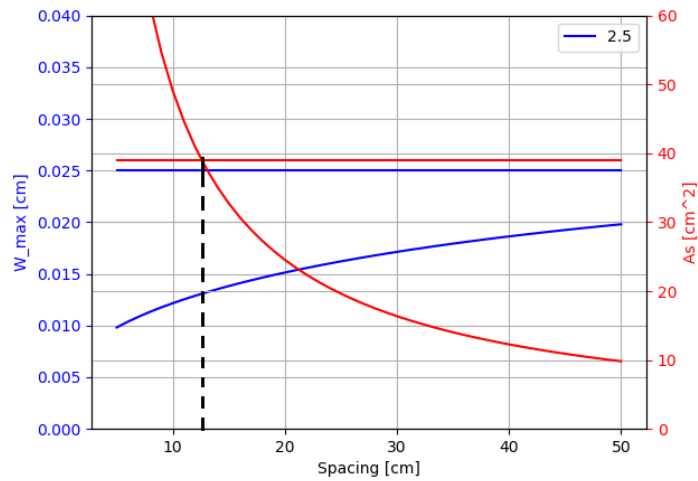


Figure A.4: Minimal required reinforcement (QR24) in red based on strength with the right-hand y-axis and the configuration of bar diameter and mutual bar spacing in blue to fulfil the crack width limitation with the left-hand y-axis.

**Example class B bridge with steel quality QR40**

A class B bridge from 1965 with assumed steel quality of QR40 is RE. The higher steel quality leads to less required reinforcement but the crack width control is now governing for the dimensioning of the reinforcement. A smaller spacing between the longitudinal bars, so more bars per meter slab width need to be applied in order to fulfil the crack width limitation. A smaller bar diameter also lowers the expected crack width.

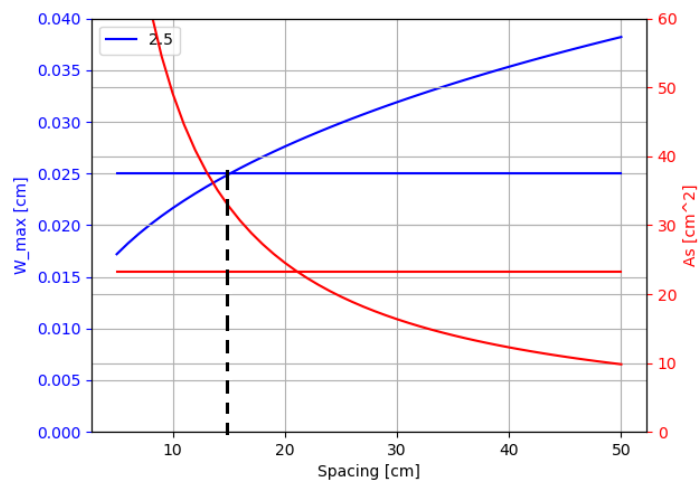


Figure A.5: Minimal required reinforcement (QR40) in red based on strength with the right-hand y-axis and the configuration of bar diameter and mutual bar spacing in blue to fulfil the crack width limitation with the left-hand y-axis.

Print out of the Guyon-Massonnet method in Excel, with example values filled in, Figures A.6-A.8.


Berekening krachtsverdeling met theorie voor lastspreiding Guyon-Massonnet						 Royal HaskoningDHV Enhancing Society Together		
Project:	Herberekening	Datum:	5-9-2019	Norm:	VOSB1933			
Projectnummer:	1	Naam:	Thomas Harrewijn	Programma:	GuyMass			
Omschrijving:	Constructie X	Verzie:	v0.1	Authorisatie:				
<b>1. Invoer geometrie brugdek</b>								
Isotrope toelastijve plaat	$\alpha$	=	1.000			Controlecel		
Equivalente veldlengte (tussen de M-nulpunten)	$L = 2a$	=	7.422 m	10.8 m				
Equivalente deklengte $B_{equivalent} = 12 \cdot l / h^2$	$2b$	=	20.300 m	=> Specifieke plaatverhouding: $b/2a =$		1.36205		
Voor K1 gerekend met een dwarscontractie-coëfficiënt	$\nu$	=	0.00					
Uitvoer in punt (vanaf rechter rand)	$y$	=	1.500 m	8.65 m vanaf hart plaat				
Dikte plaat	$h$	=	0.490 m					
Breedte wiel	$j$	=	0.300 m					
afstand 2-3 wiel	$i$	=	0.300 m					
afstand wiel- rand	$g$	=	0.200 m					
	$\beta$	=	0.690					
<b>2. Invoer belastingen (conform Eurocode 1, NEN-EN 1991-2)</b>								
Randafstand rechts	$to_v b/2$	=	0.7 m					
Randafstand links	$to_v -b/2$	=	0.7 m					
Breedte rijweg	$w$	=	18.900 m					
Breedte theoretische rijstrook	$w_{th}$	=	3 m					
(max.) aantal theoretische rijstroken	$n_{th}$	=	6					
Aantal zware vrachtwagens per jaar per rijstrook	$N_{skw}$	=	2.00E+03					
De lijnlast excentriciteit $e$ wordt opgegeven t.o.v. het dekmidden.								
Excentriciteit Rijstrook I ten opzichte van as dekplaat:	$a_1$	=	7.95 m	$Q_{skwI}$	$q_{skwI}$	$q_{skwI} \cdot w_{th}$	Wegingfactor	
Excentriciteit Rijstrook II ten opzichte van as dekplaat:	$a_2$	=	4.95 m	4	0.8	9.6 kN/m	0.50	
Excentriciteit Rijstrook III ten opzichte van as dekplaat:	$a_3$	=	1.95 m	4	0.8	9.6 kN/m	0.50	
Excentriciteit Rijstrook IV ten opzichte van as dekplaat:	$a_4$	=	-1.05 m		0.8	0 kN/m	0.00	
					0.8	0 kN/m	0.00	
				$Q_{skw}$		19.2 kN/m		
Spoorbreedte Laststelsels								
Excentriciteit Laststelsels tov rijstrook		=	0.75 m					
Positie wiel 1 tov hart rijstrook	$a_{w1}$	=	-0.375 m	Positie wiel 2 tov hart rijstrook	$a_{w2}$	=	0.375 m	
				$Q_1$	$q_{13}$	$q_{13} \cdot Q_1$	Wegingfactor	
				200	0.8	160 kN	0.50	
				200	0.8	160 kN	0.50	
				100	0	0 kN	0.00	
				100	0	0 kN	0.00	
				$P_{tot}$		320 kN		
$\theta = b/2a \cdot (\sqrt{j})^2 \cdot (L/4)$		=	1.36					
$\theta = 0.7a/\beta i$		=	1.36					
DAF		=	1.15					
<b>3. Berekening constanten afhankelijk van geometrie dek</b>								
$\theta$		=	1.362	$(1-\nu)$	=	1	$\lambda = m\theta/(bv^2)$	0.2981
$\theta m$		=	4.2790	$(1+\nu)$	=	1	$2\lambda b$	6.051
$\sinh(\theta m)$		=	36.077	$\sinh(2\lambda b)$	=			212.36
$\cosh(\theta m)$		=	36.0913	$\sin^2(2\lambda b)$	=			0.0528
$\sinh^2(\theta m)$		=	1301.6	$\sinh^2(2\lambda b)$	=			45096
$\theta m \cdot \cosh(\theta m)$		=	154.44					
$\theta m \cdot \cosh(\theta m) - \sinh(\theta m)$		=	118.36					
$2 \cdot \sinh(\theta m) + \theta m \cdot \cosh(\theta m)$		=	226.59					
$[(3+\nu) \cdot \sinh(\theta m) \cdot \cosh(\theta m) - (1-\nu) \cdot \theta m^2 \cdot (L-\nu)]$		=	3902.0					
$[(3+\nu) \cdot \sinh(\theta m) \cdot \cosh(\theta m) + (L-\nu) \cdot \theta m^2 \cdot (L-\nu)]$		=	3910.5					
$(1-\nu) \cdot \theta m \cdot \cosh(\theta m) - (1+\nu) \cdot \sinh(\theta m)$		=	118.36					
$(1-\nu) \cdot \theta m \cdot \cosh(\theta m) + 2 \cdot \sinh(\theta m)$		=	226.59					
<b>4. Berekening K0-factoren</b>								
Gelijkmatig verdeelde belasting per rijstrook								
Een strookbelasting wordt tot 4 gelijke lijnlasten F1 t/m F4 geschematiseerd.								
Rijstrook	1	2	3	4				
Positie [m]	$K_0$	Positie [m]	$K_0$	Positie [m]	$K_0$	Positie [m]	$K_0$	
F1	9.075	5.803	6.075	2.188	3.075	0.151	0.075	-0.290
F2	8.325	4.910	5.325	1.479	2.325	-0.064	-0.675	-0.283
F3	7.575	3.952	4.575	0.907	1.575	-0.197	-1.425	-0.256
F4	6.825	3.024	3.825	0.469	0.825	-0.267	-2.175	-0.218
gem Q	4.422		1.261		-0.094		-0.262	

Figure A.6: Excel sheet (1/3).



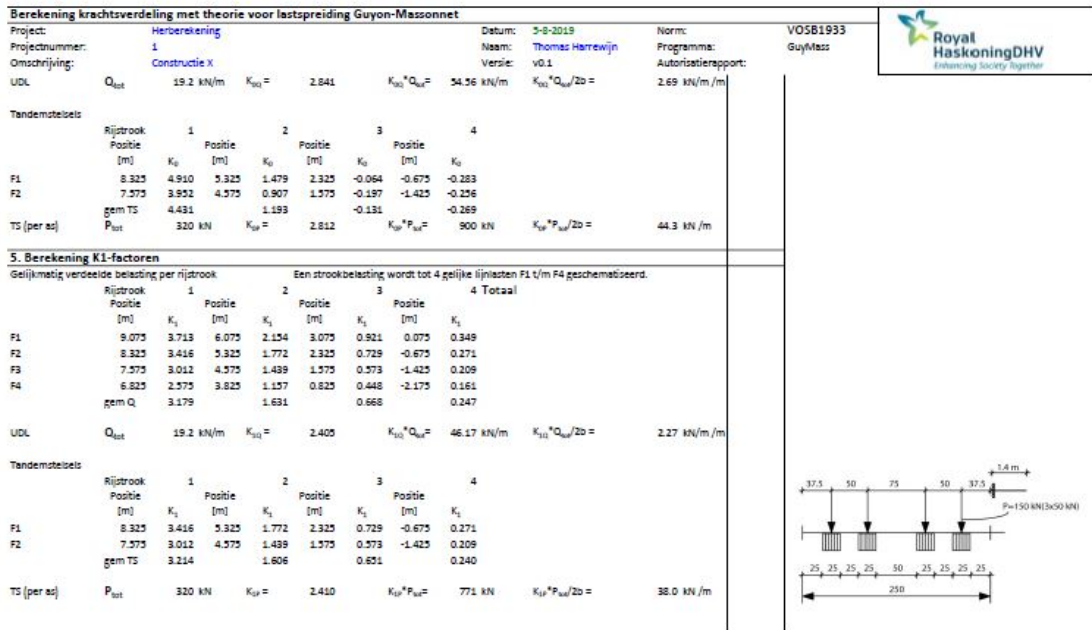


Figure A.7: Excel sheet (2/3).

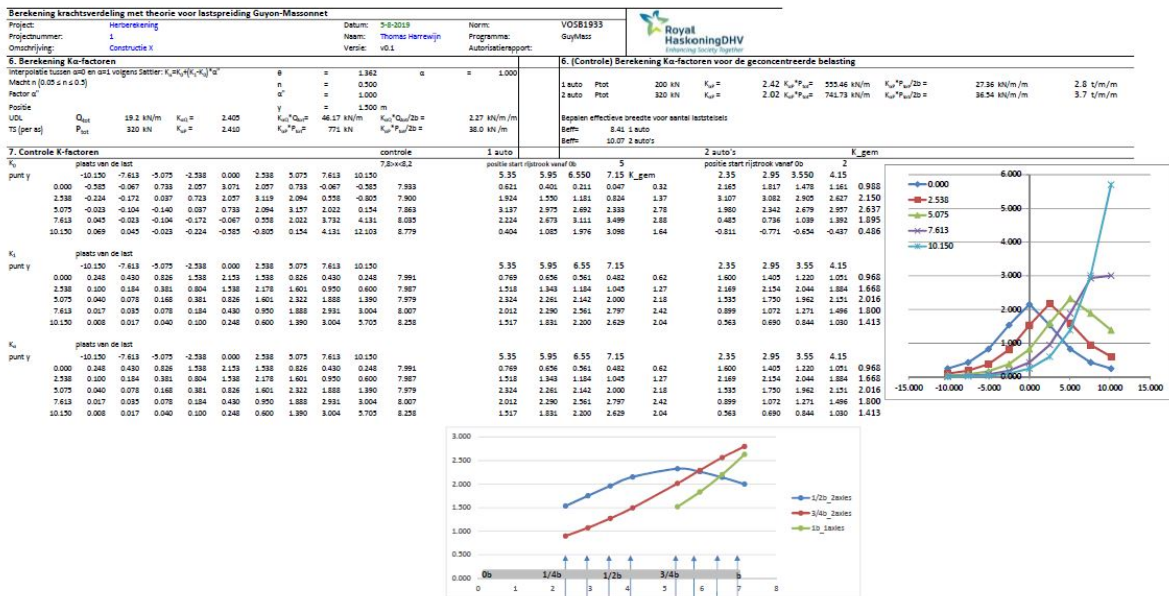


Figure A.8: Excel sheet (3/3).

**Graphical method**

W. van der Schrier (van der Schrier, 1938) developed a graphical method to calculate and design shear reinforcement. This method is developed for a beam with distributed loading. The graphical method draws from a base point, arc beams in order to sketch trapezes whereof the surface should be determined. From the centre of gravity of each trapeze a line at 45 degrees is drawn towards the beam to mark the location of the bent bar, see Figure A.9 for an impression of the graphical method. The area between B-C, AD and h1 and H, is the effective shear stress and should be divided in to equal parts, where h1 is equal to  $\rho$ , and H to D. This leads to an equal load distribution for the bent bars, where the mutual distances decrease in direction of the support. For a combination of concentrated- and distributed loading the method is more complicated and is not discussed in the literature.

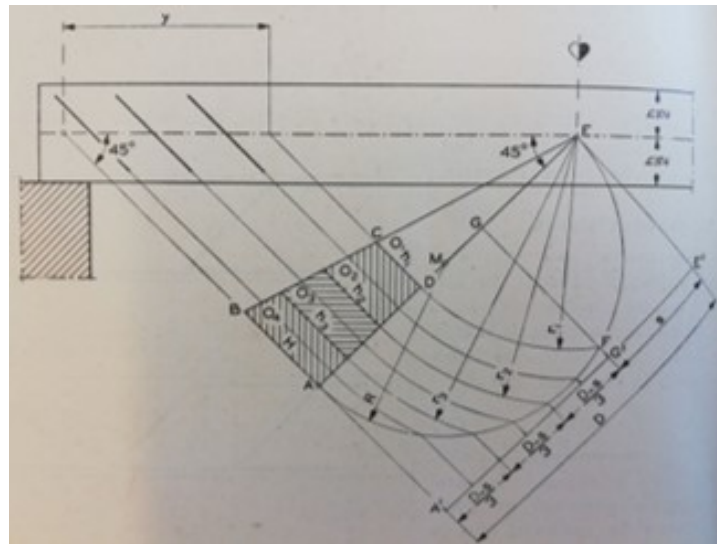


Figure A.9: Graphical method to determine the position of the bent reinforcement, from 'Bouwen in gewapend beton' (van der Schrier, 1938)

# B

## Appendix - Chapter 3: Reverse Engineering

### Influence lines

In Figure B.1 below, an example of an influence line of a four span bridges loaded by a point load in its second span. The ODE with its unknown integration constants to solve for boundary and interface conditions are written in Figure B.2.

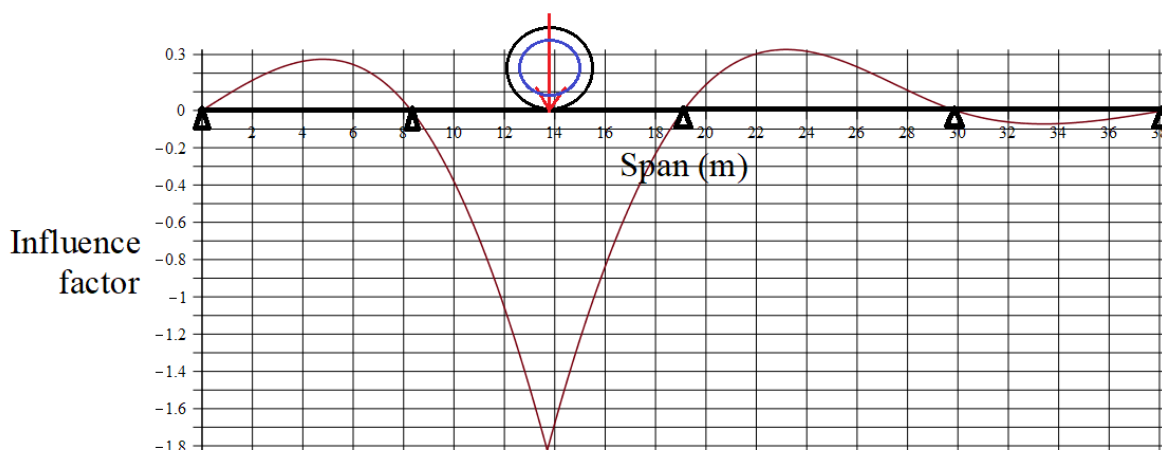


Figure B.1: Illustration of the influence line for a wheel load schematised to a point load at span 2, leading to the maximum influence value.

```
> restart;
> # Influence line for a static indeterminate beam:
> ODE1 := -EI1*diff(w1(x), x$4) = -q1 :
> ODE2 := -EI2*diff(w2(x), x$4) = -q2 :
> ODE3 := -EI2*diff(w3(x), x$4) = -q2 :
> ODE4 := -EI1*diff(w4(x), x$4) = -q3 :
> ODE5 := -EI1*diff(w5(x), x$4) = -q4 :
> sol := dsolve({ODE1, ODE2, ODE3, ODE4, ODE5}, {w1(x), w2(x), w3(x), w4(x), w5(x)}): assign(sol);
> w1 := w1(x): w2 := w2(x): w3 := w3(x): w4 := w4(x): w5 := w5(x):
> phi1 := -diff(w1, x): kappa1 := diff(phi1, x): M1 := EI1*kappa1: V1 := diff(M1, x):
> phi2 := -diff(w2, x): kappa2 := diff(phi2, x): M2 := EI2*kappa2: V2 := diff(M2, x):
> phi3 := -diff(w3, x): kappa3 := diff(phi3, x): M3 := EI2*kappa3: V3 := diff(M3, x):
> phi4 := -diff(w4, x): kappa4 := diff(phi4, x): M4 := EI1*kappa4: V4 := diff(M4, x):
> phi5 := -diff(w5, x): kappa5 := diff(phi5, x): M5 := EI1*kappa5: V5 := diff(M5, x):
> # Boundary and interface conditions:
> x := 0: eq1 := w1 = 0: eq2 := M1 = 0:
> x := L1: eq3 := w1 = 0: eq4 := w2 = 0: eq5 := phi1 = phi2: eq6 := M1 = M2:
> x := L1 + a: eq7 := w2 = w3: eq8 := M2 = M3: eq9 := V2 = V3: eq10 := phi3 - phi2 = 1:
> x := L1 + L2: eq11 := w3 = 0: eq12 := w4 = 0: eq13 := phi3 = phi4: eq14 := M3 = M4:
> x := L1 + L2 + L2: eq15 := w4 = 0: eq16 := w5 = 0: eq17 := M4 = M5: eq18 := phi4 = phi5:
> x := L1 + L2 + L2 + L1: eq19 := w5 = 0: eq20 := M5 = 0:
> sol := solve({eq1, eq2, eq3, eq4, eq5, eq6, eq7, eq8, eq9, eq10, eq11, eq12, eq13, eq14, eq15, eq16, eq17, eq18, eq19, eq20}, {_C1, _C2, _C3, _C4, _C5, _C6, _C7, _C8, _C9, _C10, _C11, _C12, _C13,
_C14, _C15, _C16, _C17, _C18, _C19, _C20}): assign(sol);
```

Figure B.2: Calculation procedure of the influence line for a point load at span 2.

Influence values are determined at steps of 1/10 of the span length in former bridge design, and is compared with a structure with known influence values from former calculation.

Table B.1: Calculation and comparison of the influence values for KW7.

Position	Influence value former calculation	Influence value Maple	Accuracy
1	1,59	1,59	100%
2	2,67	2,63	99%
3	3,17	3,14	99%
4	3,36	3,35	100%
5	3,21	3,18	99%
6	2,96	2,94	99%
7	2,26	2,25	100%
8	1,51	1,48	98%
9	0,60	0,57	95%
10	2,74	2,74	100%
11	0,72	0,70	97%
12	1,75	1,74	99%
13	2,73	2,72	100%
14	3,38	3,34	99%
15	3,52	3,47	99%

### B.1. Force lines

Figure B.3 shows the overview of the force coefficients due to distributed loading from the GBV1940.

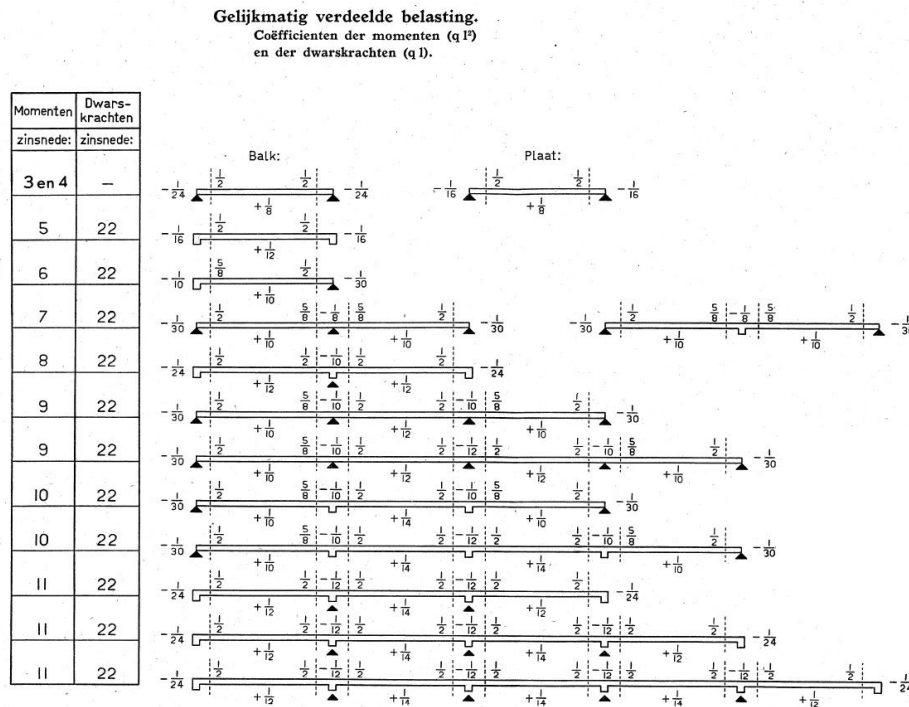


Figure B.3: Schematic overview of the coefficients of bending moments and shear forces for distributed loads.

Figure B.4 shows the overview of the force coefficients due to concentrated loading from the design truck from the GBV1940.

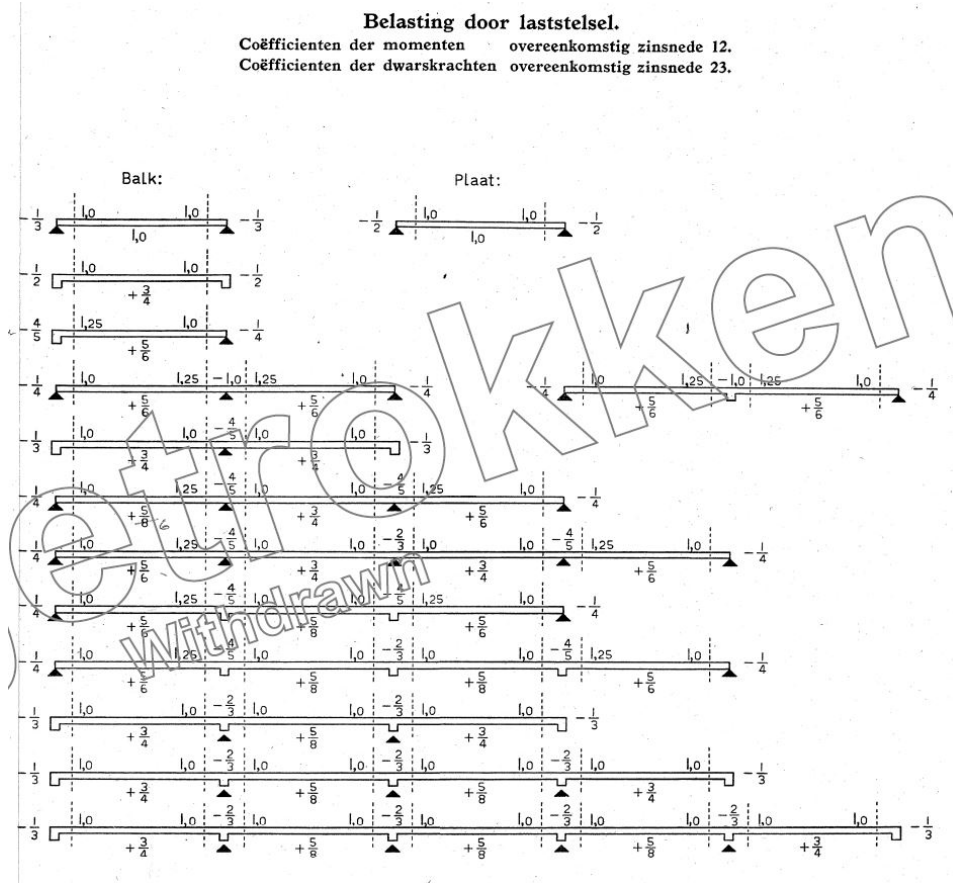


Figure B.4: Schematic overview of the coefficients of bending moments and shear forces for the design truck.

With the use of the following calculation procedure in Maple can the governing span moments due to permanent loads and distributed traffic load, and governing support moments due to permanent loads, distributed- and concentrated traffic load be calculated.

```
> restart;
KW7-distributed traffic load
> w1:=(q+q1)*x^4/(24*EI)+C1+C2*x+C3*x^2+C4*x^3;
> w2:=(q+q2)*x^4/(24*EI)+C5+C6*x+C7*x^2+C8*x^3;
> w3:=(q+q3)*x^4/(24*EI)+C9+C10*x+C11*x^2+C12*x^3;
> phi1:=-diff(w1,x): kappa1:=diff(phi1,x): M1:=EI*kappa1: V1:=diff(M1,x):
> phi2:=-diff(w2,x): kappa2:=diff(phi2,x): M2:=EI*kappa2: V2:=diff(M2,x):
> phi3:=-diff(w3,x): kappa3:=diff(phi3,x): M3:=EI*kappa3: V3:=diff(M3,x):
> x:=0: eq1 :=w1=0: eq2:=M1=0:
> x:=L1: eq3 :=w1=0: eq4:=M1=M2: eq5:=phi1=phi2: eq6 :=w2=0:
> x:=L1+L2: eq7:=w2=0: eq8:=M2=M3: eq9:=phi2=phi3: eq10:=w3=0:
> x := L1 + L2 + L1 : eq11 := w3 = 0 : eq12 := M3 = 0 :
> sol:=solve({eq1,eq2,eq3,eq4,eq5,eq6,eq7,eq8,eq9,eq10,eq11,eq12},{C1,C2,C3,C4,C5,C6,C7,C8,C9,C10,C11,C12}): assign(sol): x:=
'x':
> L1:=8.65: L2:=10.8:s:= 1+3/(10+(L1+L2)/2): q1:=0*0.8*S^4: q2:=1*0.8*S^4: q3:=0*0.8*S^4:q:=1*17.06: EI:=10000:
> with(plots):
> AA:=plot(-M1,x=0..L1,thickness=2,color="red",size=[1000,500],axis = [gridlines = [linestyle = dot]],labels = ["x","kNm"],
labelfont = ["utopia", 16], legend = ["Moment-line"]):
> BB:=plot(-M2,x=L1..L1+L2,thickness=2,color="red"):
> CC:=plot(-M3,x=L1+L2..L1+L2+L1,thickness=2,color="red"):
> AV:=plot(V1,x=0..L1,color="blue",thickness=2, labels = ["x","kNm"], labelfont = ["utopia", 16], legend = ["Shearforce-
line"]):
> BV:=plot(V2,x=L1..L1+L2,color="blue",thickness=2):
> CV:=plot(V3,x=L1+L2..L1+L2+L1,color="blue",thickness=2):
> display(AA,BB,CC,AV,BV,CV);
```

Figure B.5: Ordinary differential equations with boundary- and interface conditions

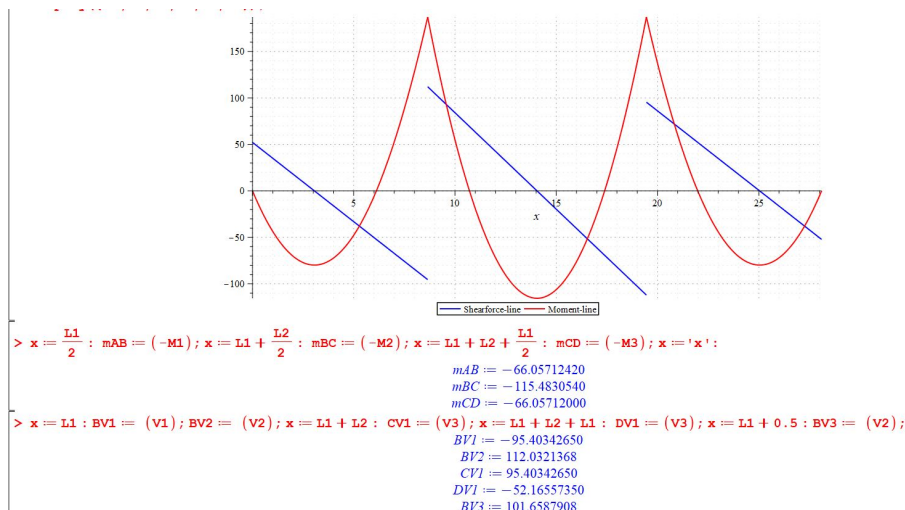


Figure B.6: Resulting bending moment-line and shear force line.

## B.2. Shear force

The difference in shear reinforcement amount for a second and third support of a four span bridge is shown in the reinforcement drawings in Figure B.8 and B.8. Both support adjoin the same span leading to the same design shear force, but different amounts of bend reinforcement can be obtained from the technical drawings. The amount of stirrup reinforcement is equal for both supports.

The estimated required reinforcement to bear the effective bending moments are presented with a bar chart in Figure B.11.

### Example of a shear force check for a bridge from Waalwijk

The shear check is executed at support B, for span 2 and support C, for span 2. A list of different types of loading is obtained for the Waalwijk bridge in Table B.2. The assumption is made that 100% of the loading can be transferred to the edge beams.



```

> b = 8.44 : #Meewerkende breedte 2 auto's
> F1 = 0.9·S·400 ; F2 = 0.9·S·400 ; F3 = 0.9·S·400 ; L3 = L1 : EI = 1000 : s1 = 4 : s2 = 5 : a1 = L2 / 2 - x : a2 = a1 + s1 : a3 = a1 + s2 :
    b1 = L2 - a1 : b2 = L2 - a2 : b3 = L2 - a3 :
> eq1 = M_b·L1 / (3·EI) + F1·a1·b1·(L2 + b1) / (6·EI·L2) + F2·a2·b2·(L2 + b2) / (6·EI·L2) + F3·a3·b3·(L2 + b3) / (6·EI·L2) - M_b·L2 / (3·EI) - M_c·L2 / (3·EI) :
> eq2 = F1·a1·b1·(L2 + a1) / (6·EI·L2) + F2·a2·b2·(L2 + a2) / (6·EI·L2) + F3·a3·b3·(L2 + a3) / (6·EI·L2) - M_b·L2 / (3·EI) - M_c·L2 / (3·EI) - M_c·L3 / (3·EI) :
> sol = solve((eq1, eq2), (M_b, M_c)) : assign(sol) :
> evalf(M_b) : evalf(M_c) :
> with(Optimization) : Mb = maximize(M_b, x = -5..5) ; Mc = maximize(M_c, x = -5..5) ;
    Mb = 108.8826931
    Mc = 114.7120329
> plot(M_b, x = -5..5) :
> p = 2 : F4 = 200·S : F5 = 200·S : F6 = 200·S : #loadsystem width
> V_b1 = (F4 / p) · (L2 - 0) / L2 + (F5 / (p + 2·(s2 - s1))) · (L2 - (s2 - s1)) / L2 + (F6 / (p + 2·s2)) · (L2 - s2) / L2 ;
    V_b1 = 177.7918603
> V_b2 = (F4 / p) · (L2 - 0) / L2 + (F5 / (p + 2·s1)) · (L2 - s1) / L2 + (F6 / (p + 2·s2)) · (L2 - s2) / L2 ;
    V_b2 = 140.0288692
> x = L1 : mB = (-M1 + Mb) ; x = L1 + L2 : mC = (-M2 + Mc) ;
    mB = 295.8864073
    mC = 301.7157489
    
```

Figure B.7: Formulae to determine the support-moment due to concentrated loading from the design truck.

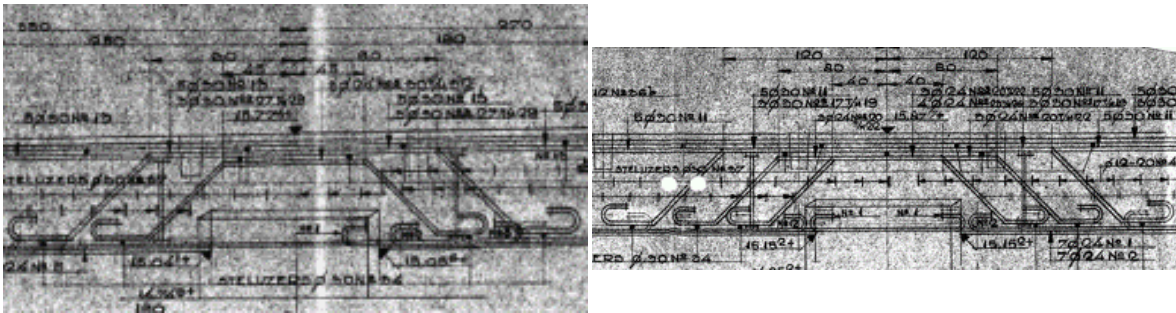


Figure B.8: Detailing of shear reinforcement at a support.

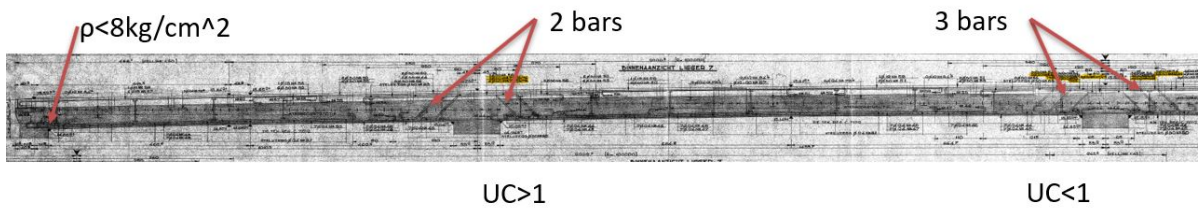


Figure B.9: Longitudinal cross-section of a RC bridge deck to overview the reinforcement, and unity checks for shear force, leading to no need for additional shear capacity from reinforcement for the end-supports.

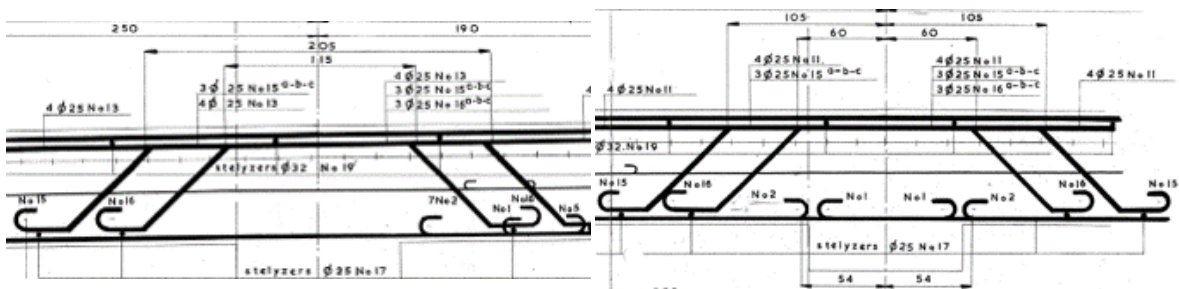


Figure B.10: Two figures showing the bend reinforcement and their mutual distances.

In case  $\rho > \sigma'_B$ , additional reinforcement is required for the shear force.

$$\rho = \frac{3 D}{2 bh} = \frac{3 \cdot 1382}{2 \cdot 318 \cdot 71.25} = 9.2 \text{ kg/cm}^2 \tag{B.1}$$

$$D8 = \sigma'_B \cdot b \cdot z = 8 \cdot 318 \cdot 51 = 1271 \text{ kN} \tag{B.2}$$



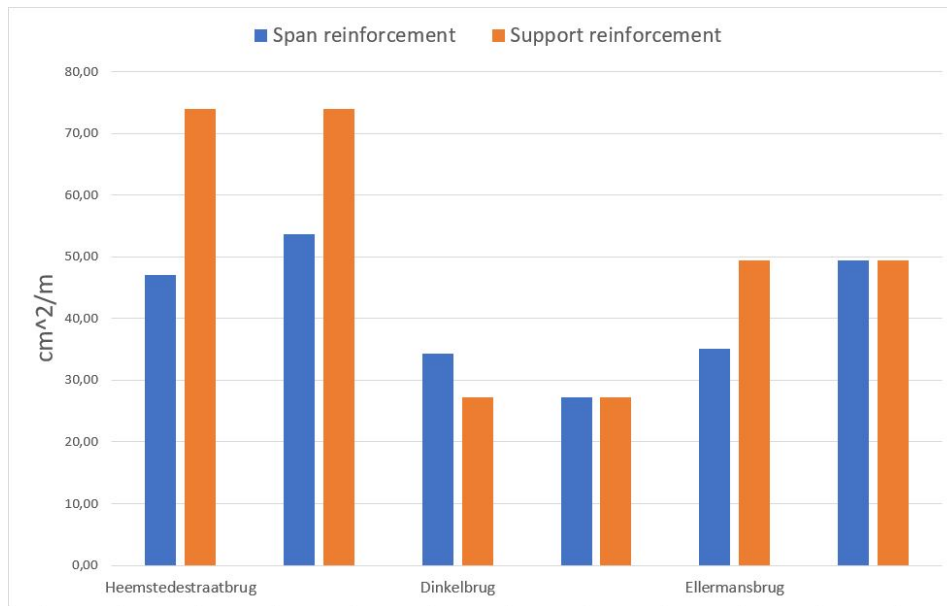


Figure B.11: Field- and support reinforcement amounts RE, where the first blue and orange bars are from the first span and the support at the right side of the span. The second blue and orange bars are of the second span and the support at the right side of the span.

Table B.2: List of shear forces and distributed loading at the Waalwijk bridge.

Shear force	kN	Distributed load	kN/m
$D_{slab}$	628	$q_{slab}$	87.4
$D_{beams}$	421	$q_{beams}$	58.6
$D_{vl}$	172	$q_{vl}$	24
$D_{TS}$	138	$q_{TS}$	19.2
$D_{total}$	1359	$q_{total}$	190

$$y = \frac{D - D8}{q_{total}} = \frac{1359 - 1271}{190} = 46.6 \text{ cm} \quad (\text{B.3})$$

$$F_{y0} = \frac{\frac{8+\rho}{2} \cdot 100 \cdot y}{\sqrt{2} \cdot \sigma'_a} = \frac{\frac{8-9.2}{2} \cdot 318 \cdot 46.6}{\sqrt{2} \cdot 1500} = 59.99 \text{ cm}^2 \quad (\text{B.4})$$

Reinforcement applied:

$$A_s = 2 \cdot \left(6 \cdot \frac{1}{4} \pi 2.5^2\right) = 58.9 \text{ cm}^2 \quad (\text{B.5})$$

Without the contribution of the stirrup reinforcement is the Unity Check for the shear capacity:

$$UC = \frac{F_{y0}}{A_s} = 1.0 \quad (\text{B.6})$$

The calculation of the Unity Check for shear force, results in the additional stirrup reinforcement to be superfluous in terms of strength. Meaning that the bend reinforcement can bear all possible acting shear loading on the bridge.

## Appendix - Chapter 4: Reverse Engineering

### C.1. Parametric geometry

Below in Table C.1 an overview of all input parameters/information and the output of the computer model.

Table C.1: Overview of the input and output from the computer model.

Input parameters	Style	Output parameters	Style
Name bridge	Text	Design code/class	Text
Design year	Number	Effective width	Number
Location	Text	Bending moments	Number
Number of spans	Number	Shear forces	Number
Span ratio	Number	Cross-sectional forces	Number
Steel quality	Text	Reinforcement cross-sectional area	Number
Concrete quality	Text	Bar diameter	Number
Concrete cover	Number	Unity checks	Number
Slab width	Number		
Span length	Number		
Slab thickness span	Number		
Slab thickness support	Number		
Edge distance	Number		
Width transverse beam	Number		
Applied asphalt layer	Number		
Bar distance	Number		
Reinforcement layer distance	Number		
Available bar diameter	Number		
Input for the Assessment	Text		
New edge distance	Number		
Extra applied asphalt layer	Number		
Assessment level	Text		
Actual carriage use	Text		

### C.2. Assumption

The assumption of equal stiffness's of the boundary conditions in the calculation of the support moments is examined. In a software program for beam calculations (Technosoft) are the support moments determined and compared to the result of the computer model. The result of the computer model gives a bending moment of 81.5 kNm for both supports, where Technosoft gives bending moments of 82 kNm and 79 kNm, see figure C.1. Here can be concluded that the method applied in the computer model does not deviate much from the 'exact' method in Technosoft.

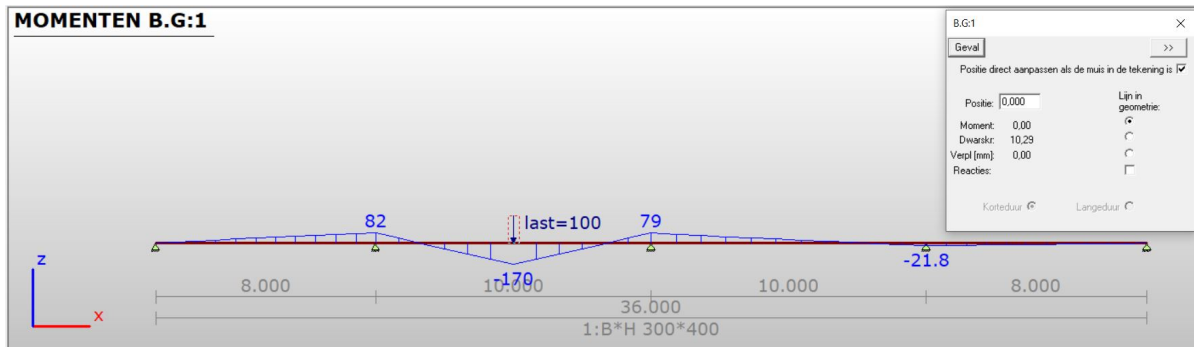


Figure C.1: Bending moment line as a consequence of a concentrated load in span two, determined with the use of Technosoft.

**Reduction of forces in presence of a transverse beam**

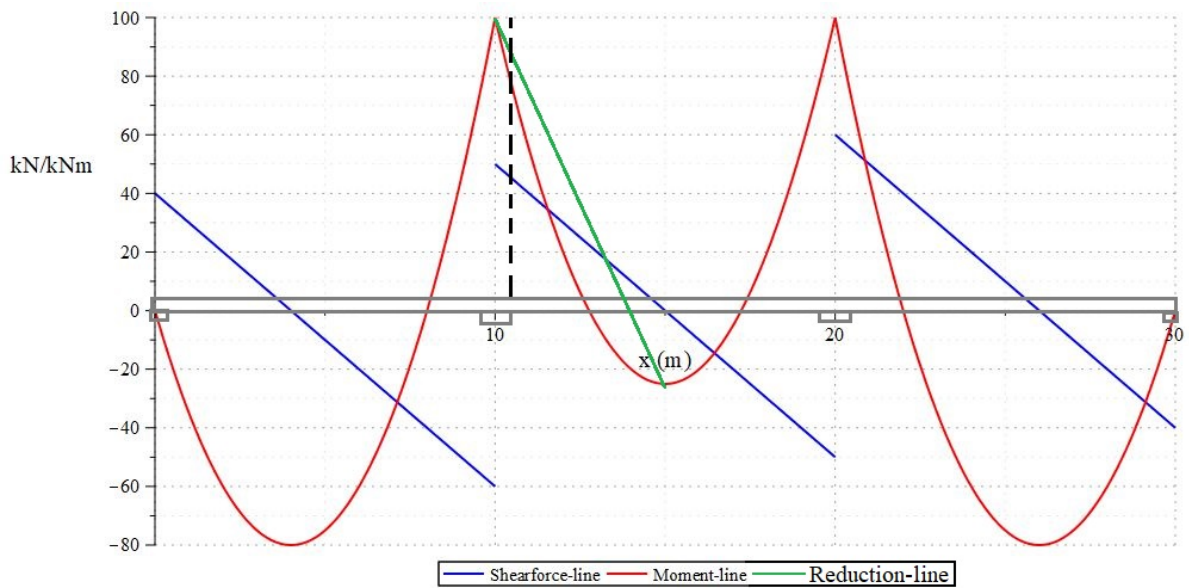


Figure C.2: The reduction of the support moment in case of the presence of a transverse beam is shown with the linear green line.

Table C.2: Partial load factors  $\gamma$  for the ULS for the assessment level 'Disapproval' for CC2 with  $\beta_b = 2.5$ , from the (NEN8700, 2011) Table A2.2(C).

	Permanent load (unfavourable)	Traffic load	$\psi_1$
Load combination (eq. 6.10a)	$\gamma_{Gj,sup}$	$\gamma_{Q,1}$	
Consequence Class 2 (eq. 6.10b)	1.1	1.1	0.8
Consequence Class 2	1.1	1.1	1.0

**Load reducing values**

The Tables C.3 and C.4 provide load reduction factors for specific reference periods and/or influence lengths. For different reference periods and/or influence lengths may one apply linear interpolation.

Table C.3:  $\psi$ -factors for shorter reference periods.

Reference period	$\psi$ -factor
100 years	1.00
50 years	0.99
30 years	0.99
15 years	0.98
1 year	0.95

Table C.4: Reduction factor  $\alpha_{trend}$  for the influence of the trend related to the year 2060, for the traffic loads from LM1 and LM2.

Influence length L [m]	Reduction factor $\alpha_{trend}$					
	2010	2020	2030	2040	2050	2060
0	1.00	1.00	1.00	1.00	1.00	1.00
20	0.89	0.91	0.93	0.96	0.98	1.00

### Graphical user interface

A graphical user interface (GUI) is made in order to interact with the computer model. An input sheet provides the possibility to adjust all required parameters to execute a detailed assessment of the existing RC slab bridge. During running of the model, determined force lines pop-up to control (intermediate) results. An output sheet pops-up when the RE bridge is assessed. The input sheet is presented in Figure C.3.

File

**Reverse Engineering of an existing reinforced concrete slab bridge:**

Input for Reverse Engineering:

The name to the bridge:

The design year:

Location of the bridge in a ... network:

Number of spans:

Reinforcement steel quality:

Concrete quality:

Concrete cover (cm):

Slab width (m):

Span length (end-span) L1 (m):

Span length (mid-span) L2 (m):

Slab thickness at mid-span (m):

Slab thickness at the support (m):

Edge distance (m):

Width of the transverse beam (m):

Applied asphalt layer (cm):

Applied additional permanent load (kN/m):

Input of the reinforcement layout:

Guess the bar distance (cm):

Reinforcement layer distance (cm):

Available bar diameters (cm):  12  18  19  20  22  25  28  30  32  36

Input for the Assessment:

Fill in the new edge distance (m):

Extra applied asphalt layer (cm):

Extra permanent load (kN/m):

Assessment level (CC2):

Reference period (years):

Number of cycles of heavy trucks (>3.5ton):

Actual carriageway use:

Figure C.3: Input sheet of the GUI.

The force distributions are presented by the output function of the AnaStruct package as in Figure C.5 and in Figure C.5. The governing positions for the distributed traffic loading are explained in Chapter 3, the visual explanation of an example bridge with four spans can be found in Figures C.6 and C.7.

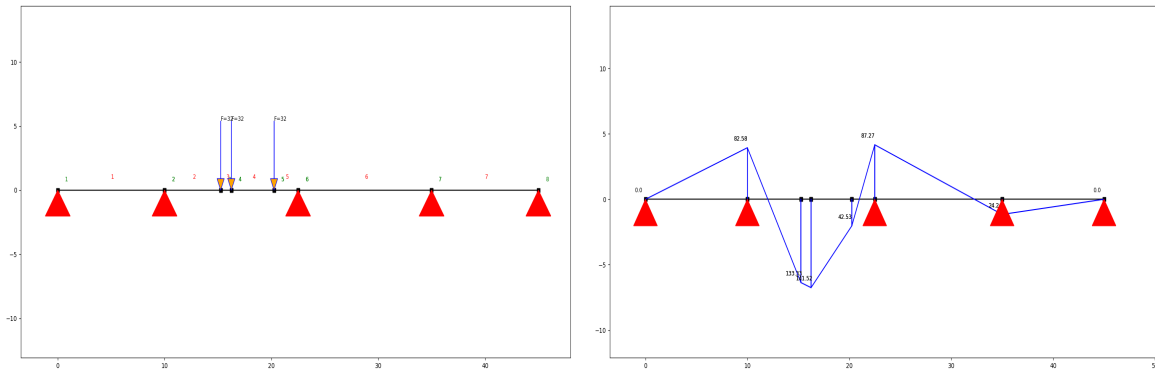


Figure C.4: Pop-up screens of force lines from the AnaStruct package. Left: example of a structure loaded by a design truck and right: Corresponding maximum sagging bending moment line

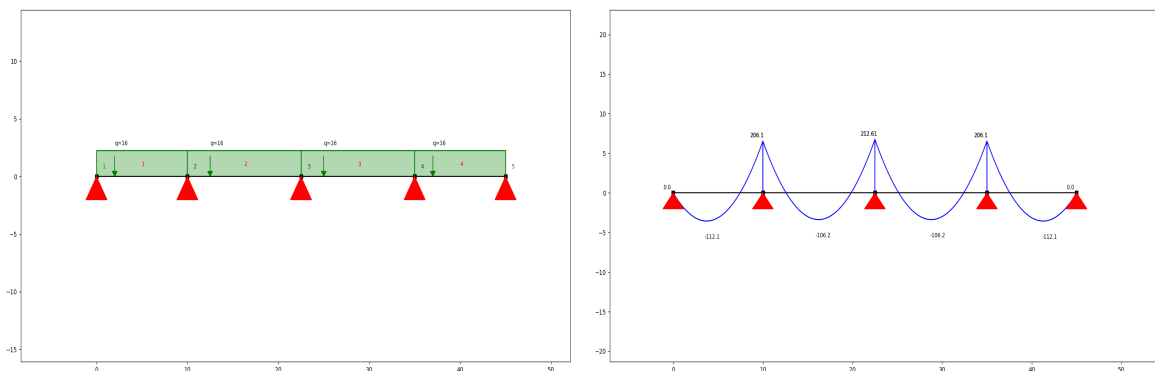


Figure C.5: Pop-up screen of force lines from the AnaStruct package. Left: example of a structure loaded by a self-weight and right: corresponding bending moment line.

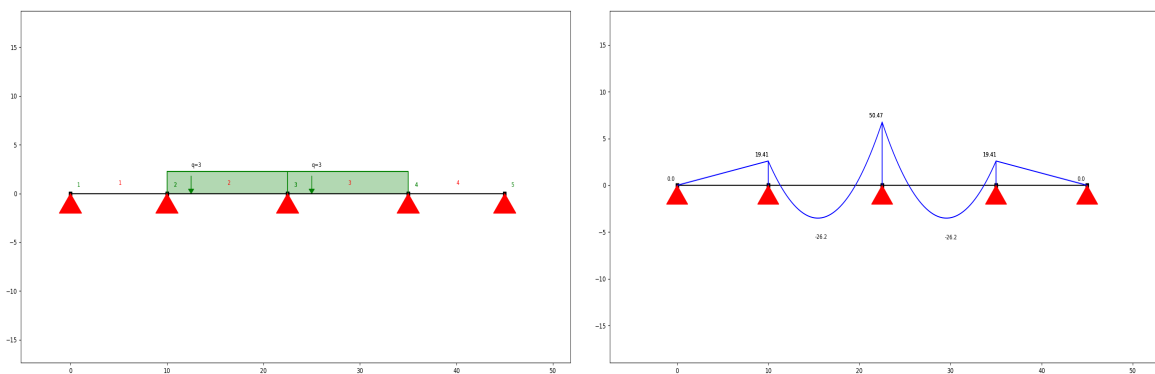


Figure C.6: Pop-up screen of force lines from the AnaStruct package. Left: example of a structure loaded by a distributed traffic load and right: corresponding bending moment line.

The output screen containing the result of the RE and assessment of the bridge is presented in Figure C.8. An reinforcement table in Excel is created to define the reinforcement configuration.

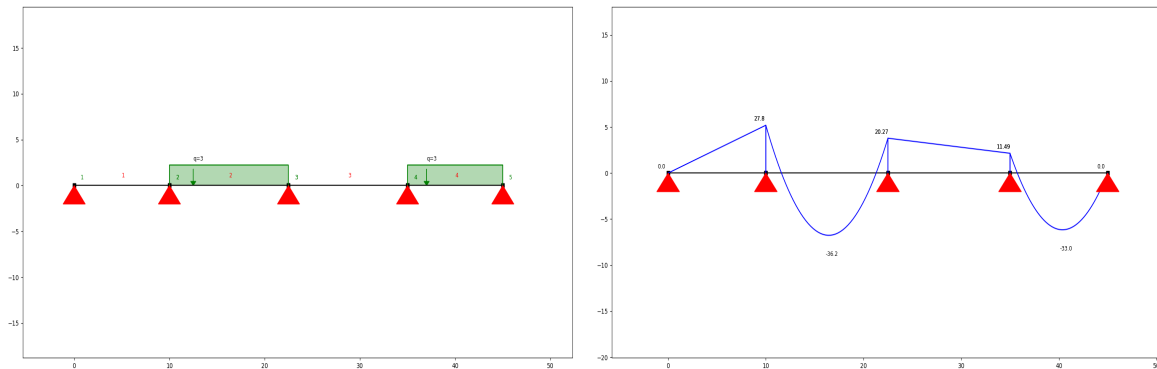


Figure C.7: Pop-up screen of force lines from the AnaStruct package. Left: example of a structure loaded by a distributed traffic loading and right: corresponding bending moment line with maximum sagging bending moment.

tk
— □ ×

### Results from Reverse Engineering

The name of the bridge is Groeneboog  
 The former design code is GBV1962 with the Load VOSB1963 because the bridge is build in 1966  
 The corresponding load class is the Class 60  
 The total number of traffic lanes taken into account is/are 2  
 The effective width are 11.49 m and 9.65 m of which the governing one is chosen for futher calculations.  
 The span moments are -322.19kNm from deadload, -80.49kNm from distributed traffic load, and -237.27kNm from concentrated traffic load.  
 The total bending moment in the governing mid-span is -639.95 kNm  
 The support moments are 433.92kNm from deadload, 93.99kNm from distributed traffic load, and 145.16kNm from concentrated traffic load.  
 The total bending moment in the governing mid-support is 673.08 kNm  
 The required reinforcement amount according to the former design code in the mid-span is 71.89cm<sup>2</sup>.  
 The required reinforcement amount according to the former design code in the support is 75.96cm<sup>2</sup> consisting of 75.96cm<sup>2</sup> in layer 1, and 0cm<sup>2</sup> in layer 2.

Reinforcement Tables

### Results from the Assessment

The span moments are -390.6kNm from deadload, -139.41kNm from distributed traffic load, and -278.41kNm from concentrated traffic load.  
 The total bending moment in the governing mid-span is -808.43 kNm  
 The support moments are 526.07kNm from deadload, 154.95kNm from distributed traffic load, and 102.92kNm from concentrated traffic load.  
 The total bending moment in the governing mid-support is 783.93 kNm  
 The required reinforcement amount according to the assessment code in the mid-span is 62.53cm<sup>2</sup>  
 The required reinforcement amount according to the assessment code in the mid-support is 60.35cm<sup>2</sup> consisting of 60.35cm<sup>2</sup> in layer 1, and 0cm<sup>2</sup> in layer 2.  
 The bending moment capacity with reverse engineered reinforcement at the mid-span is 910.17kNm.  
 The bending moment capacity with reverse engineered reinforcement at the mid-support is 952.94kNm.  
 The Unity Checks (load/capacity), where the load is defined according to the Eurocode with load factors from assessment level Reconstruction and the capacity determined with the reverse engineered reinforcement, result in: 0.89 at mid-span, and 0.82 at the mid-support.  
 The shear force capacity with Reverse Engineered reinforcement at the mid-support is 364.79kN.  
 The acting shear force from the assessment at the mid-support is 380.52kN.  
 The Unity Check for shear at the governing mid-support at 2.5d from the centre of the support is 1.04.

Quit

Figure C.8: Output screen of the GUI.

### C.3. Reinforcement table

The reverse engineered reinforcement from the model is determined with optimisation for a unity check of 1.0. Therefore a lower limit of the required reinforcement is made because from the validation can be concluded that the applied reinforcement in the existing bridge is in all cases slightly larger. By filling in the required reinforcement in Table C.5, the possible multiplication of bar distance times bar diameter are shown. In case a second reinforcement layer is present, a second reinforcement table will be filled in.

Table C.5: The reinforcement table with possible configurations of bar distance times bar diameter, filled in for an example required reinforcement amount.

Layer 1  
Lower limit of reinforcement: 18.6 cm<sup>2</sup>

Bar diameter	Distance [cm]	18	19	20	22	25	28	30	32	36
9	28	32	35	42	55	68	79	89	113	
10	25	28	31	38	49	62	71	80	102	
11	23	26	29	35	45	56	64	73	93	
12	21	24	26	32	41	51	59	67	85	
13	20	22	24	29	38	47	54	62	78	
14		20	22	27	35	44	50	57	73	
15		19	21	25	33	41	47	54	68	
16			20	24	31	38	44	50	64	
17				22	29	36	42	47	60	
18				21	27	34	39	45	57	
19				20	26	32	37	42	54	
20				19	25	31	35	40	51	
21					23	29	34	38	48	
22					22	28	32	37	46	
23					21	27	31	35	44	
24					20	26	29	34	42	
25					20	25	28	32	41	
26					19	24	27	31	39	
27						23	26	30	38	
28						22	25	29	36	
29						21	24	28	35	
30						21	24	27	34	
31						20	23	26	33	
32						19	22	25	32	
33						19	21	24	31	
34							21	24	30	
35							20	23	29	
36							20	22	28	
37							19	22	28	
38							19	21	27	
39								21	26	
40								20	25	

### C.4. Effective width

The resulting effective width depending on the span length can be plotted from the model. Figures C.9 and C.10 show the effective width according to the GBV methods and the Guyon-Massonnet method for different loading cases determined with the RE-tool and with Maple. The RE-tool chooses the governing effective width for the Guyon-Massonnet method based on slab size, edge distance, and chooses the loading situation resulting in largest forces from one or two design trucks. The determined graphs of the effective width from the RE-tool match the graphs from the calculations in Maple, only the different input values in both methods lead to different resulting effective widths.



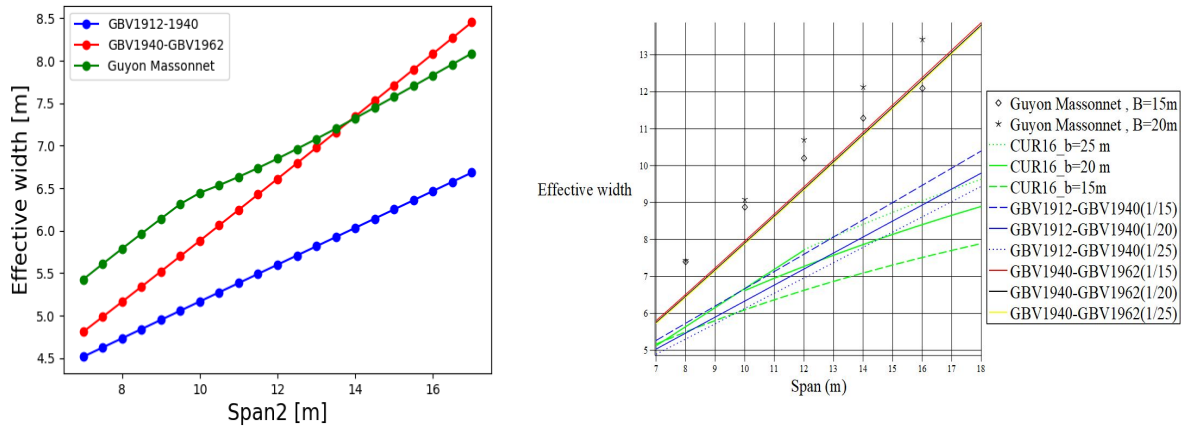


Figure C.9: Comparison of the determined effective width for loading by one design truck at the edge of the slab, the left figure determined with the RE-tool and the right figure with calculations in Maple.

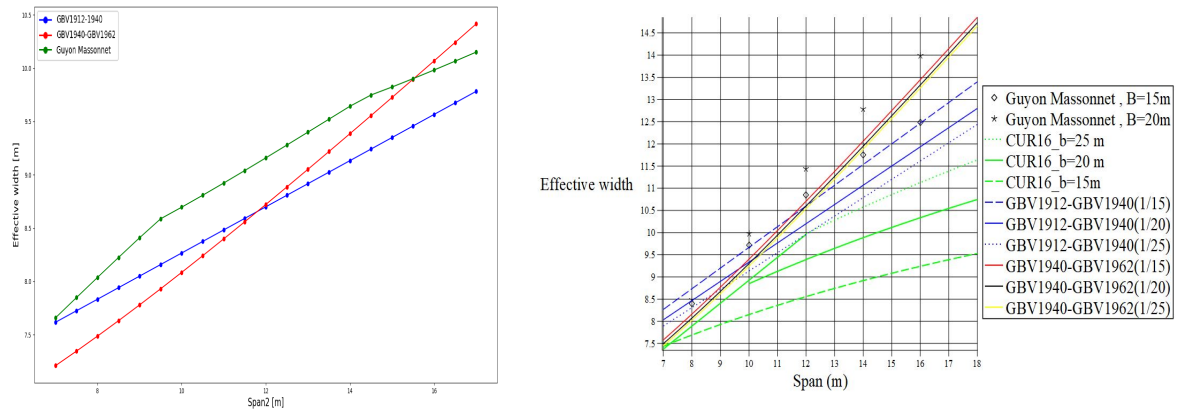


Figure C.10: Comparison of the determined effective width for loading by two design trucks in the middle of a slab, the left figure determined with the RE-tool and the right figure with calculations in Maple.



### C.5. Required reinforcement amounts and reinforcement ratio

For the span the required reinforcement is for the former load class and the EC RE. Dividing these two amounts results in a reinforcement difference ratio, shown in Figures C.11, C.12 and C.13. In these results is the minimum slab thickness of 400mm not included and the load reduction values for a reduced reference period and the traffic load trend are not included.

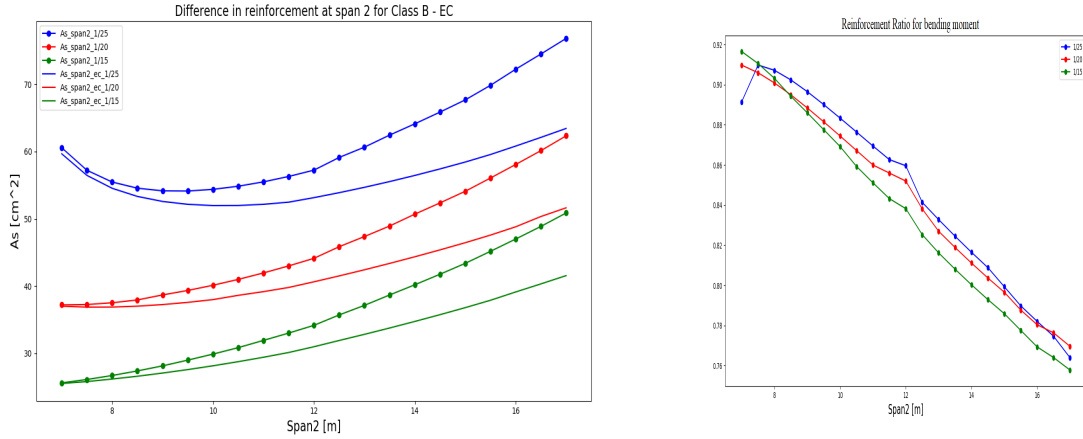


Figure C.11: RE reinforcement amounts at mid-span for load class B and the EC (left) and reinforcement difference ratio (right) for the period 1930-1940, for a variable mid-span length for three slenderness' 1/15, 1/20 and 1/25.

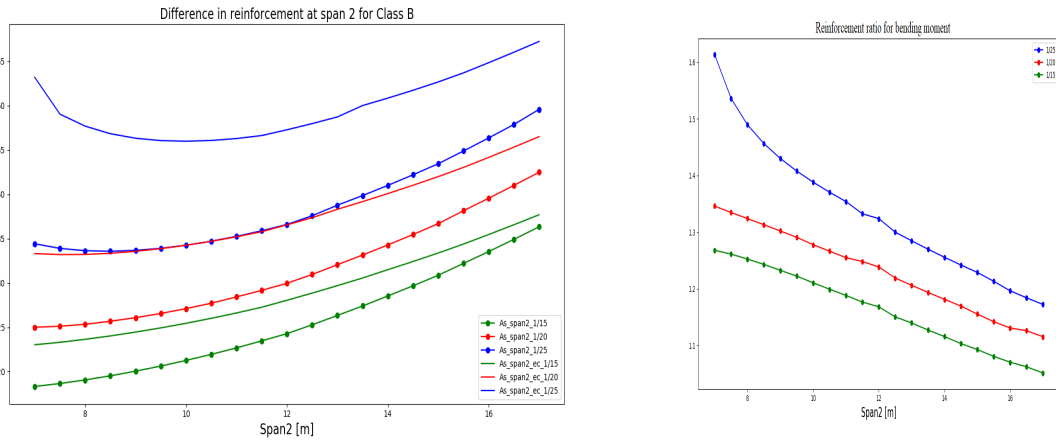


Figure C.12: RE reinforcement amounts at mid-span for load class B and the EC (left) and reinforcement difference ratio (right) for the period 1940-1950, for a variable mid-span length for three slenderness' 1/15, 1/20 and 1/25.

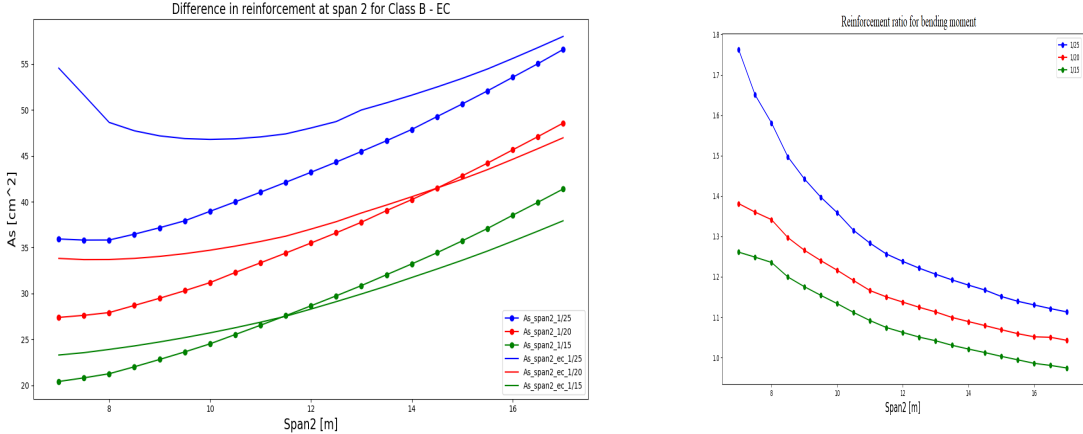


Figure C.13: RE reinforcement amounts at mid-span for load class 45 and the EC (left) and reinforcement difference ratio (right) for the period 1962-1970, for a variable mid-span length for three slenderness' 1/15, 1/20 and 1/25.

### C.6. Assessment

The assessment of existing structures has to be executed for the ULS of the structure, according to the (NEN8700, 2011). For each design period, the required reinforcement amounts at the governing support is determined. Consequently the corresponding Unity Checks are given. Now, a minimum slab thickness of 400mm is included and the load reduction values for a reduced reference period and the traffic load trend are included. An additional calculation report received through the cooperating company (RHDHV) is used to verify the results from the assessment with the EC, but it is not obtained in this report.

#### Support reinforcement load class B/45

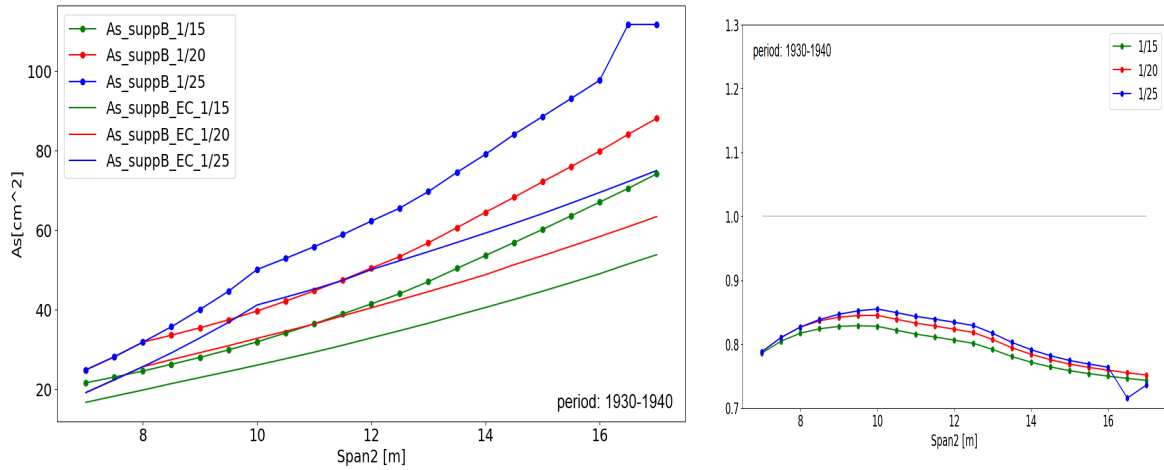


Figure C.14: RE support reinforcement amounts at a mid-support for load class B and the EC (left) and corresponding Unity Checks (right) for the period 1930-1940, for a variable mid-span length for three slenderness' 1/15, 1/20 and 1/25.

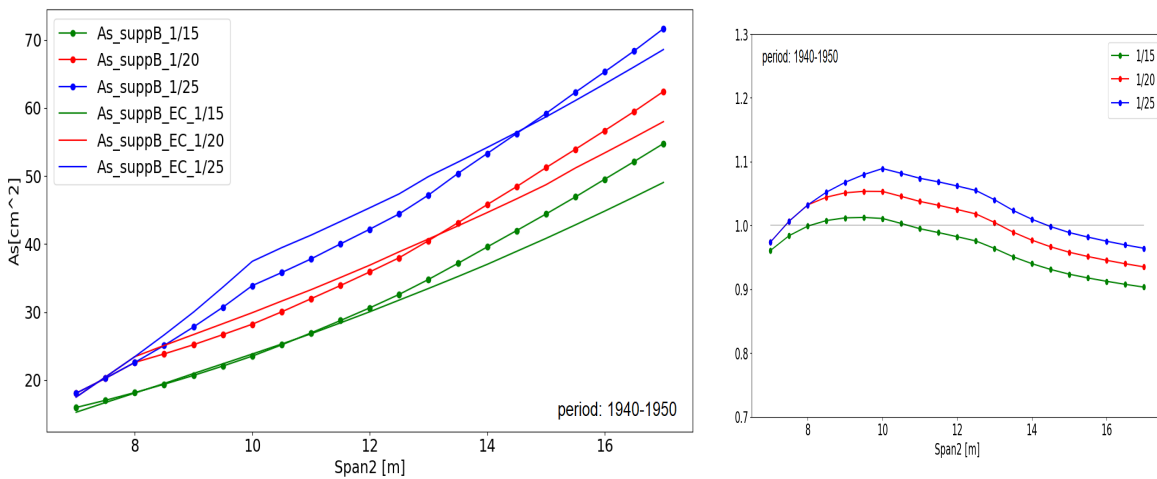


Figure C.15: RE support reinforcement amounts at a mid-support for load class B and the EC (left) and corresponding Unity Checks (right) for the period 1940-1950, for a variable mid-span length for three slenderness' 1/15, 1/20 and 1/25.

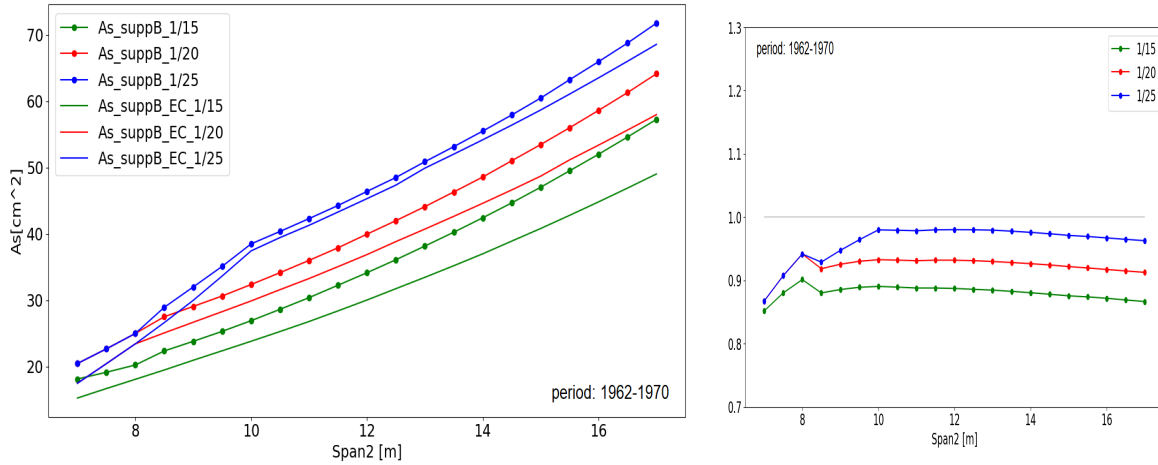


Figure C.16: RE support reinforcement amounts at a mid-support for load class 45 and the EC (left) and corresponding Unity Checks (right) for the period 1962-1970, for a variable mid-span length for three slenderness' 1/15, 1/20 and 1/25.

**Results load class A**

The governing period of bridge design is the period from 1950-1962, meaning that design in general led to the smallest bending moment capacity. For load class A in this period the span and support reinforcement, the bending moment UC and the UC for shear force is determined for a variable span and slenderness, see Figures C.17, C.18 and C.19.

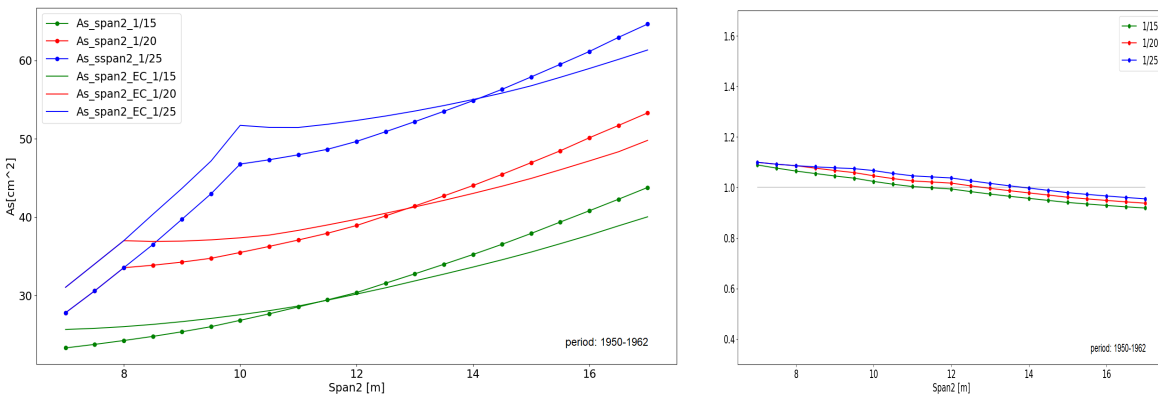


Figure C.17: RE span reinforcement amount at a mid-span for load class 60 and the EC (left) and corresponding Unity Check (right) for the period 1950-1962 for class A, and according to the assessment calculations, for a variable mid-span length for three slenderness' 1/15, 1/20 and 1/25.

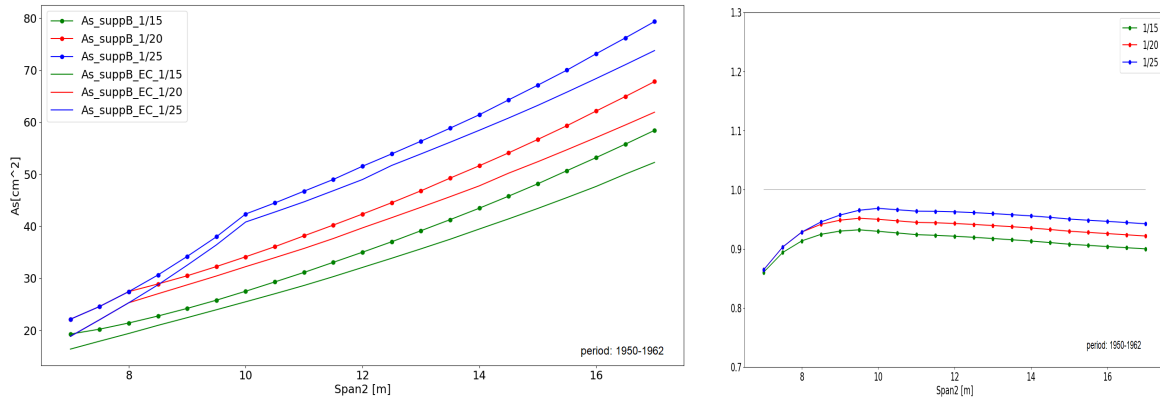


Figure C.18: RE support reinforcement amount at a mid-support for load class 60 and the EC (left) and corresponding Unity Check (right) for the period 1950-1962 for class A, and according to the assessment calculations, for a variable mid-span length for three slenderness' 1/15, 1/20 and 1/25.

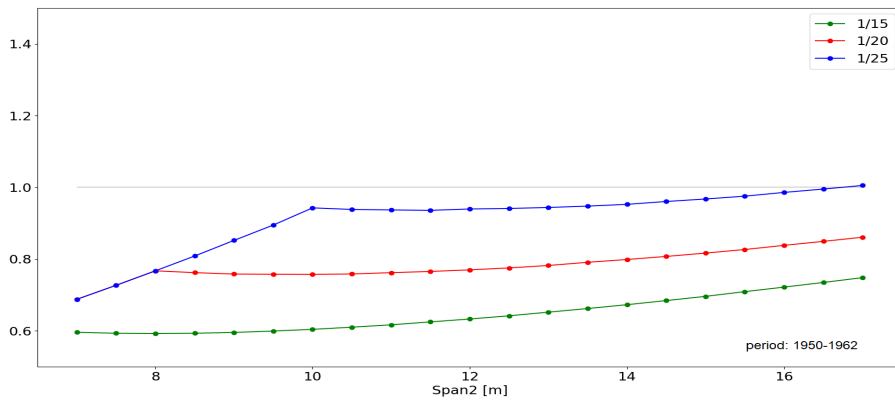


Figure C.19: Unity Check for the shear force for period 1950-1962 for load class A, assessed for the EC. Geometry with a variable mid-span length for three slenderness' 1/15, 1/20 and 1/25.

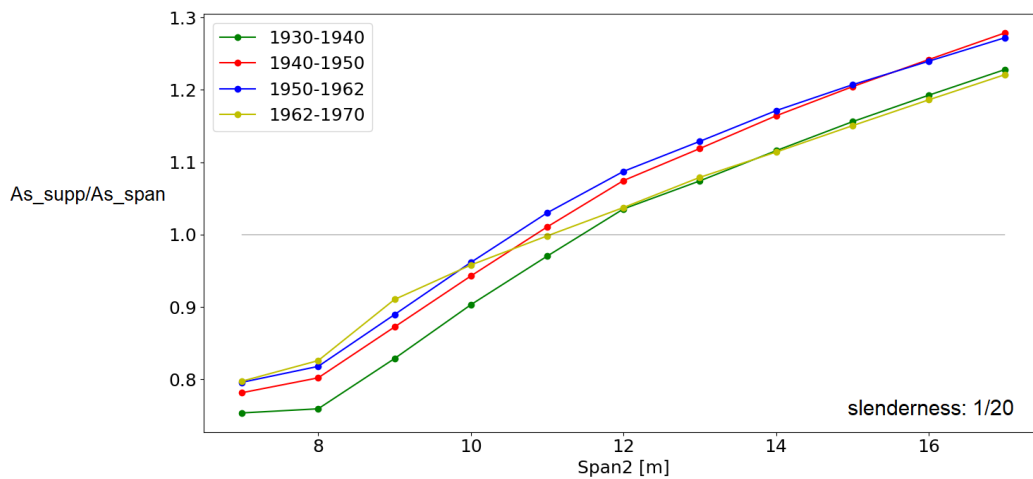


Figure C.20: Reinforcement ratio between the RE support reinforcement and the RE span reinforcement for load class A/60 for  $L1/L2 \leq 0.8$ , a slenderness of 1/20 and a minimum slab thickness of 400mm.

**Decentralised load model**

In addition to the conditions mentioned in Section 4.7 the DC load model is applicable for bridges in the following category: Incidental exemptions for heavy transport are only permitted after an individual assessment. The bridge is not frequently loaded by traffic with a deviating high load rate (access route of industry or transshipment area) or by wheel configurations which deviate unfavourable from the table NB.6-4.7 from the national annex belonging to the EN 1991-2. The following situation does not occur: entire renovation of the structure or the adjustment of the structure within 15 years after realisation.

The basis for the analysis is formed by the measurement data from the Weigh in Motion (WIM) system in the national road A16, where annual exemption traffic data is filtered-out. From earlier analysis (Vrouwen-velder et al., 2000) is obtained that the A16 is a relative heavy loaded national road, assuming that the use of the applied dataset leads to a conservative set of traffic loading compared to city bridges within the scope of application. The traffic load factors for concentrated- distributed traffic loading developed by TNO are applied for all three remaining design periods. The Figures C.21, C.22, C.23 show the determined required span reinforcement from RE and from the assessment, and the unity checks for bending moment. The period 1930-1940 shows unity checks almost independent of the slenderness of the deck. This leads for the same ratios between the capacity determined with former RE reinforcement and the loading by the DC load model, for all slenderness. All determined UC's for all design periods, the assessment with the DC load model result below 1.0.

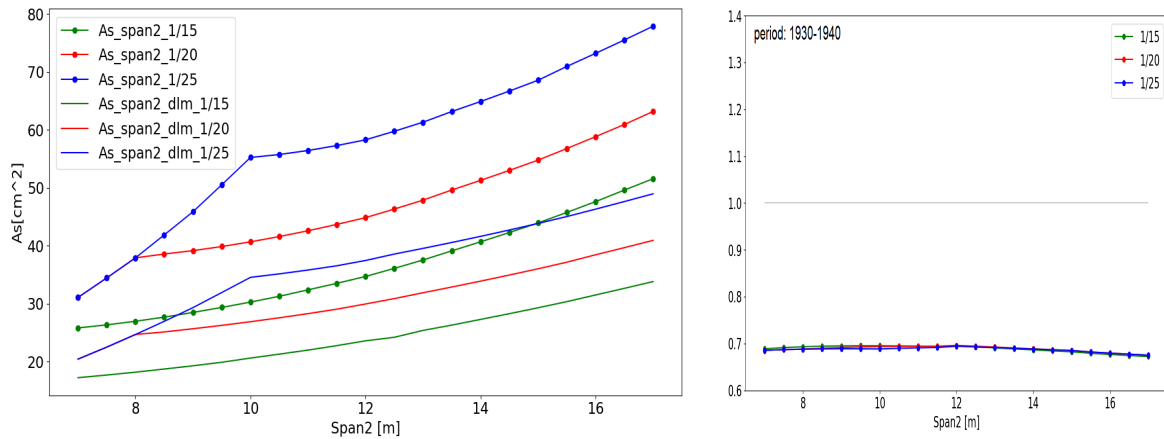


Figure C.21: RE span reinforcement amounts for bending according to load class B and assessed according to the DC load model (right) and corresponding Unity Checks (b) for the period 1930-1940, for a variable mid-span length for three slenderness' 1/15, 1/20 and 1/25, and minimum slab thickness of 400mm.

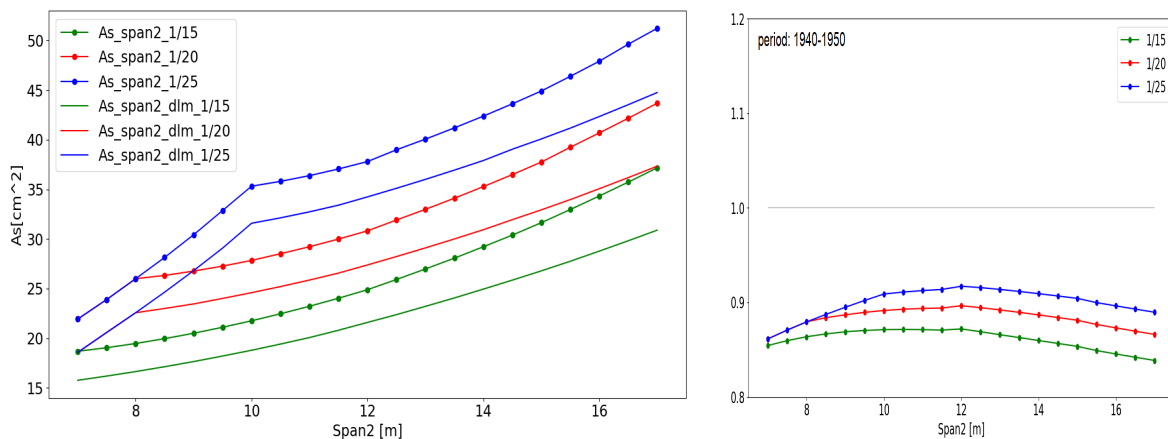


Figure C.22: RE span reinforcement amounts for bending according to load class B and assessed according to the DC load model (right) and corresponding Unity Checks (b) for the period 1940-1950, for a variable mid-span length for three slenderness' 1/15, 1/20 and 1/25, and minimum slab thickness of 400mm.

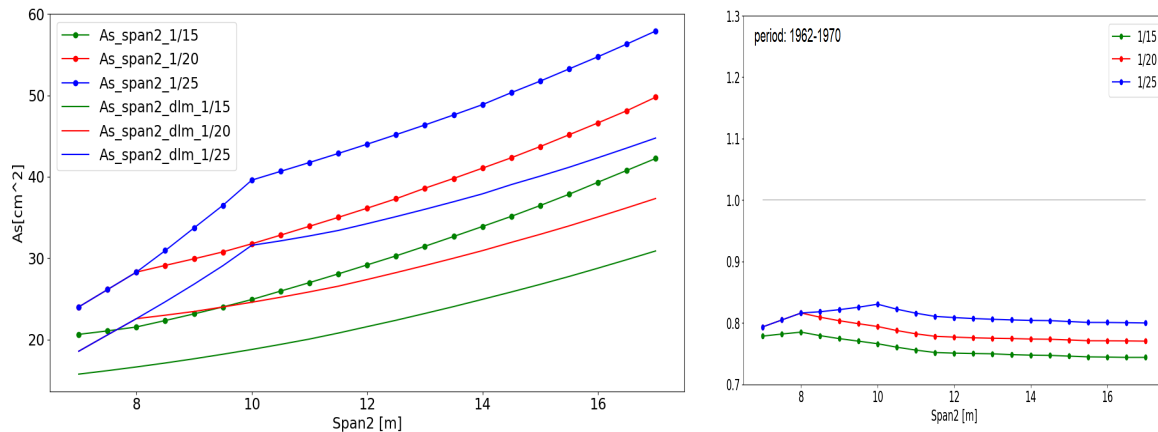


Figure C.23: RE span reinforcement amounts for bending according to load class B and assessed according to the DC load model (right) and corresponding Unity Checks (b) for the period 1962-1970, for a variable mid-span length for three slenderness' 1/15, 1/20 and 1/25, and minimum slab thickness of 400mm.

**Summary of the results of class A/60 bridges**

The Unity Checks of the bending moment capacity at the mid-span and at the mid-support and of the shear force capacity, for the different load models are presented in table C.6. In the parametric study are the load reduction factors from Section 4.4.1 included in the assessment. The assessment is performed with a reference period of 15 years for the EC and the DC load model.

Bridges designed for load class A/60 should carefully be checked if the bridge suffices the conditions for assessment with the DC load model. In general are class A/60 bridges located in the National road network and will not meet the conditions. However, the DC load model can be applicable for bridges designed in the local road network for load class A/60.

Table C.6: Overview of the Unity Checks from bending moment and shear force results for RE class A bridges, designed in the period 1950-1962.

Unity Checks for 1950-1962	EC	EC, with span reinforcement	DC load model	DC load model, with span reinforcement
Span	0.95 - 1.09		0.74 - 0.77	
Support	0.85 - 0.97	0.7 - 1.2	0.6 - 0.8	0.5 - 1.08
Shear force	0.6 - 1.04		0.4 - 0.85	- <sup>1</sup>

The results from the bridges designed for load class A show a more critical design for shear force compared to bridges designed for load class B. Class A bridges have in general more reinforcement from bending due to the higher former traffic load class. This increases the bending capacity but does almost not effect the shear capacity.

**C.7. How accurate is the computer code?**

Unless the computer code is verified to check if its well-engineered and error-free, the reliability of the computer code cannot be 100%. All computer codes are wrong in some degree, but the question is 'how accurate is the computer code and are the results reliable enough'? Behind the result maps and graphs are varying degrees of uncertainty attributable to accuracy of the input data, modelling uncertainties, degree of validation and verification, data discretisation and computational accuracy.

Modelling of uncertainties are dealt with by making assumptions within the scope of the thesis. All assumptions and modelling decisions are captured in Section 4.2. The degree of code validation can be judged upon the results of the validation table 4.3, where is estimated if the tool meets the actual needs. Discretisation is the process of converting continues features (input parameters) into discrete counterparts. For example, when existing bridge design is assessed for the variable 'time', in discretisation is only the function value de-

<sup>1</sup>The Unity Checks of shear force in combination with RE reinforcement from span and the DC load model is not determined, because the influence of the reinforcement amount is limited for shear compared to the share of concrete.

terminated for discrete time values. The computational accuracy is influenced by a numerical error in the finite element analysis package AnaStruct and the optimisation package from Numpy. The numerical error can be a combined effect of the finite precision of the floating-point or integer values and the truncation error. The Guyon-Massonnet method is an approximation of the actual distribution of loading on a slab structure and results in general in slightly higher forces according to de Boon (2018). However, the computer code including its uncertainties and limitations can be ensured to be fit-for-purpose, used appropriately and is producing reliable and defensible results.



# D

## Appendix - Chapter 5: Risk Analysis

### D.1. Geometrical uncertainties

The effect of the constant input parameters in the parametric study is examined by changing the individual parameters. The graphs belonging to the Table 5.1 from Chapter 5 are presented below in Figures D.1-D.4. The effect of the parameter can be obtained by comparing the new graphs (light coloured) with the original graphs (dark coloured). In the legend is also the resulting graph including the geometrical modification highlighted with an asterisk (\*). Most of the geometrical modifications effect the support moment, only the concrete cover and additional dead-load effect the RE required reinforcement at the span. The effect of the material properties on the required RE reinforcement is only reasoned based on horizontal forces equilibrium in a cross section. A higher material quality leads to lower required reinforcement and visa versa. However, this effect is expected to have small influence on the RE method.

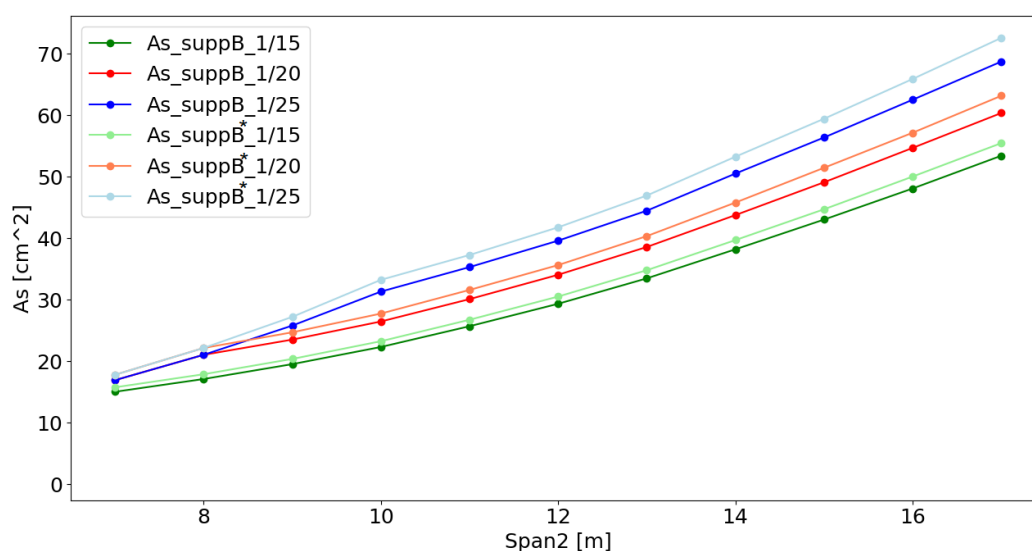


Figure D.1: Effect of the removal of the extra slab thickness on the RE required reinforcement amounts at the support.

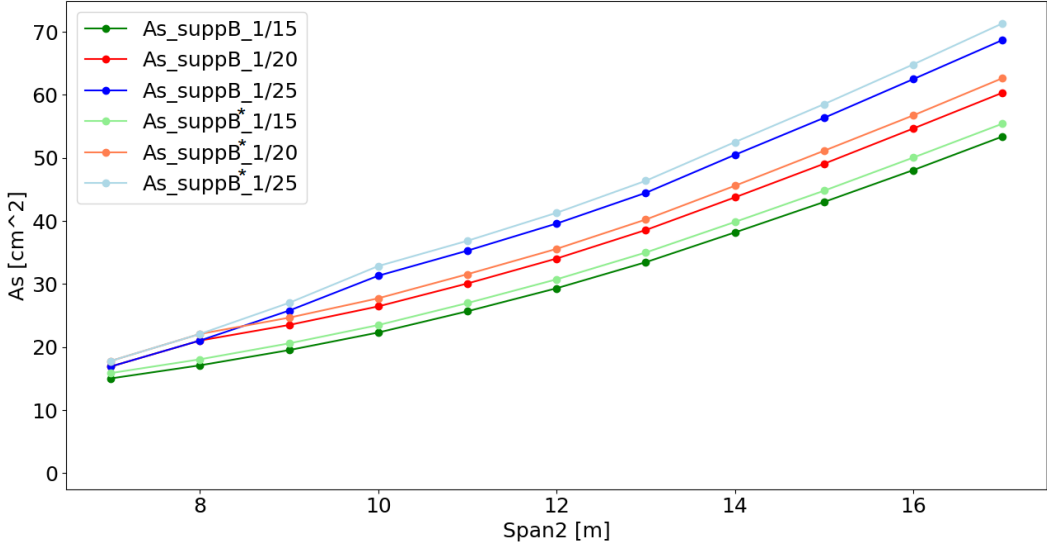


Figure D.2: Effect of the removal of the transverse beam on the RE required reinforcement amounts at the support.

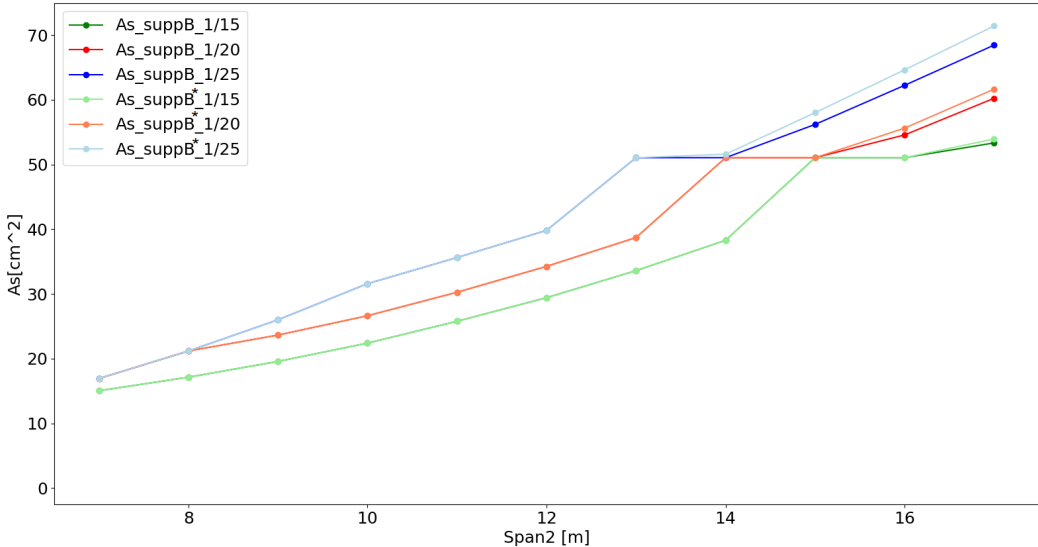


Figure D.3: Effect of the addition of the reinforcement layer distance of 2.0cm on the RE required reinforcement amounts at the support.

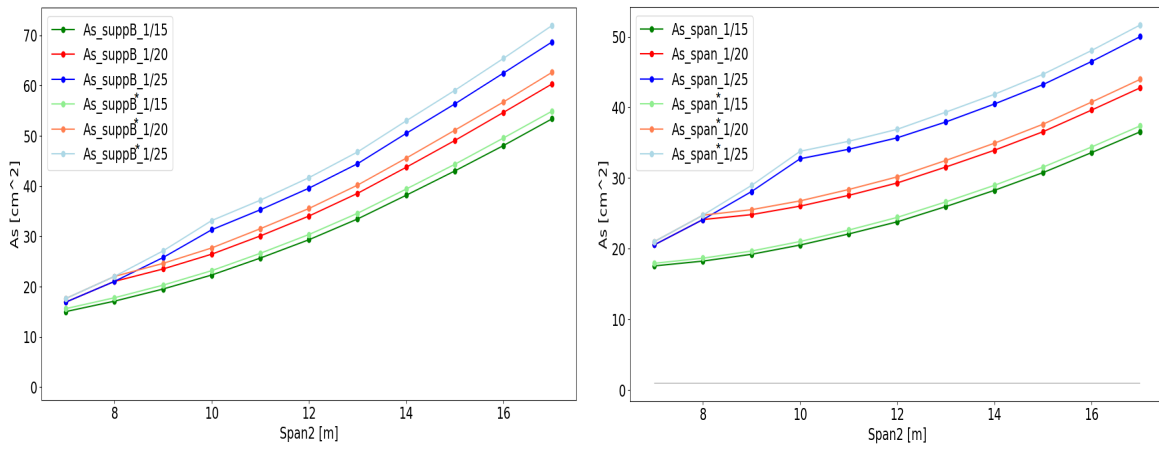


Figure D.4: Effect of the addition of extra dead load on the RE required reinforcement amounts at the support (left) and span (right).

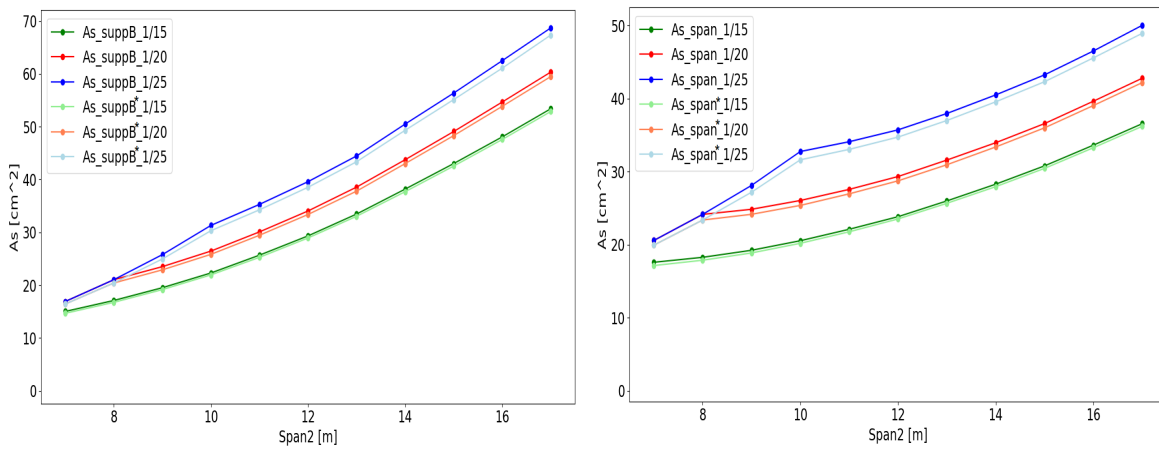


Figure D.5: Effect of a lower concrete cover 2.0cm relative to 3.0cm on the RE required reinforcement amounts at the support (left) and span (right).

**Effect of the slab width**

The effect of a variable slab width on the RE required reinforcement is examined. Here, former structural design is also divided by the four periods from Figure 2.21 according to the timeline. Figures D.6 show a constant RE required reinforcement amount for bridges with a variable slab width for the different design periods.

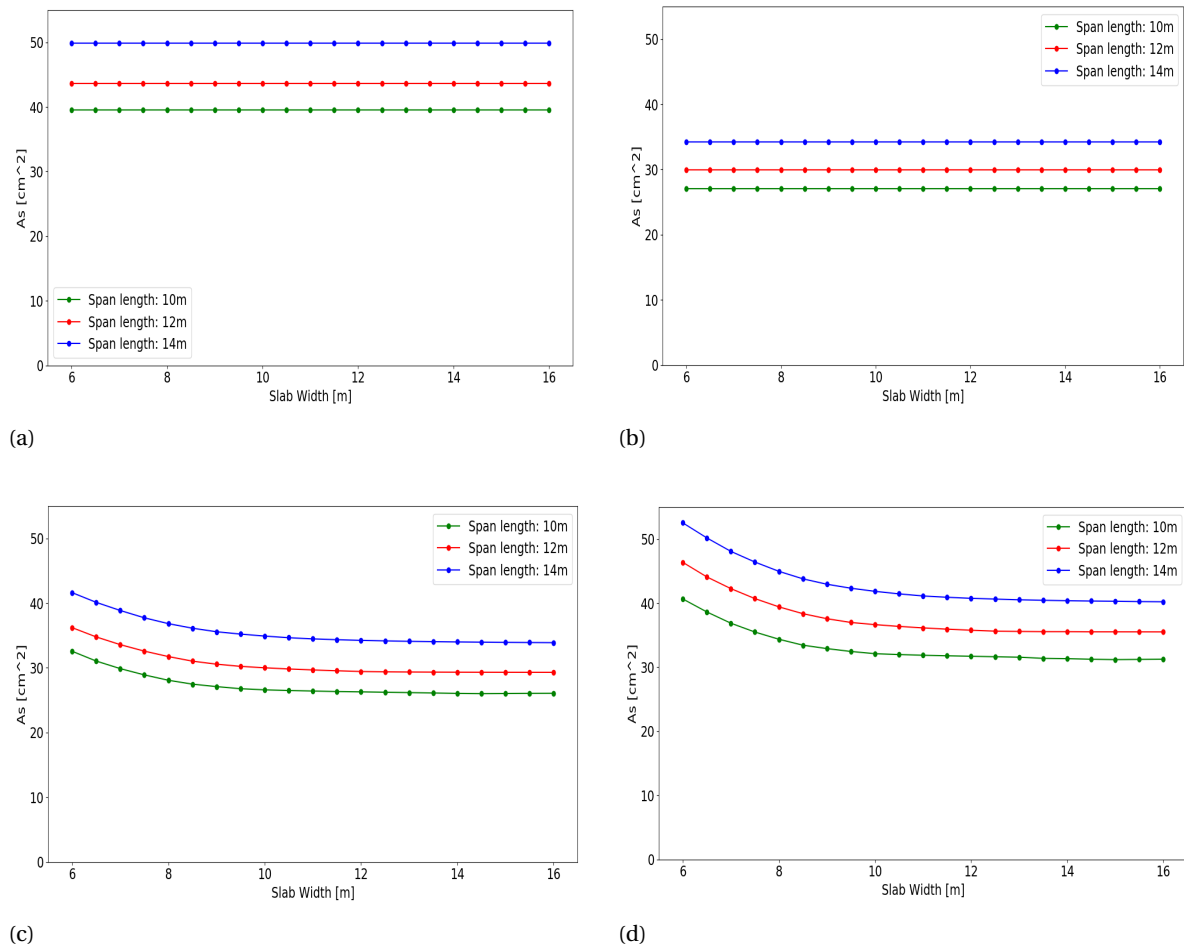


Figure D.6: Unity check for the midspan reinforcement for a bridge with variable width and span length of 10, 12 and 14m. Design in the period 1930-1940 (a), 1940-1950 (b), 1950-1962(c) and 1962-1970 (d) for load class 45.

The effect of the slab width on the Unity Checks of bending moment for the span is examined for assessment according to the EC. The four graphs of the determined Unity Checks for a variable slab width are shown in Figure D.7. From these figures can be concluded that for slab widths from 10 meter the influence on the the Unity Checks is negligible. This can be argued that from approximately 9 meter slab width (depending on the edge distance) two design trucks or -tandems fit on the slab next to each other. If the slab width is smaller than 9 meter, only one design truck or -tandem will fit on the slab.

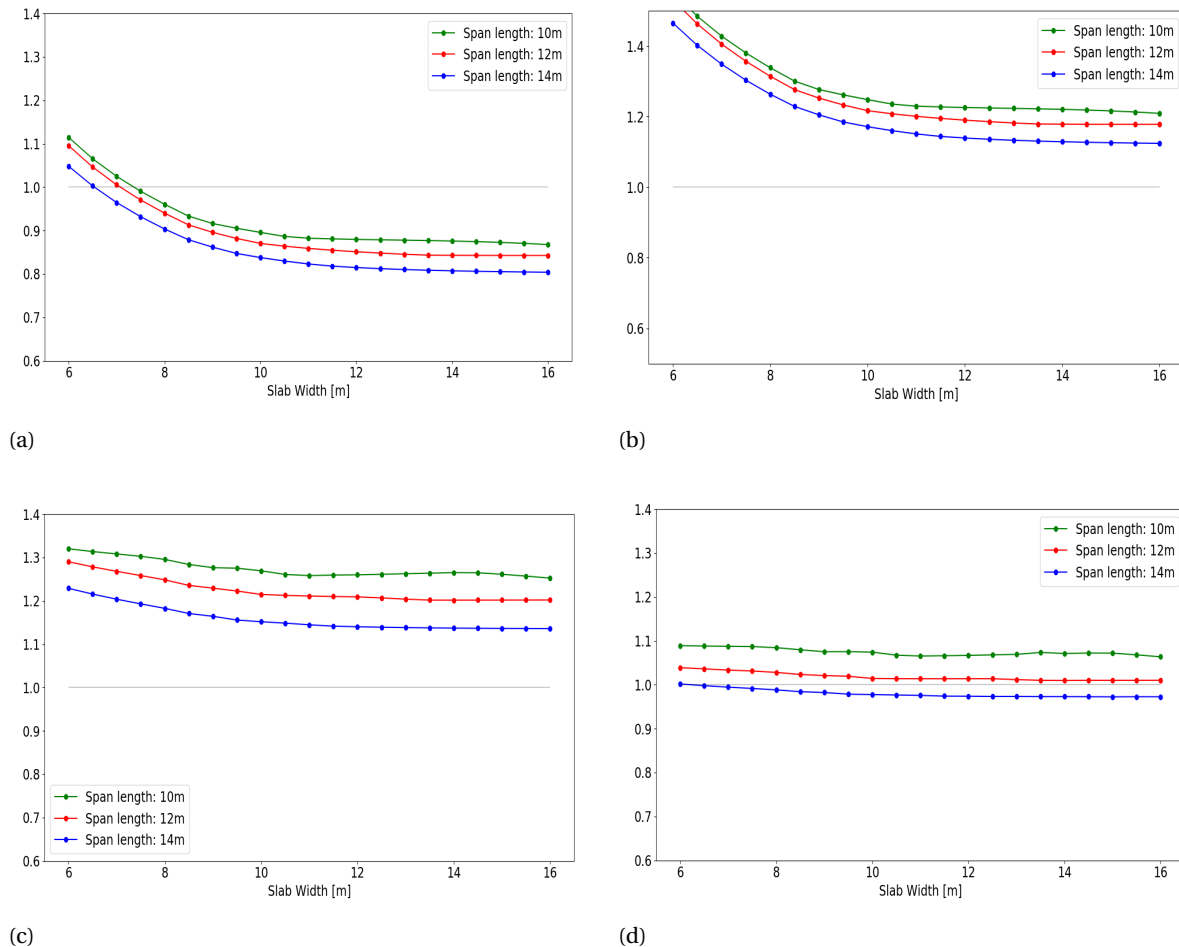


Figure D.7: Unity check for the midspan reinforcement for a bridge with variable width and span length of 10, 12 and 14m. Design in the period 1930-1940 (a), 1940-1950 (b), 1950-1962(c) and 1962-1970 (d) for load class 45.

In case the uncertainty of the design year fits within a design period, the scatter originates from the uncertainty in the geometry, as can be seen in Figure D.8.

## D.2. Reliability Methods

In the lecture notes from Jonkman et al. (2017) of the department of Hydraulic Engineering from Delft University of Technology the elaboration of a level I and level III method is explained.

Level I method (semi-probabilistic design): The uncertain parameters are modelled by one characteristic value for load and resistance as for example in codes based on the partial coefficients ( $\gamma$ 's) concept

Level III methods (numerical): The uncertain quantities are modelled by their joint distribution functions. The probability of failure is calculated exactly, e.g. by numerical integration.

## D.3. Protocol

Figure D.9 is a flowchart explaining the steps and checks to perform, in the process of RE and assessing an existing RC slab bridge. The protocol aims to perform a quick assessment for bridges with CC2 and a reference period of minimal 15 years (green) for RC slab bridges. However, the NEN8700 (2011) recommends in general, a residual lifetime and consequently a reference period for CC2 of 30 years. Two steps of collecting information for an assessment can be distinguished. Step 1 is the collection of information from the archives and requires low effort. Step 2 is an additional collection of information in case more detailed calculations need to be performed. Here, more physical effort and most likely more costs are accompanied. If in step 2 (all) additional information is collected, the uncertainty in the input parameters is deducted and conse-

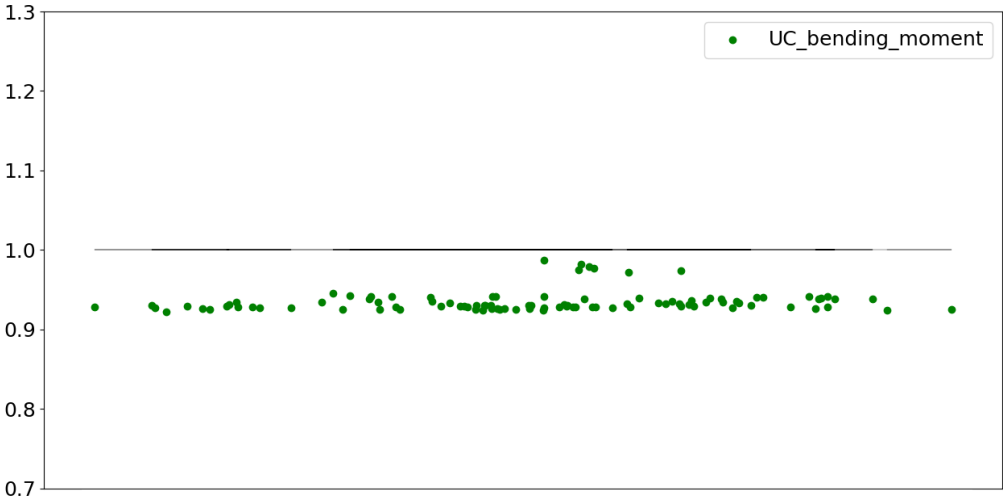


Figure D.8: Scatter plot of the Unity Checks for bending moment at midspan, with RE reinforcement designed for load class B, assessed for the DC load model with a ND design year of 1955.

quently suffices a Unity Check of 1.0 instead of 0.95. In the protocol, the Unity Check is the legal safety check for minimal reliability of the structure. Meaning that a Unity Check lower than 1.0 leads to sufficient reliability ( $\beta$ -value) according to the design codes, and a Unity Check higher than 1.0 leads to insufficient reliability according to the design codes. So, in case a Unity Check higher than 1.0 is obtained, follow-up action is required indicated by the protocol. The protocol functions as an example for the assessment of existing RC slab bridges and does not declare the only approach of assessment.

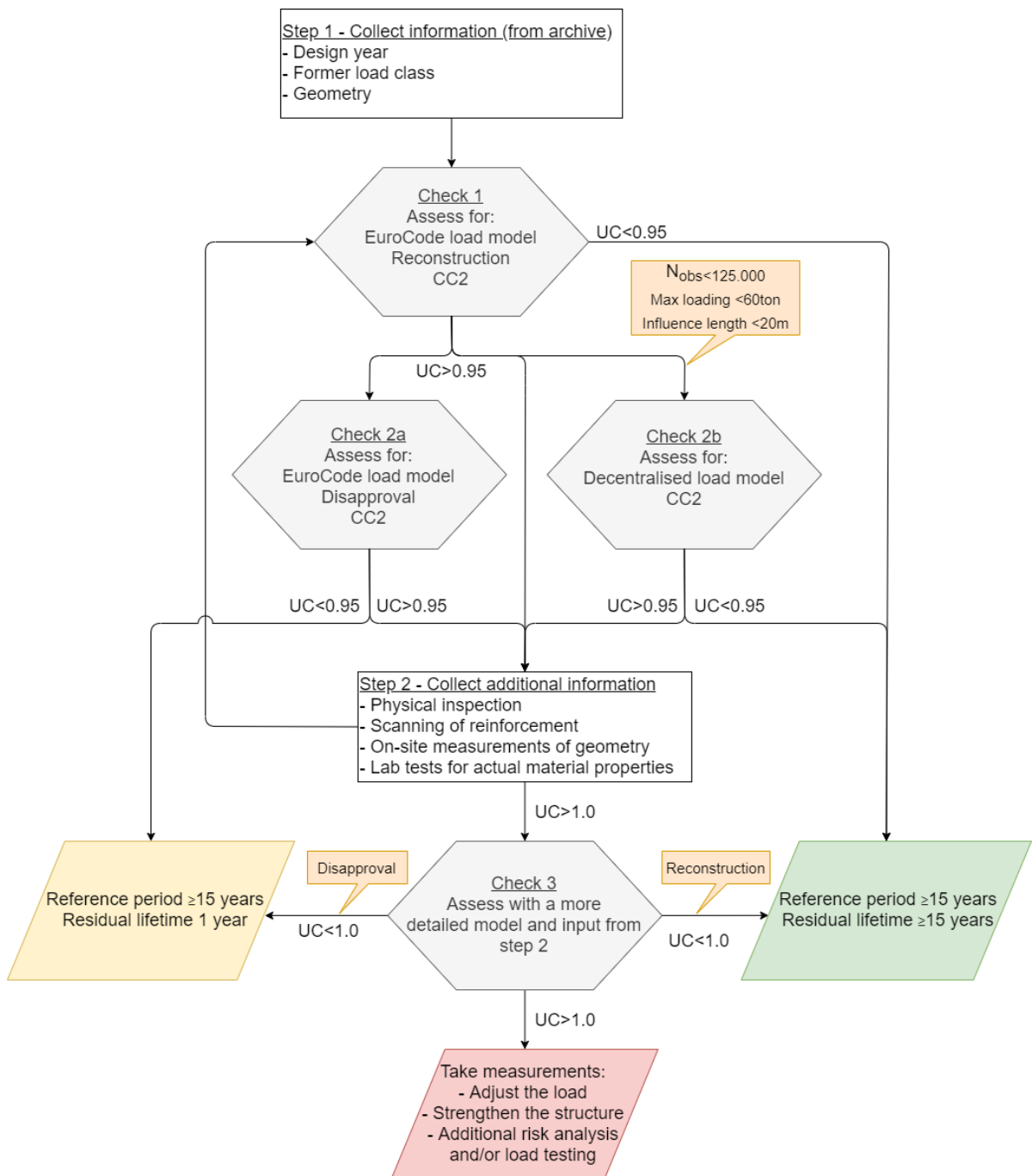


Figure D.9: Protocol for the assessment of existing RC slab bridges.



